Refining a Post-Stroke Pharmacological and Physical Treatment to Reduce Infarct Volume or Improve Functional Recovery, Using Gene Expression Changes in the Peri-Infarct Region to Examine Potential Mechanisms in Male and Female Rats

A dissertation submitted in partial fulfillment of the
requirements for the degree of
Doctor of Philosophy

By

MONER A. RAGAS
B.Sc., Omar Al-Mukhtar University, 1998

2016

WRIGHT STATE UNIVERSITY

WRIGHT STATE UNIVERSITY

GRADUATE SCHOOL

July 28, 2016

I HEREBY RECOMMEND THAT THE DISSERTATION PREPARED UNDER MY SUPERVISION BY Moner A. Ragas ENTITLED Refining a Post-Stroke Pharmacological and Physical Treatment to Reduce Infarct Volume or Improve Functional Recovery, Using Gene Expression Changes in the Peri-Infarct Region to Examine Potential Mechanisms in Male and Female Rats BE ACCEPTED IN PARTIAL FULFILLMENT OF THE REQUIREMENTS FOR THE DEGREE OF Doctor of Philosophy.

Adrian M. Corbett, Ph.D.
Dissertation Director

Mill W. Miller, Ph.D.
Director, Biomedical Sciences Ph.D. Program

Robert E. W. Fyffe, Ph.D.
Vice President for Research and
Dean of the Graduate School

Committee on Final Examination

Adrian M. Corbett, Ph.D.

Michael B. Hennessy, Ph.D.

Jeffery M. Gearhart, Ph.D.

David R. Ladle, Ph.D.

Debra Ann Mayes, Ph.D.

ABSTRACT

Ragas, Moner A. Ph.D., Biomedical Sciences Program, Department of Neuroscience, Cell Biology, and Physiology, Wright State University, 2016. Refining a Post-Stroke Pharmacological and Physical Treatment to Reduce Infarct Volume or Improve Functional Recovery, Using Gene Expression Changes in the Peri-Infarct Region to Examine Potential Mechanisms in Male and Female Rats.

Stroke, a life-threatening medical condition, is the fifth-leading cause of death in the United States with an estimated annual cost of treatments above $70 billion. A combination of innovative approaches was used in our lab to optimize the pre-clinical stroke research design by choosing the most appropriate animal model and methodologies to increase the translational capability of the stroke research.

The first study, modeled after ongoing clinical trials using fluoxetine, refined the appropriate timing of fluoxetine and ascorbic acid delivery if a rat was on simvastatin for 7 days pre-stroke and throughout the remainder of the study. Administration of fluoxetine and ascorbic acid at 6-12 hours or 48-54 hours (the time used in clinical trials) after stroke in male 10-12 month old rats resulted in larger infarct volume and indicated a high risk of hemorrhagic transformation, while administration of the same drugs 20-26 hours after stroke dramatically reduced infarct volume and the risk of bleeding in the brain. The ability of the combination therapy (fluoxetine and simvastatin) to improve motor recovery following stroke was estimated in both rehabilitated and non-rehabilitated female 10-12 month rats. The combination of drugs and rehabilitation improved motor function recovery,

but ultimately, the same functional recovery was seen with the drugs when there was no rehabilitation, making this treatment potentially useful for stroke patients who cannot undergo rehabilitation. The Forelimb Asymmetry test for the motor function was refined so that it showed greater sensitivity and correlated better with results from the Montoya's staircase grasping test. Finally, the potential mechanisms by which the pharmacological treatment works to aid recovery were investigated, exploring any putative sex-specific pattern of gene expression in the peri-infarct region in male and female rats at post-stroke day 7. A preliminary genetic analysis along with protein-protein interaction prediction reveal a fundamental role of animal sex in the response to drug treatment. The study shows a variation in the influences of the drug on pro- and anti-inflammatory biomarkers of microglia, regulation of neurotrophic factors and synaptic plasticity, with a new possible role of a neuropeptide Orexin and receptors in mediating the functional recovery in male rats.

TABLE OF CONTENTS

TABLE OF CONTENTS (Continued)

TABLE OF CONTENTS (Continued)

LIST OF FIGURES

LIST OF FIGURES (Continued)

LIST OF FIGURES (Continued)

LIST OF TABLES

LIST OF TABLES (Continued)

ACKNOWLEDGMENTS

I would like to extend my sincere gratitude and appreciation to my advisor, Dr. Adrian M. Corbett for helping me make a long-standing dream a reality. Dr. Corbett's professional knowledge and patient guidance have led me so far in my academic pursuits. She has been a great source of motivation through all the time. She is always challenging me to think critically, develop ideas and figure out how to solve problems on my own. She provided insightful feedbacks and constructive suggestions on my dissertation. Her relentless commitment to advancing stroke treatment, as demonstrated through her *tour de force* research, was very inspirational.

I would like to thank my dissertation committee, Dr. Michael Hennessy, Dr. Jeffery Gearhart, Dr. David Ladle and Dr. Debra Ann Mayes for their time and efforts. I sincerely appreciate their willingness to support me and ensure my success. Special thanks go to Dr. Ashot Kozak for his advice and input at the early stage of this work.

I am very appreciative of the generous support I received from the Biomedical Sciences Ph.D. Program throughout the course of my graduate studies, without it I would not be able to achieve my goal. Special thanks to Dr. Gerald Alter, Dr. Mill Miller, and to Ms. Karen Luchin.

Finally, I want to express my deepest love and thanks to my family. I would not have gone to graduate school without the encouragement of my parents, and I would not have been able to get through it without the love and support of my wife, Nada and my little boy, Ali.

To my greatest inspiration, my beloved mother and father
who have made me the person I am today

CHAPTER I
INTRODUCTION

1.1 Stroke and its Current Treatment

Stroke is a life-threatening medical condition that occurs when the normal blood supply to the brain is interrupted. There are two main types of strokes: ischemic, which happens when a thrombus or embolus blocks a cerebral artery supplying blood to the brain. This leads to deprivation of oxygen and nutrients to one area of the brain followed by cellular death in the affected area. The second type of stroke is hemorrhagic, which occurs when a weakened blood vessel ruptures and leaks either near the surface of the brain resulting in subarachnoid hemorrhage or into the tissue deep within the brain, as in intracerebral hemorrhage. In addition to these two forms of stroke, a transient ischemic attack (TIA), known as a mini-stroke, may occur as a short-term episode of transient neurologic dysfunction when the blood supply to part of the brain is briefly interrupted. The TIA is considered a warning sign of stroke risk.

According to the American Heart Association, stroke is the fifth-leading cause of death in the United States (Mozaffarian et al., 2016). The majority of strokes, ~ 87%, are ischemic (Rosamond et al., 2008). In ischemic stroke, there is an immediate loss of neurons after the initial insult depends upon where the stroke was, resulting in permanent damage to the brain, and increasing the risk of long-lasting disabilities (Saver, 2006). Stroke can affect people of all ages and backgrounds. In the United States, every 40 seconds someone

has a stroke and, on average, every 4 minutes one American dies of a stroke (Mozaffarian et al., 2016). Approximately 800,000 strokes occur every year in the United States. Depending on the location of stroke and severity of the attack, patients may experience serious problems with speech, walking, seeing, and understanding. The condition can potentially be fatal if not timely treated. The estimated annual direct and indirect costs associated with stroke treatment in the United States was $71.55 billion in 2010 and that expected to double by 2030 (Mozaffarian et al., 2016).

Ischemic stroke is a leading cause of the majority of long-term disabilities. One ongoing cardiovascular cohort study, the Framingham study, shows that survivors of an ischemic stroke who were at least 65 years of age experienced serious disabilities after stroke (Gore-Felton et al., 2003). Some of the limitations observed were muscular weakness on one side of the body, inability to walk, aphasia, depression, and dependence in daily living tasks.

Intravenous thrombolysis with recombinant tissue plasminogen activators (rt-PA), such as alteplase, reteplase, and tenecteplase, are the only FDA-approved pharmacological therapies available for ischemic stroke. These clot buster medications are believed to be effective in breaking up blood clots if given within 3 to 4.5 hours after symptom onset ("Tissue plasminogen activator for acute ischemic stroke. The National Institute of Neurological Disorders and Stroke rt-PA Stroke Study Group," 1995). However, a recent review indicated uncertainty for the short time window data; and recommended re-evaluating the safety and efficacy of the treatment within that time window (Alper, Malone-Moses, McLellan, Prasad, & Manheimer, 2015)

Stroke sufferers arriving at a hospital outside of this therapeutic window may not be eligible to receive the therapy, as later application results in hemorrhagic transformation (Lees et al., 2010). Unfortunately, only a small percentage of stroke patients reach the hospital in time to be considered for the clot buster (Wahl & Schwab, 2014). Patients presenting within 48 hours of symptom onset are given the anti-coagulant agent, aspirin, to keep blood clots from forming and to reduce the risk of early recurrent ischemic stroke.

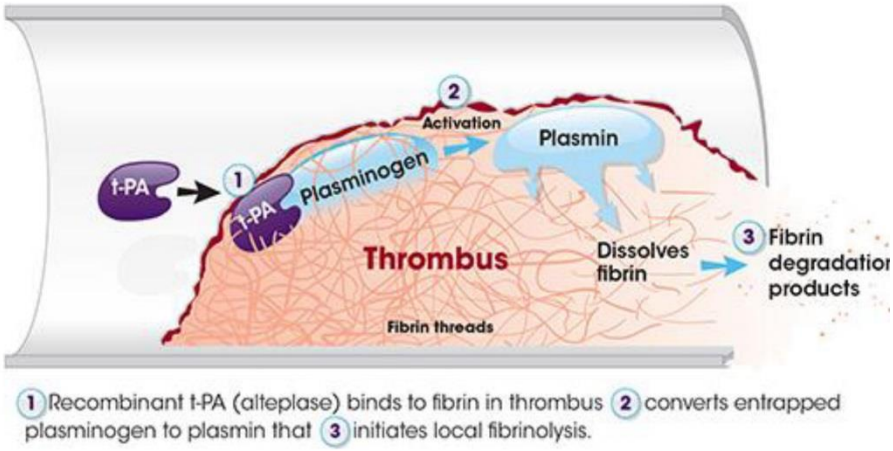

Figure 1. Mechanism of action of recombinant t-PA (Adapted from (Chhabra, 2014)

According to the guidelines from the American Heart Association/American Stroke Association for the initial management of patients with acute ischemic stroke, intravenous rt-PA (such as Alteplase) can only be given to a selected group of patients within a short time window of the onset of stroke symptoms (Del Zoppo, Saver, Jauch, Adams, & American Heart Association Stroke, 2009). Patient must be under 80 years of age, have no history of previous stroke or diabetes, not be taking any oral anticoagulant medications, or have an NIH Stroke Score greater than 25 (Adams et al., 2007). The National Institutes of Health Stroke Scale, or NIH Stroke Scale (NIHSS) is a tool used by healthcare providers to objectively quantify the impairment caused by a stroke. The use of rt-PA in stroke

patients beyond that therapeutic time frame could lead to potential side effects such as bleeding complications and angioedema (Miller, Simpson, & Silver, 2011). Currently, less than 8.5% of patients are able to take the only available pharmacological treatment, rt-PA, within the required time after the onset of stroke symptoms (A. M. Corbett et al., 2015). This limitation has necessitated studies to come up with a more efficient treatment that is readily available and can be delayed over four and half hours.

Even with the success of endovascular therapy, in which a clot is removed under direct angiographic visualization as in the MERCI retriever (Mechanical Embolus Removal in Cerebral Ischemia), intravenous rt-PA within the first 4.5 hours remains the standard of care. That is because not all patients are suitable candidates for MERCI retriever and sometimes even ideal candidates have major complications after a mechanical removal of the thrombus. Endovascular therapy is for patients who have (NIHSS) ≥ 6 and demonstrated large occlusion in middle cerebral artery, internal carotid artery, or anterior cerebral artery on imaging. For these reasons, there is a pressing need to identify a pharmacological therapy that can safely be administered beyond that short time window for the majority of stroke patients.

For fifteen years after rt-PA was approved, several experimental studies failed to translate their data into clinically useful neurorestorative therapies for acute ischemic stroke (Dirnagl, 2006). The majority of these preclinical studies were performed using rodent models of permanent or transient focal cerebral ischemia in which induction of middle cerebral artery occlusion (MCAo) is done by insertion of a surgical filament into the external carotid artery to block the middle cerebral artery at its origin (Longa, Weinstein, Carlson, & Cummins, 1989). This widely used model, however, is susceptible

to issues of anatomical accuracy and requires careful practice to avoid surgical complications, such as damage to adjacent tissues and bleeding. In addition, the MCAo model produces a larger infarct volume in animal brain and always have a higher mortality rate in aged rats, which limit the assessment of functional disabilities in adult animals after stroke (R. Y. Wang, Wang, & Yang, 2003).

In 2011, a randomized, double-blind placebo-controlled trial called FLAME (Fluoxetine in Motor Recovery of Patients with Acute Ischemic Stroke) examined the influence of the anti-depressant selective serotonin reuptake inhibitor, fluoxetine, on functional motor recovery after acute ischemic stroke (Chollet et al., 2011). This study led to a fundamental change in ischemic stroke treatment and re-ignited hope that this drug could improve motor recovery and reduce post-stroke disabilities. Experimental studies in our lab have shown that administration of a drug combination consisting of the anti-depressant fluoxetine and the cholesterol-lowering drug simvastatin in addition to L-ascorbic acid (Vitamin C), in an adult rat model of ischemic stroke 20-26 hours after symptom onset, successfully improves motor recovery and reduces functional impairment in the rats. Furthermore, the drug combination significantly increased neurogenesis up to 19-fold in treated animals versus controls (A. M. Corbett et al., 2015). The underlying mechanisms by which this drug combination works to enhance functional motor recovery in stroke patients are not at all clear. Based on animal studies in our laboratory and others, there are some potential mechanisms whereby fluoxetine might augment functional recovery in ischemic brain. These include stimulation of neurogenesis, where a robust pool of newly generated neurons migrate to ischemic areas; stimulation of angiogenesis; regulation of neurotrophic factors; and synaptic plasticity (Siepmann et al., 2015).

A modified procedure to induce focal ischemic stroke by endothelin-1 (A. M. Corbett et al., 2015) was performed in these animals to produce relatively small infarcts compared to the widely used model of MCAo with a gradual injury perfusion similar to that in humans. A post-stroke drug combination of fluoxetine and simvastatin, in addition to L-ascorbic acid (FSA), was orally delivered in a stress-free environment to improve functional motor recovery after stroke and to complement the limited availability of the only available pharmacological therapy, tissue plasminogen activator (tPA) (A. M. Corbett et al., 2015).

By reviewing pre-clinical studies on stroke, there are gaps in previous research that contributed to the unsuccessful translation. Some questions were asked: What would be the best animal model with biological similarities to the human brain that can efficiently simulate the pathological processes after ischemic stroke? How could we design appropriate methodologies to mimic the clinical situation closely? The lack of translation could not be entirely attributed to the choice of animal model, but also in how such models and their resultant data are applied (Howells et al., 2010).

1.2 Problems with Translating Pre-Clinical Animal Studies to Human Clinical Trials

Despite tremendous investments in advancing translational stroke research, many pre-clinical studies failed in translating their findings from animal studies into human clinical trials, thus have not been adopted into clinical practice. The main factors causing the failures of neuroprotective treatments have been explained in the STAIR (Stroke Therapy Academic Industry Roundtable) guidelines for preclinical stroke trials (Stroke Therapy Academic Industry, 1999). The factors include inappropriate time windows of drug administration, ineffective dose, using medications that can not cross the blood-brain-

barrier, the age of the animal is young, morbidities and mortalities in young animals, and the heterogeneity of stroke subtypes in patients. In addition to animal age, sex bias is another essential factor that should be considered when translating research from preclinical studies. Young male animals are usually employed in preclinical studies (Beery & Zucker, 2011). Some other explanations of this unsuccessful translation could be related to poor experimental design: lack of randomization or using inappropriate animal models that do not accurately mimic the disease condition in a human. An example of poor experimental design is choosing animal strains for particular study without taking into account the variation in their drug metabolism, which can lead to an unclear conclusion regarding the efficacy and toxicity of the medicine treatment. Moreover, not all animal models used for inducing focal ischemic stroke have brain blood vessel collateralization that mimics human cerebral vasculature. Also, using ineffective assessment methodologies along with inappropriate statistical analyses may contribute to the failure of research translation. The number of animals that are employed in the experimental studies is imperative, an inadequate statistical power when few animals are used, along with inaccurate statistical analyses can substantially influence results. A publication bias is another important factor contributing to this failure (S. Liu, 2009). Studies suggest that research directions of authors and reviewers (Joyce, Rabe-Hesketh, & Wessely, 1998), conflicts of interest (Perlis et al., 2005), research funding sources (Liss, 2006) are few examples of factors influencing publication bias.

1.3 Randomization in Animal Studies

A growing body of evidence is indicating that randomization and blinding outcome assessment in pre-clinical studies can minimize the potential risk of bias (Bath, Macleod,

& Green, 2009). Some of the key solutions to avoid any possible biases are random assignment of test animals to experimental and control groups without any prejudice. Being blinded to groups in functional assessments and when evaluation and analysis performed is vital. No information should be known to the observer who performs the analysis besides animal's number. In our experiments, we have controlled for bias, and we have tried to be as objective as possible. In cases where there may be some subjectivity in the observation (*e.g.* examining whether only tips of fingers or palms of the hand are touching a wall in Forelimb Asymmetry tests), we typically use one observer to perform an entire series of evaluations, so the same bias is present throughout a study. To confirm that a proposed change in methodology is reliable, we have multiple different observers use the same method and evaluate the results across the different monitors to determine the inherent variability due to subjectivity.

1.4 Animal Models of Stroke and Age of Model

Animal models are essential to preclinical stroke research. Due to the complexity of interactions in the brain vasculature during the stroke, there is no *in vitro* model that can properly mimic these complicated pathophysiological mechanisms in humans. We chose rats as rodents are one of the most relevant animal models used in stroke research (Casals et al., 2011). Rats have been employed in stroke research due to their close resemblance to cerebrovascular physiology and anatomy to human, and reproducibility of stroke damage (Ginsberg & Busto, 1989). Nevertheless, no single animal model can precisely represent the variables affecting ischemic stroke patients (Bacigaluppi, Comi, & Hermann, 2010). We previously have done multiple studies on different strains of rats such as: Fisher, Long-Evans, Wister, and Sprague-Dawley, to determine which one would make a better model

of the medical situation in humans. The majority of stroke studies are conducted using young animals which might react differently to stroke injury by initiating spontaneous neurogenesis (Casals et al., 2011). A large number of preclinical studies on stroke use 2-month-old animals (100 grams) with MCAo method of stroke induction for preclinical studies on ischemic stroke. In contrast to these studies, we utilized a group of 10-12-month-old rats (400-600 grams) because they have more similarity to human patients, who in most cases are middle-aged or older. Also, neurogenesis typically decreases with age (Walter, Keiner, Witte, & Redecker, 2011), hence requiring the drugs to be tested under similar conditions in both rats and humans. In our lab, adult male and female Sprague-Dawley rats were favored over all other strains for their brain blood vessel collateral circulation resembles that in people and because of the animal age correlates with the middle-aged person in clinical trials.

1.5 Sex-dependent Differences

Increasing evidence suggests that an animal's sex may influence the results of stroke studies by multiple mechanisms, therefore animal's sex is a potentially informative consideration for the development of new pharmacological treatment for stroke. The effectiveness of the drug may vary depending on animal sex (K. Li et al., 1996). A study indicated that there are sex differences in rat and mouse brains; and that gonadal hormones modulate prostaglandins (PGE2) in brain. (Dean, Knutson, Krebs-Kraft, & McCarthy, 2012). The PGE2 regulates the response to injury after stroke with female rats showing better outcomes than males to the same injury. An experimental study using MCAo models of stroke has demonstrated that female rats have a prominently reduced infarct volume compared with male rats, and ovariectomized rats have infarct volumes that are similar in

size to male rats (Alkayed et al., 1998). Female steroid hormone estradiol plays a role in this neuroprotective effect in rats. Studies showed that administration of exogenous estrogen decreases infarct volume size in both male and female rats (Toung, Traystman, & Hurn, 1998). An interesting study showed that the amount of hydrogen peroxide produced by macrophages from male mice is more than female animals, and causing more tissue damage than macrophages from females (Y. Chen & Johnson, 1993). A study on human granulosa-luteal cell culture demonstrates that high concentrations of estrogen inhibit the activity of the inflammatory interleukin-1 (IL-1). IL-1 is a highly inflammatory molecule released early in ischemic tissue, which activates many inflammatory processes through activation of T cells and induce expression of acute-phase proteins. IL-1 plays a role in the neuronal injury that occurs following stroke (Polan, Daniele, & Kuo, 1988).

We examined the drug combination, FSA, in both male and female animals to explore possible sex-de pendent changes in response to treatment. The findings are presented in details in the results section.

1.6 Post-Stroke Physical Rehabilitation

One of the criticisms of stroke work in animal studies is that they do not include physical rehabilitation, whereas human stroke patients undergo some form of rehabilitation. Choosing the right animal model of rehabilitation is important when interpreting results. We used Sprague-Dawley rats for the similarities to the neurovascular branching and the limb movements of the human arm (Yamori, Horie, Handa, Sato, & Fukase, 1976) and (Whishaw et al., 2002). One rehabilitative method that encourages the use of impaired limb while constraint the unaffected limb called constraint-induced movement therapy (CIMT). This technique was developed by Taub et al. (Taub, Uswatte,

Mark, & Morris, 2006). Studies showed that CIMT after stroke can improve functional reorganization and plasticity of the brain in the adult rats (Qu et al., 2015); and in stroke patients (Nijland, Kwakkel, Bakers, & van Wegen, 2011) and (Wittenberg et al., 2003). However, other studies showed that this technique of rehabilitation increases animal stress which decreases neurogenesis (Livingston-Thomas, Hume, Doucette, & Tasker, 2013) and (Yanagita, Amemiya, Suzuki, & Kita, 2007).

We are one of few laboratories that examined whether post-stroke voluntary rehabilitation could enhance functional recovery in the impaired limb. Other studies used enriched environments to improve cognitive and social stimulation and enhance post-stroke recovery following stroke (Biernaskie & Corbett, 2001) and (Janssen et al., 2010). Although these studies may contribute to our understanding of the mechanisms of neuroplasticity, the intensity of initiated rehabilitation might not be enough to produce the desired effect. We have tested the impact of physical rehabilitation at different intensities on recovery with and without drug treatment. The findings from our studies are interesting in that they mirror some observations about rehabilitation from human clinical trials when evaluating the intensity of physical rehabilitation, and show that our drug combination may work equally well without rehabilitation (see Results section on Physical Rehabilitation).

1.7 Functional Tests in Animal Studies

Measuring the level of impairment and the influence of post-stroke treatment on motor recovery in animal models relies heavily on the applied functional assessment methods. To improve the translation of experimental therapies into clinical trials,

appropriate methods of functional measurements should be used to assess what is in the real-life clinical setting (Macrae, 2011). Due to the range of deficits that accompany ischemic stroke, a diversity of sensitive functional tests is needed. The chosen tests should precisely reflect the extent of deficit after ischemic stroke, and demonstrate the level of recovery reached by treatment. Different functional tests have been used in stroke research to assess deficits associated with ischemic stroke in rodent models. Table 1 and 2 show animal behavioral tests with a strong or weak resemblance to functional tests in human (Schaar, Brenneman, & Savitz, 2010).

Table 1. Animal behavioral tests with a strong resemblance to human trials.

Functional Test	Function
Forelimb Asymmetry Test	Measures spontaneous forelimb use and placing deficits
Montoya Staircase Test	Assesses forelimb extension, grasping skills, side bias and independent use of forelimbs
Grid Walking	Measures sensorimotor function, motor coordination and placing deficits during locomotion
Reaching Chamber	Measures skilled forepaw use and motor functioning
Pasta Test	Evaluates manual dexterity and fine motor skills
Ladder Rung Walking test	Measures stepping, placing and coordination
Corner Test	Evaluates sensorimotor and postural asymmetries
Composite Scores	Evaluates a variety of motor, sensory, reflex and balance responses

Table 2. Animal behavioral tests with a less resemblance to human trials.

Functional Test	Function
Ledged Tapered Beam	Assesses hindlimb functioning
Accelerated Rotarod	Measures motor coordination and balance
Adhesive Removal	Assesses tactile responses and asymmetries
Morris Water Maze	Measures spatial learning and memory (humans use location cues to find places everyday but the test is not applicable to human)

1.8 Methods for Post-Stroke Assessment of Motor Function in Clinical Trials

To increase the odds of translation of results from pre-clinical animal studies to human clinical trials, only accurate and reliable behavioral tests that mimic functional tests in clinical trials should be performed. In clinical studies, there are different ways to measure motor function and independence in activities of daily living (ADLs). One of the major criticisms of pre-clinical stroke studies in animals is that the post-stroke functional tests bear no resemblance to standard functional tests given to human stroke patients. In the previous section, I have evaluated whether certain post-stroke functional tests bear any resemblance to clinical tests performed on post-stroke patients. In this section, I will give more detail about what the major stroke tests for humans entail.

1.8.1 Modified Rankin Scale (mRS)

The Modified Rankin Scale (mRS) is one of the most commonly used methods to measure recovery in human stroke patients (Rankin, 1957), (Bonita & Beaglehole, 1988). This test uses a questionnaire to assess patient functional status and the ability of the patient to perform everyday life tasks by asking simple questions to both patient and caregiver.

A free Modified Rankin Scale calculator called mRS-9Q is available online (Patel et al., 2012). One of the ADL tasks evaluated in the mRS pertains to the ability of the patient to grasp an object and move it. A parallel behavioral assessment in animals includes Montoya Staircase. In this assessment the ability of each animal to grasp and hold onto an object with either forepaw is quantified and analyzed in order to evaluate gross arm movement, hand clasping, and fine finger movement control.

Table 3. Modified Rankin Scale (mRS) (Rankin, 1957).

Score	Description
0	No symptoms at all
1	No significant disability despite symptoms; able to carry out all usual duties and activities
2	Slight disability; unable to carry out all previous activities, but able to look after own affairs without assistance
3	Moderate disability; requiring some help, but able to walk without assistance
4	Moderately severe disability; unable to walk without assistance and unable to attend to own bodily needs without assistance
5	Severe disability; bedridden, incontinent and requiring constant nursing care and attention
6	Dead
	TOTAL (0–6): ____

Another assessment criterion in the mRS is the balance and strength of affected arm, and the ability of the patient to use hands to support the entire body weight when getting into and out of a chair. This test aims to recognize abnormal function and determine whether patients are getting back to their normal function by doing the daily activities or not. We utilize Forelimb Asymmetry analysis to evaluate animal functional recovery based on the animal use of full palm to support their body weight when they rear up and explore the cylinder wall (See Methods section). In our modified Forelimb Asymmetry analysis,

we define forelimb function by the placement of the whole palm on the wall of the cylinder that indicates its use for body support. We do not count a half touch (fingertip touch) as a sign of getting back to normal function but as an indicator of injury.

1.8.2 Fugl-Meyer Assessment (FMA)

The Fugl-Meyer scale is used to evaluate and measure motor recovery in post-stroke hemiplegic patients (Fugl-Meyer, Jaasko, Leyman, Olsson, & Steglind, 1975). It has been widely used in stroke patients. The test is designed to assess impairment in motor functioning, sensation, balance, joint range of motion and joint pain (See Appendix I for full protocol). Each is scored on a 3-point ordinal scale, in which 0 = cannot perform; 1 = performs partially and 2 = performs fully. The motor score ranges from 0 to 100 points, which indicate hemiplegia or normal motor performance, respectively. Out of 100 points, 66 points are for the upper extremity. This includes forearm supination/pronation, wrist flexion/extension, and tennis ball grasping, grasping of a cylinder and finger flexion (Duncan et al., 1994).

Table 4. Standard methods for post-stroke assessment of motor function and global disability. Information obtained from "Post-Stroke Rehabilitation: Assessment, Referral, and Patient Management Quick Reference Guide" by the US Agency for Health Care Policy and Research.

Assessment scale	Approximate time to administer	Strengths	Weaknesses
Modified Rankin Scale (mRS) for global disability	5 minutes	Overall assessment of disability.	Walking is the only explicit assessment criterion. Low sensitivity.
Fugl-Meyer Assessment (FMA) (Fugl-Meyer et al., 1975)	30-40 minutes	Excellent validity and reliability for assessing sensorimotor function and balance.	Very complex test and time-consuming

Depending on the severity of the stroke and its location, both dexterity and coordination might be impaired on the contralateral side, and sometimes on the ipsilateral side if the deficit is bilateral. Upper limb reaching, grasping and withdrawing are natural movement skills organized by the cerebral motor cortex. Many neurons interact with spinal circuits to regulate these locomotor movements. Brain damage to the motor cortex often impairs the contralateral arm and can affect these movements.

An experiment by Whishaw et al. (See Figure 2) evaluated rat forelimb reaching using a comparative scale to that used to evaluate human performance (Whishaw, Whishaw, & Gorny, 2008). Each forelimb reach was divided into ten movements that were rated on a 3-point scale. Damage to the motor cortex, basal ganglia, brainstem, and spinal cord alters these movements (Leisman, Braun-Benjamin, & Melillo, 2014). Disruption of corticospinal connections leads to impairment of skilled finger, hand and arm movements. One common post-stroke motor deficit is impairment in fine motor movement and extension of the fingers (Trombly, Radomski, Trexel, & Burnet-Smith, 2002), however, the mechanisms of this weakening are not well understood. A comparative analysis that was performed on 21 species, including rats, indicates a similar role of the corticospinal tract in the evolution of digital dexterity among all examined species (Heffner & Masterton, 1983). Therefore, rehabilitation that improves fine motor control and digit strength would greatly enhance the lives of stroke patients. Here we examine rat forearm extension/reach, (Montoya Staircase using advance, pronation, and grasping; and Forelimb Asymmetry using touching and stabilizing) in order to evaluate the potential benefit of drug therapy or rehabilitation on forearm and digit movements post-stroke.

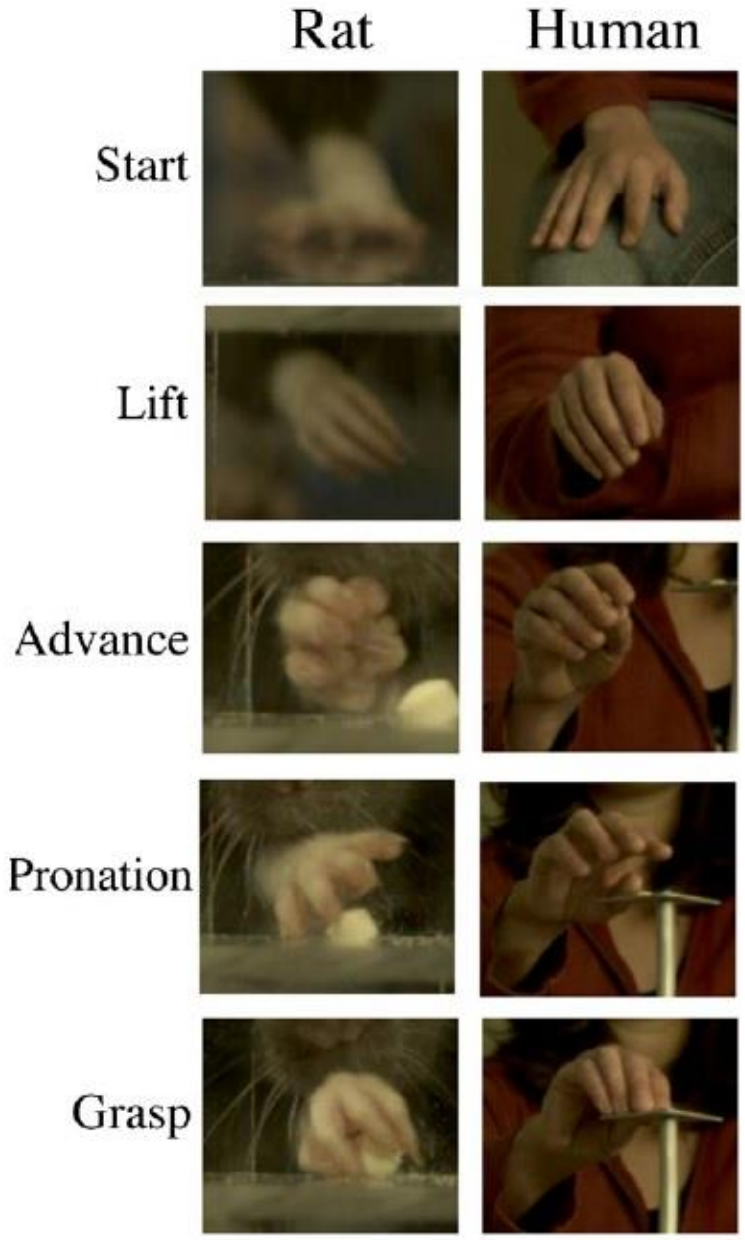

Figure 2. Similarities of hand shaping movements and position of the digits and wrist in rat and human subjects during a reaching movement. Adapted from (Sacrey, Alaverdashvili, & Whishaw, 2009).

1.9 Neurogenesis after Stroke

In order to develop an effective treatment for stroke, the acute and chronic events that are involved in ischemic stroke, as well as the associated mechanisms, must be clearly understood (Hossmann, 2006). One of the devastating effects of stroke is the loss of the neuronal circuitries, which support cognitive and sensory-motor capacities, due to neuronal cell death and dysfunction. This could lead to severe disabilities. During the first 3-6 months following a stroke, patients might be able to regain some neurological abilities, but a majority of patients stay impaired to a critical degree (Duncan, Jorgensen, & Wade, 2000). It is now known that when an individual experiences a stroke, the brain sends signals to stem cell populations to divide and to move immature neurons to areas of damage in a process of neurogenesis. This process is most active during embryonic development. It was believed that adult brain is a physiologically static organ incapable of regeneration; however, neurogenesis has been shown to continue in two locations in the adult brain: the subventricular zone (SVZ) of the lateral ventricles, and the subgranular zone (SGZ), forming part of the dentate gyrus (DG) of the hippocampus (Barlow & Targum, 2007). A resident population of neural stem/progenitor cells can provide a source of new neurons (Elder, De Gasperi, & Gama Sosa, 2006).

After ischemic insult, recruitment of neural precursor cells from the major stem cell niches within the subventricular zone (SVZ) and the subgranular zone (SGZ) of the dentate gyrus into the damaged area are imperative compensatory responses in ischemic brain (Arvidsson, Collin, Kirik, Kokaia, & Lindvall, 2002). Neuronal proliferation within the subventricular zone has been shown to peak between 7 and ten days followed by a decline in proliferation activity during three weeks post-stroke (Parent, Vexler, Gong, Derugin, &

Ferriero, 2002). However, this therapeutic response is insufficient to support a full recovery after stroke due to the limited survival of newly formed neuroblasts that migrate to the damaged area.

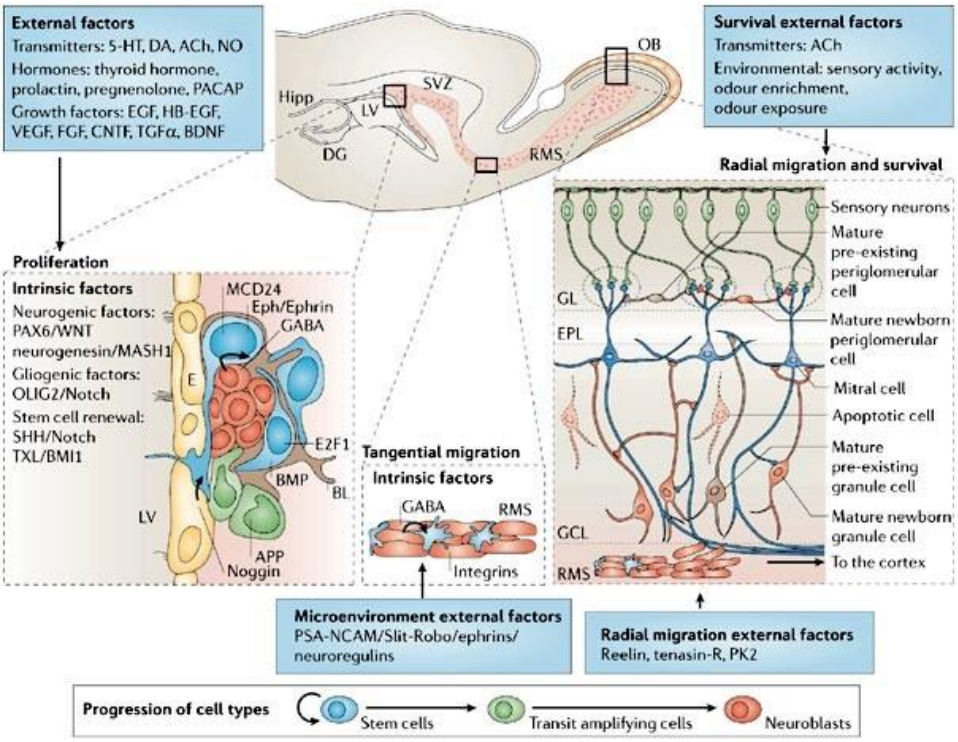

Figure 3: Intrinsic programs and external factors controlling adult neurogenesis. Adapted from (Lledo, Alonso, & Grubb, 2006).

Stroke incidence triggers neurogenesis by stimulating neural progenitor cells of the SVZ to divide and migrate to the peri-infarct area (Arvidsson et al., 2002). It is possible that radial microglia are involved with guiding migration of neuroblasts to the ischemic brain tissue (Cao et al., 2013). There is evidence that neurogenesis is linked to angiogenesis (Ohab & Carmichael, 2008), which is a process of forming new blood vessels to enhance vascularization of the surviving neuronal cells (Greenberg & Jin, 2005). For up to four

months of brain damage, neuroblasts are continuously produced in neurogenic areas including the subventricular zone (SVZ) leading to a pool of cells that can develop into fully grown neurons (Thored et al., 2007). On the other hand, neurogenesis is inhibited by inflammation that occurs during stroke recovery (Jakubs et al., 2006). Neuronal, glial, and endothelial progenitor cells release growth factors that support synaptic plasticity of surviving neurons (J. Chen et al., 2005).

1.10 Drugs Used for our Studies

In an attempt to boost the recovery of ischemic brain, we tested a combination therapy of two FDA-approved drugs as a potential delayed post-stroke treatment. These include simvastatin (Zocor) and fluoxetine (Prozac), in addition to L-ascorbic acid (Vitamin C). The drug combination showed an increase in anterior subventricular neurogenesis and neurotrophic factors in both male and female animal models of ischemic stroke, as well as enhanced neuronal survival and plasticity (A. M. Corbett et al., 2015). Some studies examining fluoxetine's effect on neurogenesis employed a synthetic nucleoside, bromodeoxyuridine (BrdU), to determine whether the brain is undergoing neurogenesis (Malberg, Eisch, Nestler, & Duman, 2000). These studies, however, are only evaluating the posterior sub-ventricular zone in the same slices as those of the dentate gyrus. The fact that this area is more caudally located than the previously examined area may explain why these studies did not highlight any effect of fluoxetine on neurogenesis. Fluoxetine is widely prescribed to treat depression and other mood disorders by blocking the presynaptic reuptake of serotonin. Simvastatin is a cholesterol-lowering drug that belongs to a group of drugs called HMG CoA reductase inhibitors. Vitamin C (L-ascorbic

acid) is an anti-oxidant that is added to the mixture to enhance the effect of the antidepressant and because of the serotonin sensitivity to oxidation. Statins have been shown to up-regulate the brain-derived neurotrophic factor (BDNF), which is a member of neurotrophic factors that mostly participate in nervous system development. The mechanism by which statins influence the BDNF up-regulation is mediated by an endothelial nitric-oxide synthase (eNOS) enzyme. Vitamin C enhances the catalytic activity of this enzyme through an unclear mechanism(s) (Huang, Vita, Venema, & Keaney, 2000). Each drug was chosen to contribute unique mechanisms when combined in the mixture to improve outcomes. Neurogenesis and BDNF are believed to be involved in the recovery of function following stroke.

The initial experiments on this drug combination were conducted on Westar male sham stroke rats that received different combinations of fluoxetine, simvastatin, and L-ascorbic acid to assess the impact of drug combination on neurogenesis versus controls. A mix of the three drugs significantly increased neurogenesis nineteen times compared to either the control or simvastatin and ascorbic acid. Fluoxetine alone producing a 10-fold increase in neurogenesis, approximately half of that seen with the drug combination (A. M. Corbett et al., 2015). A combination of low dose (0.5 mg/kg) simvastatin and 20 mg/kg L-ascorbic acid treatment showed no increase in neurogenesis over controls. However, when both were added to 5 mg/kg fluoxetine, neurogenesis nearly doubled over that when using fluoxetine alone in male sham-operated rats. The combination of drugs produced a synergistic effect rather than additive. Both simvastatin and fluoxetine are FDA-approved drugs that have been around for many years, so there is ample information on the pharmacokinetics, metabolites, and elimination of each.

Evaluation of the fluoxetine, simvastatin, and ascorbic acid compared to fluoxetine and ascorbic acid tested in functional recovery of female Long Evans rats post-stroke suggested that simvastatin and fluoxetine are both crucial to the most effective drug combination, though currently, it is not clear whether the L-ascorbic acid is essential in female rats. In these experiments, combining fluoxetine with L-ascorbic acid showed no increased functional recovery over fluoxetine alone in female rats after stroke induction. Whereas the addition of both simvastatin and L-ascorbic acid to fluoxetine showed approximately 2-fold increase over fluoxetine alone in functional recovery, which paralleled nicely the increase in neurogenesis that we observed in the subventricular zone. Taken together, this suggests that both fluoxetine and simvastatin are the key players to increasing neurogenesis and functional recovery over fluoxetine alone. Studies that have used rats to evaluate BDNF production after ischemic stroke have shown BDNF expression to rise for a limited time (eight days after a stroke) (Kokaia, Andsberg, Yan, & Lindvall, 1998), (Bejot et al., 2011). However, our delayed drug treatment (fluoxetine in addition to L-ascorbic acid) increased BDNF expression near the peri-infarct area 31 days after stroke.

1.10.1 Fluoxetine

Racemic fluoxetine (*N*-methyl-3-phenyl-3-[4- (trifluoromethyl) phenoxy]propan-1-amine), also known by trade name Prozac, is a selective serotonin reuptake inhibitor (SSRI) that was approved by the FDA for use in clinical practice since 2000. It is used to treat major depression and other mood disorders such as panic disorder, obsessive–compulsive disorder (OCD) and bulimia nervosa. Fluoxetine crosses the blood–brain barrier (Warren, 2012), and studies showed fluoxetine to increase the expression of BDNF,

which plays a role in neurogenesis (Schabitz et al., 2007) and enhances cognition in patients with vascular dementia (X. Liu et al., 2013).

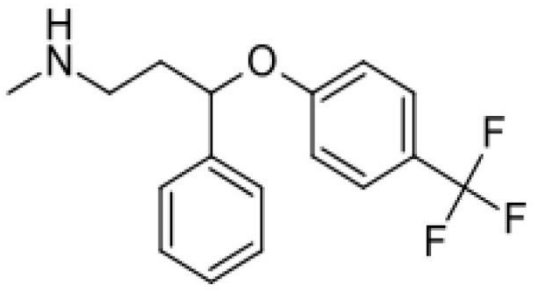

Figure 4. Chemical structure of fluoxetine

1.10.2 Pharmacokinetics of Fluoxetine

Fluoxetine binds with high affinity to plasma proteins such as albumin and α1-glycoprotein, and is metabolized in the liver by isoenzymes of the cytochrome P450 system (CYP2D6) to its active metabolite norfluoxetine (Alfaro, Lam, Simpson, & Ereshefsky, 2000). Plasma concentrations of fluoxetine and its metabolite, norfluoxetine, peak in 6 to 8 hours after oral administration. Using high-performance liquid chromatography (HPLC) method, we were able to detect fluoxetine and norfluoxetine in brain homogenate after seven days of single dose oral administration (A. Corbett, McGowin, Sieber, Flannery, & Sibbitt, 2012). Pharmacokinetic studies in rats show that distribution of the drug into tissues is similar to that in humans with faster elimination time in rats (4-7 hrs) (Benfield, Heel, & Lewis, 1986). In our study, the plasma levels of fluoxetine and norfluoxetine were detectable within 2 to 4 hours of ingestion, but not after 24 hours.

The elimination rate of fluoxetine and norfluoxetine in human is slow compared to other antidepressants due to the ability of drugs to inhibit their metabolism mediator (CYP2D6). Thus elimination half-life ranges from 1-3 days, after a single dose, to 4-6 days, after long-term use (Ouellet et al., 1998). The brain to plasma ratio of fluoxetine in patients is 2.6:1 (Strauss, Layton, Hayes, & Dager, 1997) .

Numerous experimental studies have raised as many questions as they provide answers about the efficiency of fluoxetine in treating post-stroke deficits. Some of these studies showed SSRIs (fluoxetine in particular) as an active agent in producing functional recovery after focal brain injury in rat models (Windle & Corbett, 2005). Few pre-clinical studies showed fluoxetine effectiveness on infarct size and demonstrated a potent neuroprotective action of the drug through its anti-inflammatory action on microglia (Lim et al., 2009). Moreover, fluoxetine has been shown to improve ischemia-induced spatial cognitive deficits in rats through increasing hippocampal neurogenesis after stroke (W. L. Li et al., 2009).

Although many previous studies provided convincing evidence that selective serotonin reuptake inhibitors (SRRIs) are useful in the recovery process in animal models of stroke, the drug can have varying effects on neurogenesis and overall recovery based on animal age and sex. Moreover, the timing of drug administration is a paramount factor; an appropriate therapeutic time window should be established in animal models. Also, the method of drug administration has a significant influence on the outcome, as stress would antagonize the effects of fluoxetine on the brain (Balch et al., 2015).

The FLAME clinical trial (Fluoxetine in Motor Recovery of Patients with Acute Ischemic Stroke), which was published in 2011 in THE LANCET neuro has shown that

the anti-depressant fluoxetine could help repair the damage caused by stroke and improve functional motor recovery in patients. The study was conducted in ischemic stroke patients with hemiparesis at nine stroke centers in France. A total of 113 stroke patients from different stroke centers across France were enrolled in the trial and randomized to fluoxetine (N = 57) or placebo (N= 56) groups for 90 days. Fluoxetine (Prozac) 20 mg/day or placebo was delivered for three months starting five to ten days after stroke onset. Following the FLAME trial, most of the stroke studies that examined SSRIs' effects on motor recovery have been conducted using fluoxetine more than other SSRIs, such as citalopram, sertraline, paroxetine, and escitalopram (Mead et al., 2013).

In this trial, the primary outcome was mean change in the Fugl-Meyer Motor Scale (FMMS) between baseline (day 0) and day 90. Secondary endpoints were assessed by the NIH Stroke Scale (NIHSS) and modified Rankin Scale (mRS). All patients included in this study were aged 18-85 years. The mean age of patients was 66.4 years in the fluoxetine group and 62.9 years in the placebo group. The study reported that at three months, 15 (26%) of acute stroke patients who received fluoxetine and 5 (9%) of patients allocated to placebo had a modified Rankin score (mRS) between 0 and 2, which means they can perform daily activities with no dependency on other people.

Some ongoing large-scale trials have continued to examine the effectiveness of fluoxetine when given 2-15 days following stroke onset. These include the AFFINITY (Assessment of Fluoxetine in stroke recovery) trial in Australia, the FOCUS (Fluoxetine or control under supervision) trial in the United Kingdom, and the EFFECTS (Efficacy of Fluoxetine – a randomized controlled trial in stroke) in Sweden (Mead et al., 2013).

The promising results of the FLAME clinical trial provided clear evidence of the role of fluoxetine in stroke recovery independently of depression when given to ischemic stroke patients. However, the mechanisms involved in recovery from stroke or dementia are not entirely understood (Dam et al., 1996).

Fluoxetine has neuroprotective properties that may be associated with its anti-inflammatory effects (D. Liu et al., 2011). A recently published study suggested a neuroprotective role of fluoxetine in ischemic stroke through changing inflammatory activated microglia into a neuroprotective activated microglia in a process called microglia polarization (Su, Yi, Xu, & Zhang, 2015). The study was conducted in *vitro* on both primary microglia cells and murine microglial cell line (BV-2) and demonstrated that fluoxetine significantly down-regulates the gene expression and protein production of pro-inflammatory mediators (M1 activation indexes) while up-regulating the M2 activation indexes (neurotrophins, Stat 3, Stat 6, arginase expression) in both cell line and primary cells. Nonetheless, *in vitro* studies do not necessarily correlate with *in vivo* efficacy. A study in a rat cerebral ischemia model of middle cerebral artery occlusion indicated an anti-inflammatory role of fluoxetine through suppression of microglial activation and neutrophil infiltration (Lim et al., 2009). To assess these findings, we developed our customized PCR arrays (Custom RT^2 PCR Array from Qiagen) with 38 genes of interest that have been shown to be differentially expressed in inflammation in response to activation of different types of microglia. Most pharmacological studies have been conducted using a racemic form of fluoxetine, however, increasing evidence indicates that the enantiomers of racemic drugs often differ markedly in their pharmacodynamic and kinetic properties (Williams & Lee, 1985). We tested the anti-inflammatory effects of

racemic fluoxetine and compared the effects of its enantiomers (R (-)-fluoxetine and S (+)-fluoxetine) on microglia activation using the RT^2 PCR Array technique to profile microglia markers in both female and male Sprague-Dawley rats.

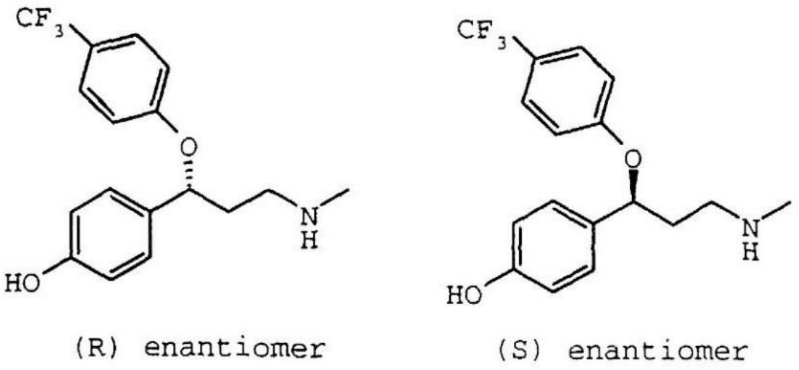

Figure 5. The (R)-enantiomer and the (S)-enantiomer of fluoxetine

In addition to its beneficial effect on neurogenesis, fluoxetine also influences angiogenesis by stimulating expression of vascular endothelial growth factor (VEGF), one of the main neurotrophic factors that mediate angiogenesis as well as neurogenesis and neuroprotection following ischemic stroke. This upregulation suggests a broad role of fluoxetine in brain recovery after stroke (Gaillard & Mir, 2011). Preclinical findings in aged mice also showed that fluoxetine induces a rise in serum concentrations of VEGF (Kubera et al., 2009). We tested the effect of fluoxetine on neurotrophins, its receptors, and synaptic plasticity genes.

1.10.3 Simvastatin

Simvastatin (also known by trade name Zocor) is a cholesterol-lowering medication that belongs to the class of drugs known as statins. Simvastatin is used mainly to treat dyslipidemia and prevent stroke and heart attacks in high-risk individuals. It has beneficial effects on coronary diseases (Alberts, 1990), and usually is used to reduce the risk of cardiovascular morbidity and mortality ("Randomised trial of cholesterol lowering in 4444 patients with coronary heart disease: the Scandinavian Simvastatin Survival Study (4S)," 1994).

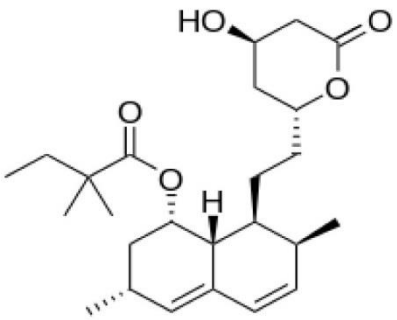

Figure 6. Chemical structure of simvastatin

1.10.4 Pharmacokinetics of Simvastatin

After an oral dose, simvastatin is quickly absorbed and metabolized from its inactive lactone prodrug form into pharmacologically active metabolite (simvastatin β-hydroxy acid), which acts by inhibiting the enzyme 3-hydroxy-3-methylglutaryl-coenzyme-A (HMG-CoA) reductase (Gotto, 1997). The HMG-CoA is a rate-limiting enzyme of the metabolic pathway responsible for the biosynthesis of cholesterol (Pedersen,

2010). Simvastatin undergoes extensive first-pass metabolism in the liver. The drug can cross blood-brain-barrier. The bioavailability of simvastatin after oral administration is 5% (about 95% is excreted), with peak plasma concentrations reached at 4 hours.

Simvastatin is known to enhance endothelial function, inhibit a thrombogenic response and reduce oxidative stress and inflammation (Liao & Laufs, 2005). Also, statins have been shown to provide neuroprotection against ischemic injury. The mechanisms by which statins provide neuroprotection are not clearly understood. However, some studies suggest statin action through upregulating of endogenous tissue plasminogen activator (Asahi et al., 2005), and restoring endothelial nitric oxide synthase (eNOS) activity during hypoxia. This enzyme generates nitric oxide in blood vessels that is involved with regulating vascular function and neurogenesis (Estrada & Murillo-Carretero, 2005; Hernandez-Perera et al., 1998; Laufs, Fata, & Liao, 1997). Others proposed a beneficial role of statins through inhibiting inflammatory response and platelet aggregation (Sanchez et al., 2008). Statins have also been shown to stimulate neurogenesis and angiogenesis, and to promote new synapses formation (Rodriguez-Yanez, Agulla, Rodriguez-Gonzalez, Sobrino, & Castillo, 2008).

Statin treatment has been shown to reduce the incidence of ischemic stroke among people who are at high risk of cardiovascular diseases, and therefore it is recommended for use in stroke patients to prevent recurrent stroke (Tuttolomondo et al., 2013). In addition to their role in ischemic stroke, statins promote neurovascular recovery after hemorrhagic stroke (Yang, Han, Zhang, Chopp, & Seyfried, 2012).

Due to its lipophilic nature (Thelen et al., 2006), simvastatin can readily cross the blood-brain barrier and passively diffuse across the endothelial cells allowing more

widespread tissue distribution (Wood, Eckert, Igbavboa, & Muller, 2010). Moreover, studies have found that simvastatin upregulates growth factors such as brain-derived neurotrophic factor (BDNF) and Vascular endothelial growth factor (VEGF), which are important in promoting neurogenesis and angiogenesis (Yang et al., 2012), (Wu et al., 2008). Simvastatin also reduces the infarct volume after ischemic stroke (Zacco et al., 2003) and has the potential to protect against neuronal excitotoxicity caused by overstimulation of glutamate receptors during an ischemic injury (Zhu et al., 2012). Recent rodent studies suggest a beneficial role of statins when combined with tPA in extending the therapeutic window for tPA as the combination drug improved thrombolysis of clot at the MCA occlusion site (L. Zhang, Zhang, & Chopp, 2012). Information from pooled data of stroke patients showed the effect of dose-related simvastatin/tPA combination on the outcome after tPA thrombolysis for ischemic stroke. The study noticed an association between the dosage of simvastatin (20mg, 40mg, and 80mg) and increased risk of intracerebral hemorrhagic transformation (2%, 6% and 13%, respectively) (Scheitz et al., 2014). Optimizing the dose of statins when combined with tPA is crucial to extend the therapeutic window for tPA (Lapchak & Han, 2010). So far there is only one trial that investigated the effect of pre-treatment with statins on brain injury in cerebral ischemia and showed a beneficial effect of statin on reducing brain injury after stroke (Blanco et al., 2007). The study also looked at the influence of statin withdrawal on the outcome of acute ischemic stroke patients and recommended that statin should be continued in the acute phase of ischemic stroke because the withdrawal was associated with increased risk of death or dependency at 90 days due to the reoccurrence of stroke.

1.10.5 Ascorbic Acid (Vitamin C)

Vitamin C or L-ascorbic acid is a potent reducing agent and effective antioxidant that protects against the potential damage caused by free radicals to lipid membrane and DNA during cell injury.

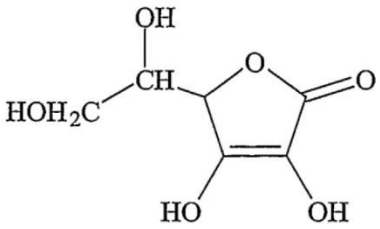

Figure 7. Chemical structure of ascorbic acid (Vitamin C)

Vitamin C can cross the blood–brain barrier in the oxidized form. This passage is mediated by BBB glucose transporters (Agus et al., 1997). A study of tissue distribution of vitamin C that calculated the concentration of radiolabeled ascorbic acid in mice showed up to 3 fold increase of ascorbic acid in the brain compared to the blood concentration (Hornig, 1975). Multiple studies have demonstrated that consumption of vitamin C rich food can lower the risk of stroke (G. C. Chen, Lu, Pang, & Liu, 2013). However, the findings are still inconclusive and need further investigation to understand the different effects of dietary vitamin C and circulating vitamin C on the risk of stroke (Rabadi & Kristal, 2007). As vitamin C is water soluble and tends to be quickly absorbed and excreted from the body, it might be beneficial to use the slow-release (extended) formulation of vitamin C rather than the plain-release form. As one study indicates that there are pharmacokinetic differences between plain and slow release formulations of ascorbic acid (Viscovich, Lykkesfeldt, & Poulsen, 2004).

Table 5. Dosing of the Pharmacologic Agents

Drug	Typical Human Adult Dose	Our Experimental Rat Dose	Human equivalent
Fluoxetine	20 mg/day	5 mg/kg	40 mg/day
Simvastatin	10-20 mg/day	1 mg/kg	8 mg/day
Vitamin C	500 mg/day	20 mg/kg	160 mg/day

1.11 Drug Delivery Method in Animal Studies

The most common routes of drug administration in laboratory animals are using oral delivery through forced feeding tube passed into the stomach (gavage), subcutaneous, intraperitoneal or intravenous injection. All of these methods of drug delivery are highly stressful for animals, as they involve some restraint, which is a major stressor for rodents. Distress due to physical restriction and morbidity are some of the common adverse reactions associated with these procedures, and they can negatively influence the outcome. Because stress can adversely affect neurogenesis (Sahay & Hen, 2007), and many physiological processes such as glucose metabolism, body temperature and cerebral blood flow (Meijer, Spruijt, van Zutphen, & Baumans, 2006), it is crucial to minimize the unnecessary stress during drug delivery by using a reliable method of voluntary drug administration. A study on rats that underwent gavage procedure indicates that a 32% mortality rate was attributable to granulomatous inflammation or asphyxia caused by impacted food and bedding material in the oropharynx (Germann & Ockert, 1994). Our laboratory sought to eliminate these unwanted effects by developing a technique for voluntary oral drug administration to rats using premixed drug-cookie dough balls (A. Corbett et al., 2012). In our method, we incorporate the drug combination in a powder form

with 4 gram of sugar cookie dough and present it to the animal in a glass dish at the same time every day. This method allows for more drug delivery to the bloodstream than the gavage method due to drug absorption through lingual and buccal membranes. The voluntary oral ingestion of a drug resulted in reduced level of the stress hormone (corticosterone) in male rats when compared to a subcutaneous injection of the same drug (Goldkuhl, Carlsson, Hau, & Abelson, 2008).

1.12 Possible Drug Mechanism of Action

To understand the mechanisms by which the drug combination (FSA) works to induce motor function, I consider potential pathways that might be involved in drug action. These include:

1.12.1 Modulation of the Blood-Brain-Barrier Permeability

The Blood-brain-barrier (BBB) consists of a network of elements consisting of brain endothelial cells connected by tight junctions, a basement membrane, pericytes and astrocyte feet forming an interface between the brain and circulatory system (Hawkins, O'Kane, Simpson, & Vina, 2006). The blood-brain-barrier has a high selective permeability that separates the circulating blood from the brain extracellular fluid and allows the passage of molecules that are essential to neural function while it protects the brain from exposure to harmful molecules. After ischemic insult to the brain, impairment of the blood-brain-barrier integrity is a central event of the pathophysiology, in which the ischemic structural damage causes abnormal leaks across the blood-brain-barrier (del Zoppo & Hallenbeck, 2000). Also, endothelial cells of the BBB upregulate the expression of matrix

metalloproteases (MMPs) activation, which is a family of enzymes responsible for degrading the extracellular matrix proteins, and protease-activated receptor 1 (PAR1) in the ischemic area (Rosell & Lo, 2008). The pericytes are also involved in microvascular dysfunction after stroke through constricting the obstructed vessel (Yemisci et al., 2009). Furthermore, stroke downregulates the expression of a cell surface molecule, beta-1 integrin, which is essential for endothelial cell adhesion and migration during angiogenesis resulting in increased BBB permeability (del Zoppo & Milner, 2006).

A recent study indicates that fluoxetine suppresses matrix metalloproteases (MMPs) activation in adult male mice after spinal cord injury (J. Y. Lee, Kim, Choi, Oh, & Yune, 2012). This inhibitory action prevents disruption of blood-brain-barrier after spinal cord injury.

To investigate the effect of fluoxetine and its enantiomers (R (-)-fluoxetine and S (+)-fluoxetine) on blood-brain barrier, we used a method for determining BBB integrity based on intracardiac perfusion of an Evans Blue (EB) dye. Brain tissue homogenates from the cerebral cortex and the cerebellum were examined in each male and female rat to measure the amount of fluorescence that indicates the EB concentration. We noticed a significant difference in the BBB permeability in both cortex and cerebellum when both male and female rats treated with S-fluoxetine were compared to male rats treated with R-fluoxetine. Animals that received S-fluoxetine enantiomer treatment showed less BBB permeability than the ones treated with R-fluoxetine. However, the change was not significant among the female R- fluoxetine and S-fluoxetine groups when compared to each other. One possible explanation of this action is that S-fluoxetine is more efficient in inhibiting the breakdown of the tight junctions that connect endothelial cells of the BBB.

1.12.2 Upregulation of Neurotrophins or their Receptors

Some of the potential targets of ischemic stroke treatments are growth factors, particularly those that have been shown to get involved in promoting neural regeneration and angiogenesis, as well as inhibiting the neurotoxicity and inflammatory process within ischemic penumbra. Neurotrophins are a family of growth factors that prevent neuronal damage and promote neuronal survival and repair (Y. Zhang, Zhang, Katiella, & Huang, 2014). Administration of neurotrophins in experimental animals have shown to correlate with functional motor recovery after stroke. The potential benefit to human health that would come from a better understanding of the regulation of neurotrophins and their receptors after stroke cannot be overstated.

Studies have demonstrated that brain is not a static organ, and damage to the adult brain can induce the formation of new neurons, in a process of neurogenesis that continues throughout life (Eriksson et al., 1998). This injury-induced neurogenesis is augmented by different types of growth factors that eventually lead to efficient brain repair and recovery of function. In the first stages of ischemia, regenerative mechanisms in the brain are activated in the first few hours (Rickhag et al., 2006), followed by reduced tissue edema, some repair of injured neurons, activation of neuronal pathways and migration of neuroblasts and glial cells into the area around infarct, known as the penumbra (Marlier, Verteneuil, Vandenbosch, & Malgrange, 2015). The process is accompanied by angiogenesis in the peri-infarct zone. In surviving tissue, activation of both growth promoting and inhibiting factors occurs, but full recovery is limited due to the limited capacity for the anatomical reorganization of the brain (Carmichael, 2005). Reactivation of existing neural pathways after stroke insult seems to be one of the cellular responses

involved in functional recovery. Other strategies include combining of new neural pathways following neurogenesis (Wieloch & Nikolich, 2006). Over the past several years, many experimental studies aimed at stimulating functional recovery during the first weeks after stroke have proposed different therapeutic strategies. The plans include activating brain plasticity, changing the housing environment to an enriched environment as well as adding training and physical rehabilitation (Biernaskie & Corbett, 2001). Animal studies reported that post-ischemic administration of growth factors such as vascular endothelial growth factor (VEGF) (Z. G. Zhang et al., 2000), brain-derived neurotrophic factor (BDNF) (Schabitz et al., 2004) , epidermal growth factor (EGF) (Teramoto, Qiu, Plumier, & Moskowitz, 2003), Heparin-binding epidermal growth factor-like growth factor (HB-EGF) (Jin et al., 2004), nerve growth factor (NGF) (Dahlqvist et al., 1999), Insulin-like growth factor-1 (IGF-1) (X. F. Liu, Fawcett, Thorne, DeFor, & Frey, 2001; X. F. Liu, Fawcett, Thorne, & Frey, 2001), erythropoietin (EPO) (Leist et al., 2004), stem cell factor (SCF) (Schneider et al., 2005) and granulocyte colony-stimulating factor (GCSF) (Kawada et al., 2006) can stimulate angiogenesis, promote neurogenesis, reduce infarct volume and improve recovery in animal models of ischemic stroke. Some studies showed that improved environment can upregulate growth factors such as nerve growth factor (NGF) and enhance recovery (Dahlqvist et al., 1999), others focused on the role of some growth factors in promoting recovery of function. For example; blockade of basic fibroblast growth factor (bFGF) in ischemic rats reduces motor recovery (Rowntree & Kolb, 1997). Based on their role in angiogenesis and neurogenesis, we proposed neuroprotective properties of neurotrophins in improving the recovery after ischemic injury.

1.12.3 Orexin Receptor Upregulation

Orexin is a neuropeptide regulator of appetite, sleep and glucose metabolism. There are two types of orexins known as orexin-A and orexin-B, also called hypocretin-1 (HCRT-1) and hypocretin-2 (HCRT-2) (Sakurai et al., 1998). Orexins mediate their action through activating two G-protein-coupled receptors, orexin receptor 1 (OXR1) and orexin receptor 2 (OXR2), that are expressed in the brain (Trivedi, Yu, MacNeil, Van der Ploeg, & Guan, 1998). The activation of orexin receptors excites orexin neurons and promotes the release of presynaptic glutamate (Yamanaka, Tabuchi, Tsunematsu, Fukazawa, & Tominaga, 2010). Orexin is associated with neuronal cell apoptosis and autoimmune function (de Lecea et al., 1998). Some animal studies have recently shown that orexin-A exerts neuroprotective effects by increasing the Hypoxia-inducible factor-1 activity and reducing the oxidative stress in rats (Yuan et al., 2011). Orexin also plays a major role in modulating the inflammatory response in ischemic brain injury (Song, Kim, Kim, Song, & Lee, 2015), a study showed that orexin controls inflammation by regulating pro-inflammatory cytokines such as the IL-6 and TNF-α in microglia and protecting the neurons against oxidative stress caused by cerebral ischemia (Xiong et al., 2013). Also, two separate studies in rats (Kitamura et al., 2010) and mice (Harada, Fujita-Hamabe, & Tokuyama, 2011) indicated that intracerebroventricular injection of orexin-A into the animal brain before stroke surgery reduced infarct size. Furthermore, studies reveal that orexins play a positive role in stimulating hippocampal neurogenesis (Kim et al., 2010), and increasing the expression of brain-derived neurotrophic factor (BDNF) and neurotrophin-3 (NT-3) in cortical neuron cultures (Yamada et al., 2009), which is a primary mechanism for neuroprotection.

1.12.4 Changes in Microglial Activation

Besides the neuronal loss and cognitive dysfunction after stroke, inflammation of the central nervous system is one of the pathological processes resulting from ischemic stroke. Microglia, the resident macrophage of the CNS and the primary immune cells that contribute to neuroinflammation, is an integral component of the inflammatory immune response in the brain. There has been much debate regarding the precise origin of microglial progenitors. Studies suggest that microglia arise from peripheral mesodermal tissue in the yolk sac. Like macrophages, activation of microglia leads to multiple activities including antigen presentation, phagocytosis, cytokine production and the release of matrix metalloproteinases that deteriorate the blood brain barrier and cause peripheral leukocyte infiltration (Iadecola & Anrather, 2011). Stimulation of microglia with various signals can drive a range of different inflammatory or anti-inflammatory responses in a process called microglia polarization as shown in Figure 8.

Emerging evidence indicates that microglia polarization is involved in many types of central nervous system injuries including stroke (Hu et al., 2012). Activated microglia can be polarized into two main opposing phenotypes: cytotoxic pro-inflammatory phenotype M1, and neuroprotective, anti-inflammatory phenotype M2; which can be further subdivided into M2a, M2b, and M2c (Mantovani et al., 2004). Targeting the polarization mechanism to drive microglia from detrimental phenotype to beneficial phenotype could help in protecting brain tissue from further damage and resolve inflammation. Although immunosuppression might be an effective strategy in counteracting the inflammatory response to ischemic injury, a complete inhibition of the

inflammatory process without an increase in neurotrophic factors may worsen the outcome resulting in compromising repair mechanisms.

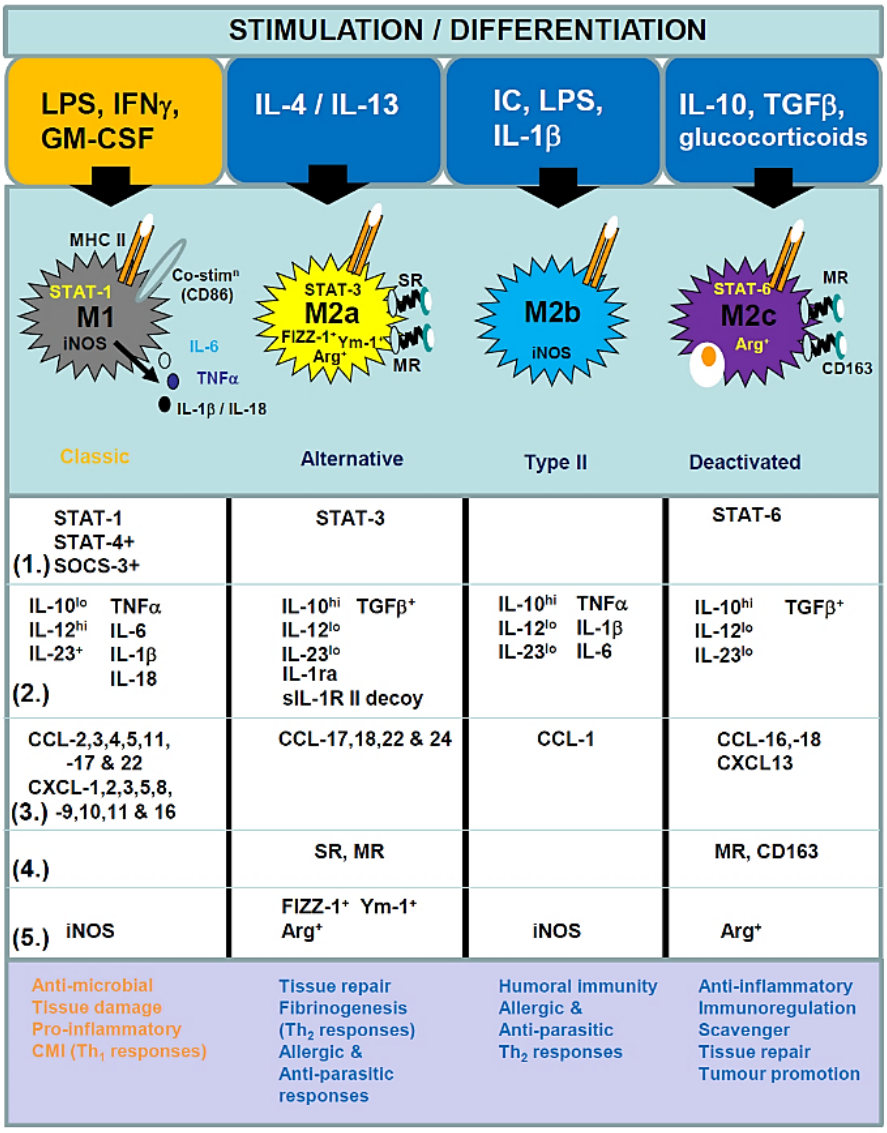

Figure 8. Microglia polarization into a range of functional phenotypes: pro-inflammatory M1 and anti-inflammatory M2 phenotypes. M2 microglia has three subsets; M2a, M2b, and M2c based on stimulating pathway (upper panel). Molecular markers of all phenotypes are categorized in the table as follow: (1.) signaling molecules, (2.) cytokines, (3.) chemokines, (4.) scavenger receptor expression and (5.) tryptophan metabolism effector molecules (AD, 2012).

1.13 Hypotheses

Three hypotheses were proposed:

1) That earlier delivery of the combination drug would result in smaller infarct size, and a closer examination of the wall touches in Forelimb Asymmetry test may allow us to refine the analysis and get similar contralateral deficits to Montoya Staircase.

2) That post-stroke physical rehabilitation can boost motor recovery when combined with the combination drug therapy.

3) That the drug combination exerts sex-dependent neuroprotective effects by modulating microglia activities from pro-inflammatory to anti-inflammatory.

1.14 Specific Aims

Specific Aim I

A). To examine whether administering the combination drug at an earlier time point after the onset of stroke symptoms would reduce infarct volume.

B). To improve the sensitivity of the Forelimb Asymmetry test by refining wall touches into a more specified parameter that correlates better with functional tests from Montoya staircase**.**

Specific Aim II

To investigate the impact of moderate rehabilitation with the impaired arm on functional recovery with and without post-stroke drug treatment.

Specific Aim III

To explore sex-dependent changes in gene expression of inflammation and polarization markers expressed by microglia in the peri-infarct zone in response to combination drug treatment. Neurotrophic factors and synaptic plasticity genes will also be examined in male rats.

CHAPTER II
MATERIALS AND METHODS

We used 10-12-month-old male Sprague-Dawley rats (generally 450-500 grams) to accomplish our specific aims 1 and part of specific aim 3. We compared our results with those from previous work in our lab in which 10-12-month-old female Sprague-Dawley rats were used for sex-dependent changes in gene expression. Female Sprague-Dawley rats were used in specific aim 2, where we evaluated the effect of rehabilitation on functional recovery with and without drug treatment. All animals are obtained from Harlan Laboratories (Indianapolis, IN) and fed Harlan rat chow. Animal experiments are approved by the Institutional Animal Care and Use Committee at Wright State University, and procedures followed are in accordance with institutional guidelines.

2.1 Surgery for Stroke Induction

All animals underwent endothelin-1-induced stroke procedure using the vasoconstrictive peptide ET-1 (Sigma, St. Louis, MO, USA). The procedure is based on modifications to Windle's protocol (Windle et al., 2006). Anesthesia was induced with 5% isoflurane, and the animals were maintained on 2-2.5% isoflurane using an anesthesia mask on the stereotactic apparatus (Stoelting Co., USA). A micro-drill was used to drill two close holes in the skull using two different set of coordinates relative to bregma to hit the forelimb motor cortex. It is critical to determine the location of stroke induction precisely to assure

destroying the forelimb motor cortex itself rather than the tissues surrounding it. Bregma position can be determined by looking at fusion lines on the skull surface where the coronal suture meets the sagittal suture. The basic surgical procedures are described in a previous study (A. M. Corbett et al., 2015), with the following modifications: two holes are drilled in the skull, with positions relative to bregma of (0.0 mm A.P., 2.5 mm M.L.) and (1.5 mm A.P., and 2.5 mm M.L.). The procedure starts with cleaning the surgical area using proviodine-iodine solution, followed by 70% ethanol then proviodine-iodine solution again. At the top of the animal head, a midline incision is made, and bupivacaine (0.25%) is administered to the incision to provide local analgesia for 12 hours. A 0.9 mm burr micro-drill is used to drill two holes in the skull (Fine Science Tools, Foster City, CA). A needle containing endothelin-1 was inserted into both holes in the skull, then lowered to a depth of 2 mm. One and one-half microliters of endothelin-1 (600 pmols) was injected into each hole over a period of 5 minutes. After that, the incision site was sutured and painted with a povidone-iodine solution to prevent infection. To avoid adverse effects of analgesics on neurogenesis (Hoehn, Palmer, & Steinberg, 2005), (Sargeant, Miller, & Day, 2008), no post-operative analgesics besides bupivacaine were used.

Endothelin-1 induced stroke surgery has advantages over the most commonly used ischemic stroke induction, the Middle Cerebral Artery Occlusion (MCAo). The ET-1 induced operation produces about 5% of ischemia in the cortex, which is similar to the majority of human strokes, compared to 45-50% injury seen in a single hemisphere in the MCAo, stroke model. It has a gradual reperfusion that closely mimics reperfusion in stroke patients (Mecca, O'Connor, Katovich, & Sumners, 2009). In addition to that, the large damage caused by blocking the middle cerebral artery and other arterial openings before

the middle cerebral artery can cause feeding difficulties in the animal and damage to the hypothalamus (Dittmar, Spruss, Schuierer, & Horn, 2003). This damage can affect drug intake and negatively influence the study outcomes. The intraluminal suture method of Middle Cerebral Artery occlusion (MCAo) has a high mortality rate in old animals. We had a smaller mortality rate in older experimental animals (under 10%) using ET-1 induced stroke model, which makes this technique a valuable model for basic and translational stroke research.

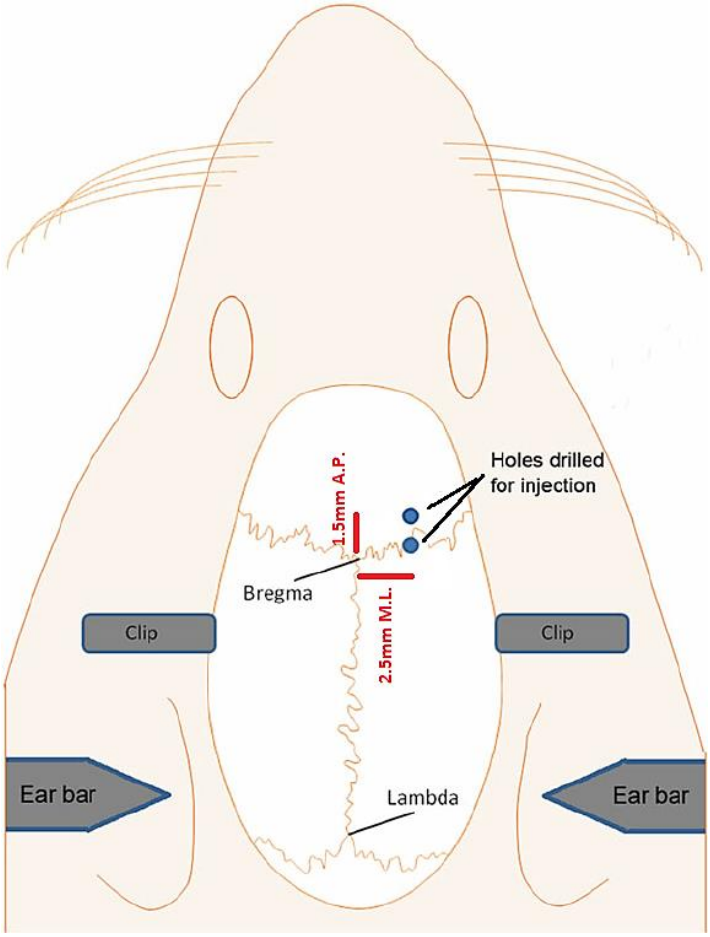

Figure 9. Schematic of a rat skull depicting the position of injection holes in accordance to bregma.

2.2 Voluntary Oral Administration of the Drug

Our method involves putting the drug in a 4-gram ball of purchased Pillsbury® sugar cookie dough. The cookie dough was weighed, rounded into a ball and then a depression pushed into the ball with a finger. The individually-weighed drugs (Pharmaceutical grade crushed tablets or contents of capsules) were put into the depression in the dough ball, and rim edges of the depression were brought together and sealed so that all the dry chemicals were enclosed in the dough ball. The dough ball was thoroughly mixed manually to incorporate all of the chemicals into the dough and reformed into a ball. The ball is presented to the animal in a glass dish at the same time every day and placed in an animal cage overnight to allow complete ingestion. Control animals receive the 4-gram ball of sugar cookie dough with no drugs added.

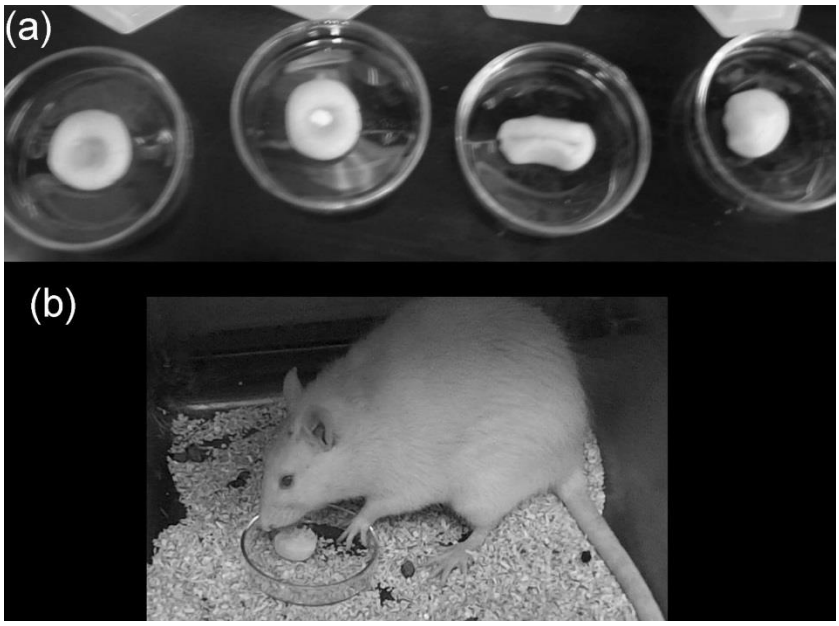

Figure 10. Voluntary Oral Administration of the Drugs. A. Drug incorporation into 4 gm of cookie dough; B. Rat is voluntarily consuming medication at the same time every day (A. Corbett et al., 2012).

2.3 Functional Tests

2.3.1 Montoya Staircase Test

Montoya staircase assesses grasping motor function, a motor function that often show deficits following stroke, which is responsible for many stroke patients' disabilities in everyday living. Thus, functional improvements in this motor function in rat models of stroke should translate well into clinical trials, which would test the same function. Rats are fasted overnight and then placed on a restricted diet consisting of 85% of their *ad libitum* rat chow while they are trained to pick up sucrose pellets, painted with maple extract, on the Montoya staircase (Montoya, Campbell-Hope, Pemberton, & Dunnett, 1991). The Montoya staircase consists of a raised platform with seven stairwells on each side containing sucrose pellets (three per stairwell), allowing left and right forelimb function to be independently assessed. Painting the sucrose pellets with maple extract or using chocolate flavored sucrose pellets is important during the training phase to entice rats through their sense of smell to reach down the sides of the platform and pick up the sucrose pellets, as they have a limited downward vision in this apparatus.

Rats must be properly trained before surgery for dependable post-operative data. Training occurred during the dark-phase consisting of 15-minute trials inside the Montoya staircase. Training lasts anywhere from 10-14 days. At the end of the training period, the rat's pre-stroke performance is determined by the best overall performance (highest total number of pellets retrieved) during the last three days of training. The majority of animals learn to retrieve between 15-18 pellets with each of their paws.

On post-stroke day 3-5, the rats are tested on the Montoya staircase again, and their best performance is used as a measure of their post-stroke baseline performance. To

normalize their performance, we divide the number of pellets taken by each paw post-stroke by the number of pellets retrieved by each paw pre-stroke. Thus, when the quotient is 1, the animal had fully regained pre-stroke function in a particular limb, and when the quotient is less than 1, that means the animal has a functional deficit in that limb. Animals that failed to reach training criteria, retrieving at least nine pellets with the left paw, on Montoya staircase test, are tested on Forelimb Asymmetry test as a backup assessment.

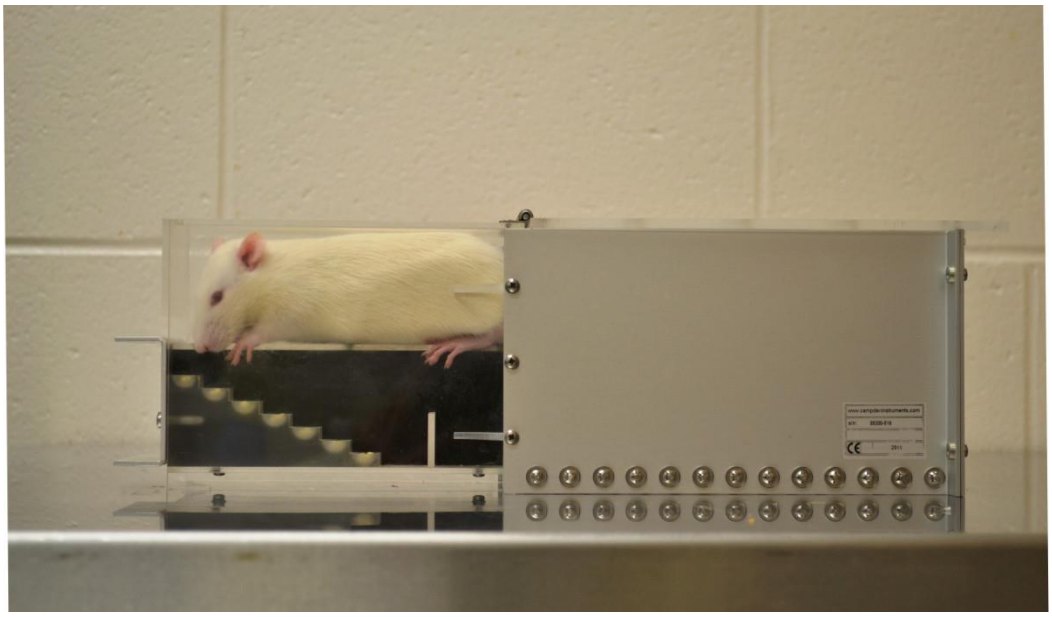

Figure 11. A rat on a central platform in the Montoya staircase box is reaching for pellets. Adapted from (Schaar *et al.*, 2010).

2.3.2 Forelimb Asymmetry Test (Cylinder test)

The animal is placed in a transparent vertical cylinder and videotaped for 5 minutes. Rats would rear up and touch the walls of the cylinder with their right and left forepaws to explore their environment. Normally before stroke induction, the majority of rats show little preference for the right or left paw during this exploration behavior. However, when rats were tested again on post-stroke day 4, they usually show a preference for touching the wall with their ipsilateral (right) paw, while they held their left paw back toward their body. Typically in this analysis, we look at the percentage of touches to the wall by right or left paw post-stroke and divide that by their pre-stroke performance percentages. However, since I am aiming to improve the sensitivity of the test, wall touches were refined into palm touches versus fingertips and palm touches to determine which of these correlate better with results obtained from Montoya staircase test.

Figure 12. A Sprague-Dawley rat is rearing up against the cylinder wall and exploring the arena. Both paws show full palm touches. Adapted from (Schallert, Fleming, Leasure, Tillerson, & Bland, 2000)

2.4 Exclusions

All animals that underwent stroke and displayed less than 20% baseline contralateral deficit in the Montoya staircase are excluded from the Specific Aim 1 (Part B) since we didn't have a Montoya Staircase functional analysis to compare with the Forelimb Asymmetry test. Animals must have learned to pick up at least nine pellets with at least their left forepaw or they are excluded from the Montoya staircase analysis. Any animal failing entirely to ingest post-stroke daily medicine or vehicle for a total of 3 days is completely excluded from the study: no animal was excluded for this reason in my work. During stroke induction surgery, movement of the needle through the cortex sometimes nicks a blood vessel and causes some bleeding, if a surgical artifact generates substantial bleeding, the animal is not included in the study: there were none excluded on this criterion in the study. When infarct volume is measured, a rat brain is excluded from the analysis if the brain was damaged either during dissection or the cryostat sectioning, such that we could not mount the individual slices or could not accurately determine the entire infarct volume. One animal was excluded based on this criterion (Rat 855 from the 6-12 hours treatment group).

2.5 Physical Rehabilitation Procedure

Recovery after ischemic stroke is a complicated process that occurs through a combination of restoration and compensation of functions as a response to both pharmacologic and physical therapies. In addition to drug treatment, post-stroke physical rehabilitation has been considered essential for enhancing functional motor recovery in stroke patients. Studies indicate that rehabilitation induces brain plasticity after stroke (Kleim, Jones, & Schallert, 2003), with an evidence of promoting neuroplasticity by

increasing BDNF production (Mang, Campbell, Ross, & Boyd, 2013). Another study shows that post-surgical rehabilitation sessions in rats that require the use of both forelimbs; therefore force the animal to use the impaired forelimb, can stimulate the BDNF production in the brain leading to improved functional motor recovery (Livingston-Thomas, McGuire, Doucette, & Tasker, 2014).

We examined whether post-stroke physical rehabilitation could improve functional motor recovery in drug-treated versus vehicle-treated rats (Ragas et al., 2015). Our lab designed a hanging rack to hold peanut butter just outside of an opening in the rat's cage (Figure 13). Because of the position of the shelf, the rat is only able to reach it with the contralateral paw (left paw) to the infarcted right hemisphere. The shelf was hung every other night with approximately 1-2 grams of peanut butter beginning eight days post-stroke and continuing for an overall period of five and half weeks. All other animals began to eat from the shelves within three days. Using this observation, we were able to determine if the animal underwent rehabilitation or not. We saw no difference in the number of completely-cleared versus partially-cleared shelves between the drug groups. This method enabled physical rehabilitation of the contralateral limb without the stress of physical restraint of the ipsilateral limb.

Rehabilitation was begun on post-stroke day 8 and continued every other day until post-stroke day 45. During rehabilitation, the hanging shelves were loaded with 1-2 grams of peanut butter and hung around 5:00 pm each day. The shelves were collected 24 hours later and evaluated for whether the animal used its impaired paw. Animals generally began to eat from the shelves within three days and continued through the end of the rehabilitation period.

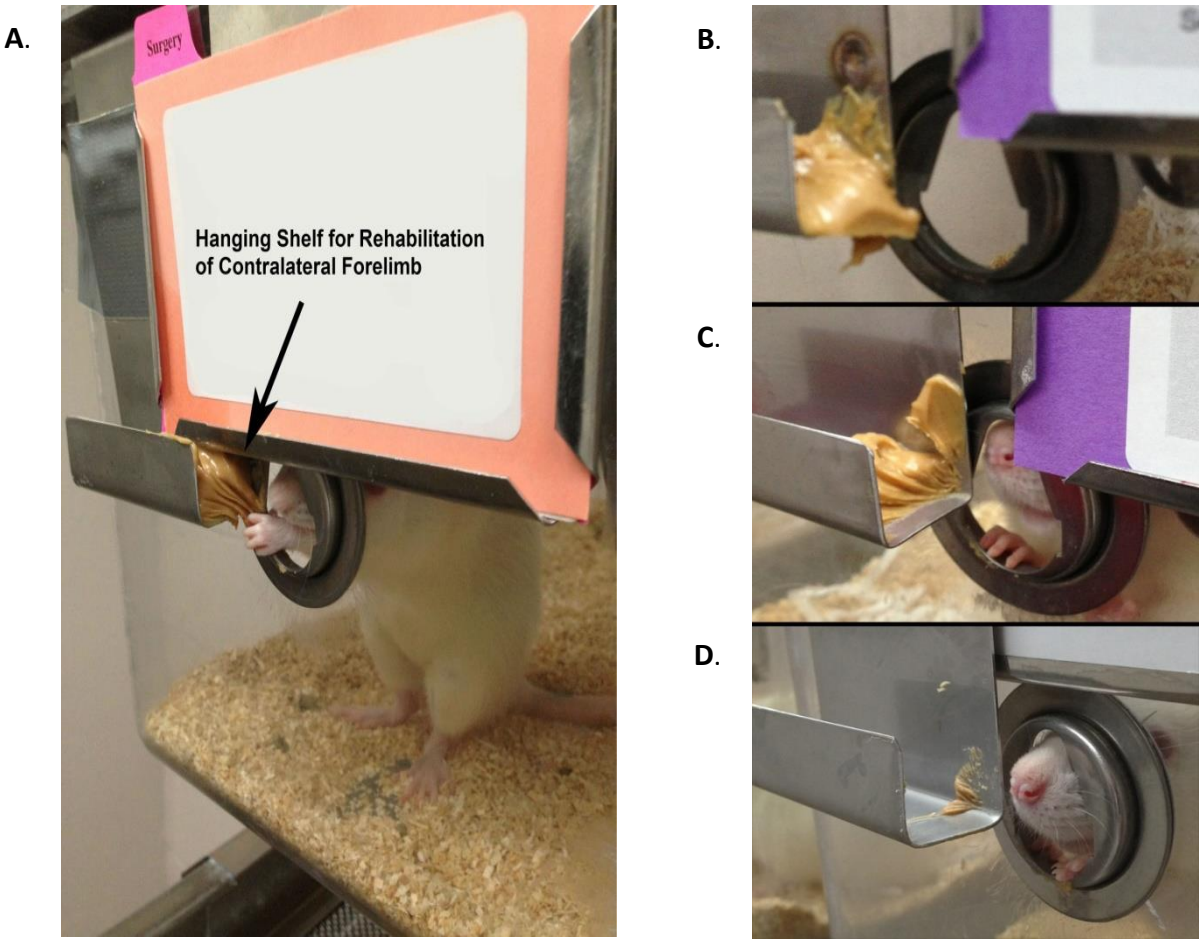

Figure 13. Voluntary Physical Rehabilitation. (A). Hanging shelf for rat rehabilitation. (B). the animal has not eaten from the shelf. (C). the animal has partially eaten from the shelf. (D). the animal has completely cleared the shelf of all peanut butter (Ragas et al., 2015).

2.6 Preparing Tissues for Immunohistochemistry (IHC) Experiment

Rats were injected with sodium pentobarbital (Euthasol; 100 mg/kg, i.p.) and returned to their cages to allow them to obtain a surgical plane of anesthesia. Animals were then perfused through the left ventricle of the heart using 100 ml of phosphate buffered solution (PBS) followed by 150 ml of 4% paraformaldehyde in PBS as a fixative. A blunt-edged cannula was used to deliver solutions through a small incision in the ventricle, to ensure it did not cross the interventricular septum. After 15-20 minutes of fixation, brains were removed and placed in the same fixative solution overnight at 4°C then immersed in 30% sucrose solution for three days at the same temperature. After that, brain tissues were stored at −80°C until use. Coronal sections of 50μm starting anterior to the infarct site were sliced on a cryostat at −25°C. Each slice was immersed into one of six vials, containing PBS, which is labeled according to the type of proposed experiment. The infarct analysis vials were labeled as 1:500 8-OHdG (8-hydroxy-deoxyguanosine antibody) and Control; the other four vials were used for other projects in our lab using different staining techniques such as H&E and Prussian blue.

Immunohistochemistry staining was performed on free-floating coronal sections in the 8-OHdG vial. The sections were incubated overnight at 4°C with a primary antibody (1:500 dilution of mouse monoclonal antibody against 8-OHdG, Abcam) to detect the nucleic acids damage by oxidative stress. Sections were then treated with horse radish peroxidase biotinylated secondary antibodies (donkey anti-mouse antibodies). Sections then rinsed twice with PBS-Tween and immunoreactivity was visualized by the Avidin-Biotin Complex method using VIP as a substrate for the horse-radish peroxidase (VIP impact kit; Vector Laboratories). Coronal slices from 8-OHdg vials and Control vials were

carefully mounted on microscope slides using a paintbrush and set aside to dry. Slides were cover slipped using DPX mountant.

2.7 Infarct Measurement

Brightfield images were taken of the sections using a 4X objective, then montaged using advanced panoramic image stitcher called Image Composite Editor (ICE) into a complete picture of a damaged region of the brain as indicated by a dark staining (infarct). Area of the infarct was determined with ImageJ (Fiji open source software) from NIH. Infarct area (mm^2) was determined for every sixth slice, then multiplied by the slice thickness (0.05 mm) and 6 to determine the complete infarct volume in mm^3.

Table 6 presents an example of infarct measurement in which the infarct volume was determined from 16 coronal brain sections collected from one animal. Slides were numbered as they were assessed for the presence of infarcts and sections on the slide were numbered left to right. Area of infarct was determined with Image J software, after setting the scale. The multiplier number varied from experiment to experiment, and in this case merely indicates that one out of every six brain coronal slices were used to measure infarcts volume with 8-OHdG. The final summed volume of the infarct for this animal is shown in the lower right part of the table.

Table 6. Summary of infarct volume calculation in one animal.

Rat ID	Slide No.	Section No.	Area mm^2	Thickness mm	Multiplier	Volume	Final volume mm^3
860	1	1	1.517	0.05	6	0.4551	
860	1	2	1.131	0.05	6	0.3393	
860	1	3	1.297	0.05	6	0.3891	
860	1	4	1.897	0.05	6	0.5691	
860	2	1	2.272	0.05	6	0.6816	
860	2	2	1.661	0.05	6	0.4983	
860	2	3	1.546	0.05	6	0.4638	
860	2	4	1.089	0.05	6	0.3267	
860	3	1	1.745	0.05	6	0.5235	
860	3	2	1.581	0.05	6	0.4743	
860	3	3	1.694	0.05	6	0.5082	
860	3	4	1.613	0.05	6	0.4839	
860	4	1	1.24	0.05	6	0.372	
860	4	2	1.608	0.05	6	0.4824	
860	4	3	1.128	0.05	6	0.3384	
860	4	4	3.511	0.05	6	1.0533	7.959

2.8 Preparing Samples for Genetic Analysis

After injecting animals with sodium pentobarbital (Euthasol; 100 mg/kg, i.p.), animals were injected with a 1ml of Evans Blue dye directly into the ventricles of the heart and then perfused with PBS to clear the dye. The brain is dissected, blocked and then the coronal portion containing the infarct dropped into a beaker containing isopentane and dry ice to freeze tissues for cryosectioning. The frozen coronal block is kept at -80 °C in a scintillation vial until the cut on the cryostat. On the cryostat, tissue was cut from the anterior-most end until the infarct was reached. An RNAseZap® cleaned microtome blade and forceps were then used to remove a block of tissue surrounding the infarct. The blocks of tissue ranged from 20-30mg in weight, are placed into pre-weighed RNase and DNase free plastic vials for the tissue homogenization step. To isolate RNA, 600 µl of lysis buffer (Qiagen RNeasy RLT Plus) were added to disrupt the tissue using a conventional rotor–stator homogenizer until it is uniformly homogeneous (about 30 seconds). Next, the lysate was centrifuged at maximum speed for 3 minutes and the supernatant was carefully transferred into a new microcentrifuge tube. Then, 600 µl of 70% ethanol were added to the cleared lysate and mixed well. A 700 µl of the sample was transferred to an RNeasy spin column placed in a 2 ml collection tube and centrifuged at 8,000 x g for 30 seconds. The flow-through volume was discarded. Next, 700 µl of a wash buffer RW1 was added to the RNeasy spin column and centrifuged at 8,000 x g for 30 seconds. The flow-through volume was discarded. A 500 µl of Qiagen RPE wash buffer was added to the RNeasy spin column and centrifuged at 8,000 x g for 30 seconds. After discarding the flow-through volume, this step was repeated with centrifugation time of 2 min. The RNeasy spin column was placed into a 2 ml collection tube and centrifuged at 16,000 x g for 1 minute to further

dry the membrane, then placed into a 1.5 ml collection tube. Forty microliters of RNase-free were directly added into the spin column and centrifuged at 8,000 x g for 1 minute to elute the RNA. The concentration of the purified RNA was determined using a NanoDrop spectrophotometer and the RNA samples were stored at -80 degrees Celsius for future analysis.

2.9 Gene Expression Analysis Using Real-Time PCR

RT^2 PCR Array technique is a reliable tool for analyzing the expression of different genes allowing us to detect genes of interest accurately by probing with cDNA, reversed transcribed from the mRNA in the peri-infarct regions of rat brain using Qiagen First Strand Kit. Both the mRNA purification kit and reverse transcription kit have a genomic DNA elimination step to remove any false positive signals that might develop as a result of contamination in RNA samples. Other quality control elements implanted within the array are: housekeeping genes for data normalization, reverse-transcription controls (RTC) for the efficiency of the first strand cDNA synthesis, and positive PCR controls to test PCR performance. Each well has a replica on the PCR 96-well plate to assess the reproducibility and validity of the data. Results from each sample and its replica are averaged before running the online data analysis which automatically performs all ΔΔCt based fold-change calculations. Average Ct values for all gene replicates were calculated first, then delta Ct value between the gene of interest and housekeeping gene for each experiment were calculated. Delta-delta Ct values obtained from delta Ct experiment – delta Ct control.

A comprehensive gene expression profile for different gene pathways can be carried out in less than 6 hours using three different Qiagen kits. Animal's tissue is first homogenized using a rotor-stator homogenizer to prepare tissue for the RNA purification.

The second step is to purify RNA using a spin-column method (the Qiagen Universal RNeasy Mini Kit). RNA was converted to complementary DNA (cDNA) by performing a reverse transcription using the First Strand Kits (contains a step for the elimination of genomic DNA). The genomic DNA elimination mix was prepared according to the RT^2 First Strand protocol and processed through a gradient thermal cycler. The next step was to mix the cDNA with the ready-to-use RT^2 SYBR® Green qPCR Mastermix and RNAse free water; this mixture is then aliquoted (25 µl per well) across the RT^2 Profiler Array. The real-time PCR cycling program runs on the ABI 7900HT thermocycler for 40 cycles, using absolute quantification.

Figures 15, 16 and 17 demonstrate custom RT^2 PCR array layouts for M1 and M2 microglia biomarkers, RT^2 Profiler synaptic plasticity PCR array and for neurotrophic genes and their receptors array, respectively. The complete lists of gene symbols, description of genes and their positions in each plate are described in Appendices II and III.

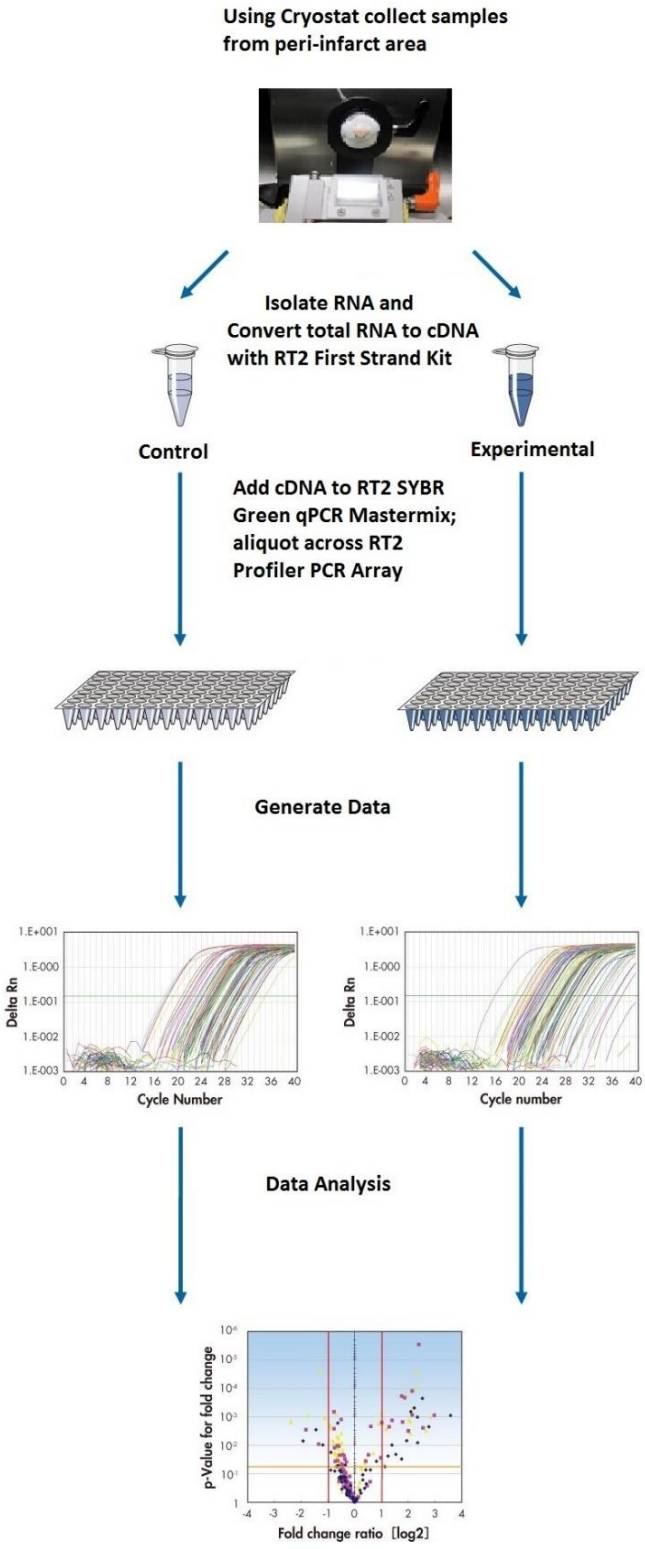

Figure 14. RT^2 Profiler PCR Workflow

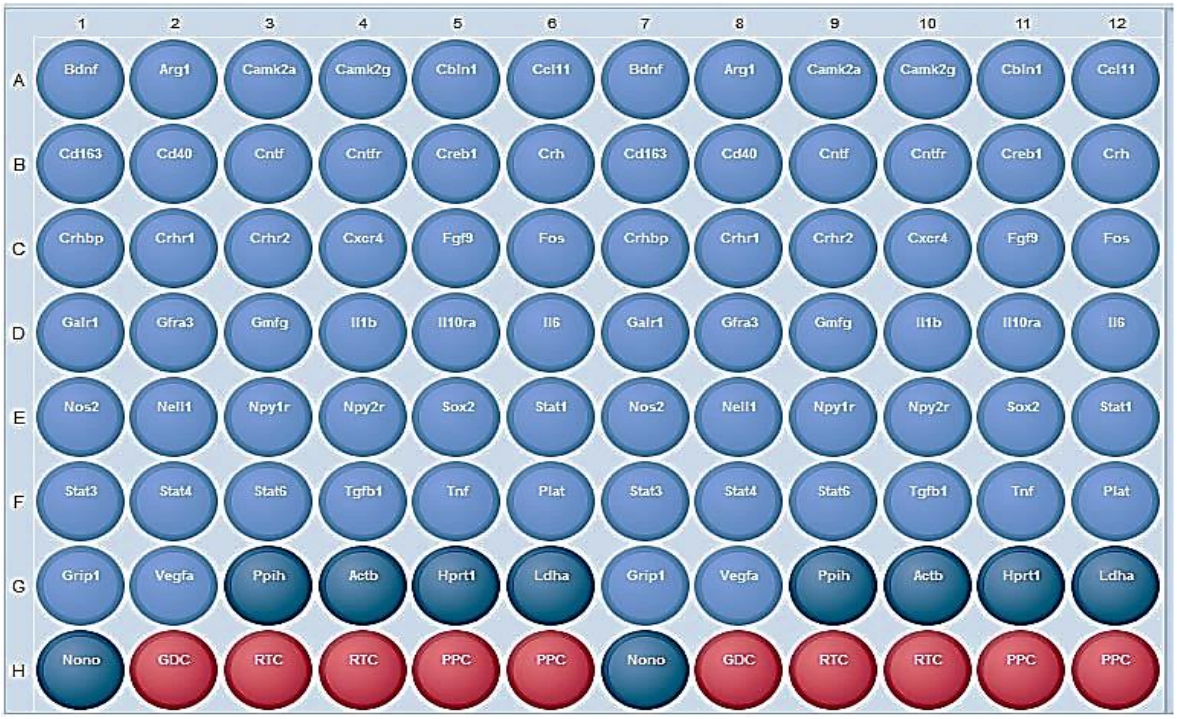

Figure 15. Custom RT^2 PCR Array layout for M1/M2 Microglia Biomarkers. Light blue wells each contain a real-time PCR primer sets for the indicated inflammatory/microglia activation related genes. All wells from column 1 to 6 are replicated in columns 7 to 12. Dark blue wells contain a housekeeping gene panel to normalize array data (Ppih, Actb, Hprt1, Ldha and Nono). Red wells H2 and H8 contain genomic DNA controls (GDC). Wells H3, H4, H9, and H10 include replicate reverse-transcription controls (RTC). Wells H5, H6, H11, and H12 include replicate positive PCR controls (PPC).

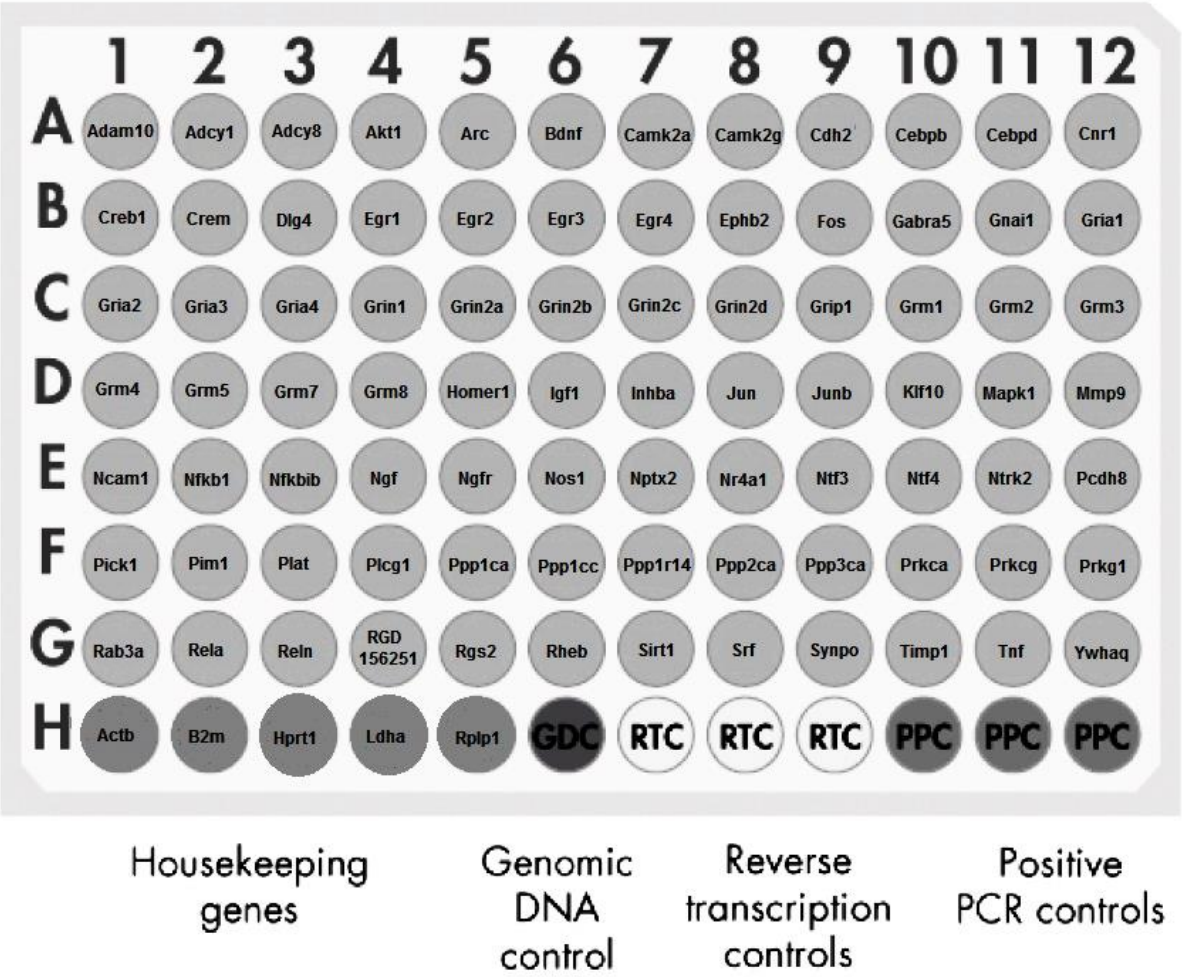

Figure 16. The diagram illustrates the layout of the 84 different primers for rat synaptic plasticity genes, controls for reaction quality (genomic DNA contamination, reverse transcription, and positive PCR controls) and five housekeeping genes for normalization.

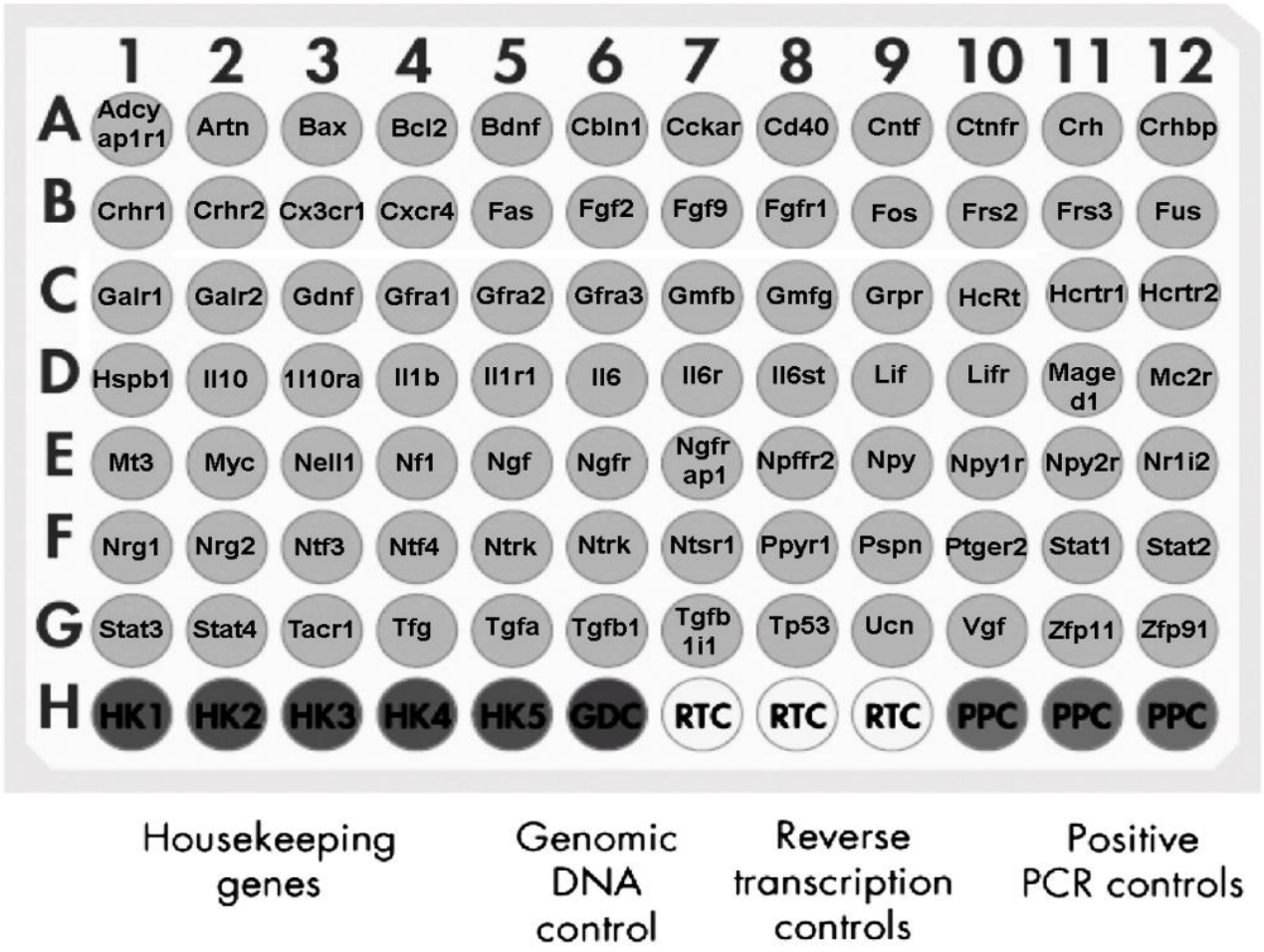

Figure 17. The diagram shows the layout of the 84 different primers for neurotrophic genes and their receptors, controls for reaction quality (genomic DNA contamination, reverse transcription, and positive PCR controls) and five housekeeping genes for normalization.

2.10 Protein-Protein Interaction (PPI) Database

To investigate the relationships between the up-regulated and down-regulated genes and the physiological significance of the interactions among them, I utilized the Search Tool for the Retrieval of Interacting Genes (STRING) version 10.0 to predict interaction information with high-confidence. The resource is accessible online at http://string-db.org. STRING is a comprehensive database that provides a computational prediction of protein-protein functional and physical associations. It is one of the widely used PPI databases that contain interaction networks from a wide variety of organisms. Adjustable confidence scores (low, medium or high confidence) are provided to each of the interactions in STRING, in addition to information on protein domains, 3D structures, and interactive network viewer that cluster networks on demand. All information can be obtained by searching for multiple proteins by names or identifiers in the program search engine and selecting the organism type (*Rattus norvegicus* strain in this study).

The current version (v10.0) of STRING database covers more than 9.6 million proteins from over 2000 organisms ranging from Bacteria, Archaea to Homo sapiens (Szklarczyk et al., 2011; Szklarczyk et al., 2015). STRING imports information from various sources, including digitized experimental data from scientists and publications such as PubMed and FlyBase (Wodak, Pu, Vlasblom, & Seraphin, 2009).

To investigate potential interactions within the genes, upregulated and down-regulated genes were considered as two separate groups. If two or more genes were identified in both the groups, they were fed into the STRING database identifier for predicting protein-protein interaction.

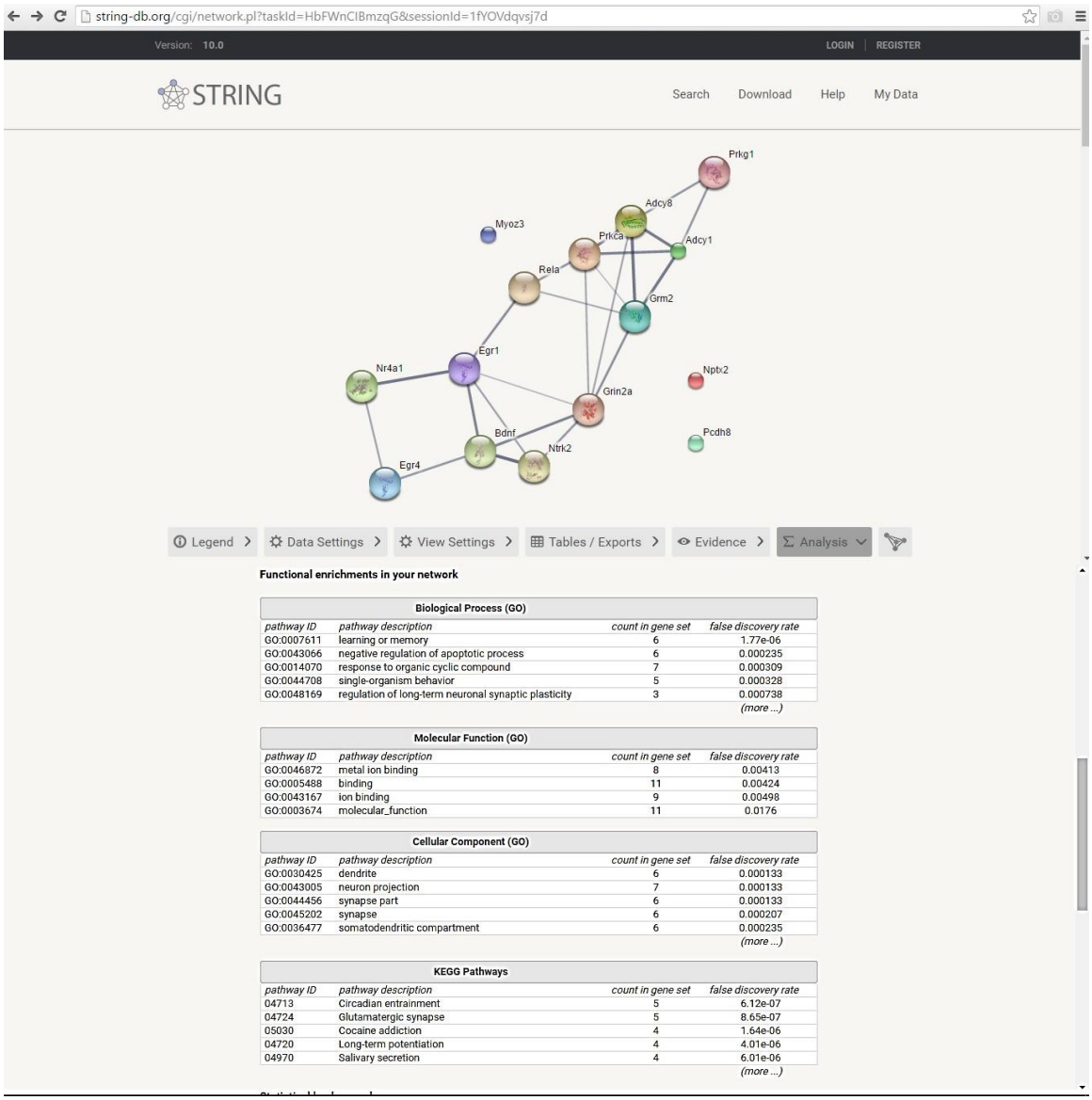

Figure 18. Screenshot of protein-protein network from the STRING website. Network can be rearranged and clustered directly in the browser window revealing tightly connected functional molecules with their role in different pathways. The thickness of lines between nodes is a rough indicator of the strength of the association. Large nodes indicate the availability of 3D protein structure information.

2.12. Research Plans

In the first part of this study, we are examining the influence of the timing of administration of fluoxetine after stroke onset on the final infarct size and the risk of developing secondary hemorrhagic transformation. Since the majority of stroke patients coming into the hospital are already on statins due to dyslipidemia, the experiment more closely modeled clinical trials by starting all animals on 1 mg/kg simvastatin seven day pre-stroke and continuing daily. Interesting findings in our laboratory on the effect of early drug delivery on infarct size in female rats have prompted us to investigate the relationship between the timing of drug administration and infarct size in male rats. Daily 5 mg/kg fluoxetine and 20 mg/kg ascorbic acid administration were begun at three initiation time points (6-12 hours post-stroke, 20-26 hours post-stroke and 48-54 hours post-stroke) in rats that pre-treated with simvastatin for one week.

We also sought to improve the sensitivity of one of the behavioral tests for the motor function: the forelimb asymmetry test. Traditionally during this test, the animal is placed in a clear vertical tube and videotaped for 5 minutes. The number of times the animal touches the wall with its right or left paw is quantified using slow motion video analysis. For pre-stroke animals, we usually see around a 50:50 use of the right and left forepaw. After the stroke surgery, we see more use of the ipsilateral paw (right paw) with inhibition in the utilization of the left paw. This test takes a long time to complete the analysis, as the number of wall touches must be quantified for each fore-paw, but it is a test that does not require any training so that it could apply to all animals in the study. The manner in which we are counting wall touches (any touch to the wall) seems to lower the sensitivity of the test to the deficit produced. We have noticed that following a stroke; the animal

tends not to put full weight on the left paw (does not flatten the palm against the wall). This behavioral test is important in that it can be applied to every rat, yet with our current method of analysis (any touch to the wall counts), it does not correlate well with functional deficits observed with the Montoya staircase test (which shows finer motor control deficits). A more precise approach has been proposed to evaluate another method for counting wall touches (differentiating between a full palm touch and a fingertip touch) to see if the full palm touches better correlates with results from the Montoya staircase test.

The second goal of this study is to determine whether physical rehabilitation might enhance functional motor recovery in drug-treated rats versus control animals. Post-stroke physical rehabilitation has been considered essential for enhancing functional motor recovery (Faralli, Bigoni, Mauro, Rossi, & Carulli, 2013). Clinical studies suggest that early rehabilitation therapy after stroke may improve physical function, increase brain plasticity and improve the skills needed to perform activities (Feigenson, McDowell, Meese, McCarthy, & Greenberg, 1977) and (Hayes & Carroll, 1986). A recent study on the effects of post-stroke rehabilitation on recovery in MCAo model rat indicates that daily rehabilitation enhances functional outcome (Sasaki et al., 2016). The degree of impairment produced in human patients after stroke differs from experimental dysfunction in rats based on stroke inducing procedure. The majority of acute stroke patients show severe impairment or total loss in upper extremity movement, while rats show a little deficit of forelimb movement in the MCAo model of focal ischemia (Kleim, Boychuk, & Adkins, 2007) . Also, the severity of rehabilitation, time of the procedure and the influence of stress are essential factors that influence the outcome. Some of the stroke studies on rats utilized intensive rehabilitation protocol in which the intact forelimb is constrained after the stroke

induction surgery to force the animal to overuse the impaired forelimb for movement and body support (Risedal, Zeng, & Johansson, 1999), (Bland et al., 2000). This type of stressful rehabilitation led to reduced functional recovery. Since physical rehabilitation in stroke patients involves assistance from the therapist in contrast to animal rehabilitation, which is totally hands-off, it is crucial to choose the right rehabilitation task in rat models to ensure that task is successful. Our method of rehabilitation using a hanging shelf filled with peanut butter accomplished rehabilitation of the impaired limb without restraint thus reduced stress during rehabilitation.

Finally, a newly discovered neuroprotective role of fluoxetine in suppressing microglia-mediated inflammation *in vitro* (Su et al., 2015) has directed us to investigate the genetic mechanisms for this inhibitory role aiming to explore other potential influences of fluoxetine on modulating microglial polarization from pro-inflammatory (M1) phenotype towards beneficial anti-inflammatory (M2) phenotype. In conjunction with previous work in our laboratory that showed fluoxetine stimulates neurotrophic factors and synaptic plasticity in female rats, in this study, the effects of fluoxetine on the neurotrophic factors and synaptic plasticity in male Sprague-Dawley rats were examined.

CHAPTER III
RESULTS

3.1 Specific Aim I

3.1.1 To examine whether administering the combination drug at an earlier time point after the onset of stroke symptoms would reduce infarct volume.

Our previous experiments had indicated that administration of fluoxetine and simvastatin at 20-26 hours post-stroke decreases the volume of ischemic infarcts in Sprague-Dawley female rats (10-12 months old) (Balch et al., 2015). This current experiment is more closely modeled on current clinical trials by starting all animals on simvastatin 7 days pre-stroke and continuing daily in male Sprague-Dawley rats. The purpose of this experiment is to determine the impact of the time to treatment of fluoxetine, in combination with simvastatin, on the infarct volume and the risk of secondary hemorrhagic transformation. Daily 5 mg/kg fluoxetine and 20 mg/kg ascorbic acid administration were begun at three initiation time points (6-12 hours post-stroke, 20-26 hours post-stroke and 48-54 hours post-stroke). We included the 48-54 hour time-point because this is the earliest time point used in three ongoing clinical trials (FOCUS, AFFINITY, EFFECTS) testing fluoxetine effects on motor recovery post-stroke. Animals were randomly assigned to either drug or control group after the surgery, but before the baseline stroke deficit was determined using either Montoya Staircase or Forelimb Asymmetry tests. After drug treatment had been begun, it was continued daily until post-

stroke day 7. All animals were euthanized on post-stroke day 7, so we could see any evidence of hemorrhagic transformation. Infarct volume was assessed at post-stroke day seven by immunohistochemical determination of 8-hydroxy-2'deoxyguanosine (8-OHdG), which locates nuclei that are under oxidative stress, using ImageJ software.

Table 7. Male treatment groups with different times of drug delivery. All groups were given 1 mg/kg simvastatin beginning 7 days before stroke induction and continuing through PSD 7. Column 2 shows any daily drug treatment for that group, with any fluoxetine and ascorbic acid administration beginning at the times indicated in Column 1, and continued daily until the euthanasia time-point (Column 5). Functional tests were administered at the times indicated in Columns 3 and 4.

Group	Oral Dose	Montoya Staircase	Forelimb Asymmetry	Euthanasia
Control (N=9)	1 mg/kg simvastatin	PSD 3-5	PSD 4	PSD 7
6-12 hrs. FSA (N=11)	5 mg/kg fluoxetine + 1 mg/kg simvastatin +20 mg/kg ascorbic acid	PSD 3-5	PSD 4	PSD 7
20-26 hrs. FSA (N=9)	5 mg/kg fluoxetine + 1 mg/kg simvastatin + 20 mg/kg ascorbic acid	PSD 3-5	PSD 4	PSD 7
48-54 hrs. FSA (N=10)	5 mg/kg fluoxetine + 1 mg/kg simvastatin +20 mg/kg ascorbic acid	PSD 3-5	PSD 4	PSD 7

A.

B.

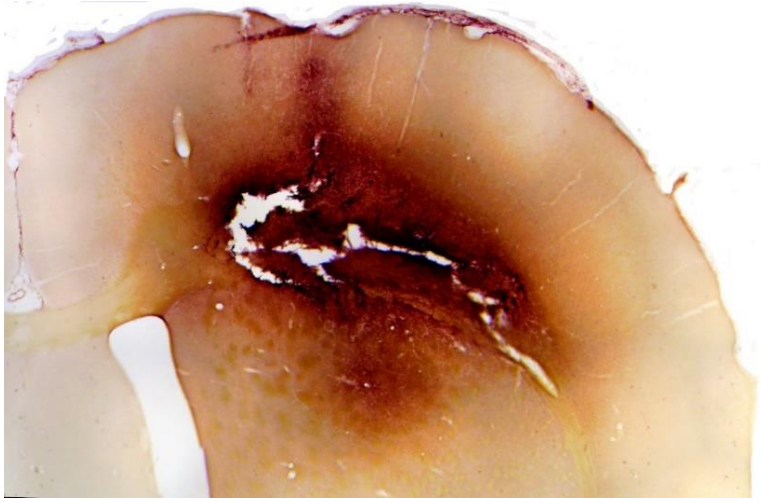

Figure 19. Representative images showing 8-OHdG staining of the infarct area indicative of oxidative DNA damage. A. This panel shows significant reduction of infarct volume when fluoxetine and the ascorbic acid combination was administered 20-26 hours after stroke surgery in simvastatin pre-treated rats. B. Infarct size in early drug delivery animal (6-12 hours after stroke induction) is similar to Control and delayed treatment groups.

In this experiment, all male Sprague-Dawley rats were on 1mg/kg simvastatin for seven days before stroke induction and continued for seven days post-stroke, then were euthanized. Typically, control animals had 5-13 mm^3 infarct volume following endothelin-1 induced stroke, when stained with 8-OHdG primary antibody (Abcam; see figure 19 for representative images from the 20-26 hour administration (Panel A) versus early drug delivery (Panel B). In the control group (see Table 8, Figure 19 and Figure 20), the mean infarct volume was 8.035 ± 0.6418 mm^3 SEM (N=10). Animals that received fluoxetine and ascorbic acid beginning 6-12 hours after stroke induction showed no significant difference in infarct volume compared to control (7.626 ± 1.009 mm^3 SEM, N=11); however, when fluoxetine delivered 20-26 hours post-stroke that resulted in significant reduction (p=0.0366) of infarct volume (4.782 ± 0.8845 mm^3 SEM, N=9). Interestingly, if the delivery of fluoxetine was delayed to 48 hours following stroke induction, the infarct size showed no significant change in comparison to control 8.202 ± 0.8754 mm^3 SEM (N=9).

Furthermore, brain sections in the delayed treatment group (48-54hrs) showed evidence of hemorrhagic transformation in the peri-infarct area when stained with H&E (see Figure 21). In figure 21, the dark blue staining was examined by pathologist Smita Krishnamurthy, M.D. and she confirmed that the extensive staining in panels A, B, and D is due to peripheral macrophage and lymphocyte infiltration, while panel C shows very little infiltration. This fits in with our previous idea that we may be eliminating reperfusion injury in this group of animals: 24 hours after stroke is when reperfusion would generally be predicted to occur in this endothelin stroked rat. Administering the drug at this time point appears to stop the reperfusion in compare to delaying treatment to 48 hours. To

examine the probability of hemorrhagic transformation occurring in drug groups to the probability of the event occurring in control group, an MD/Masters student in the lab, Neal Verma, analyzed the relative risk of hemorrhagic transformation in these groups, and found a relative risk (RR) of 1.04 (*p*-value 0.913) in the 6-12 hour administration group and 0.925 relative risk (*p*-value 0.845) in the 48-54 hour administration group compared to control, while the 20-26 hour administration group had a relative risk of 0.37, with a *p*-value of 0.14, indicating a trend. Relative risks evaluations are usually done with group sizes of 50, so it was very encouraging to see a statistical trend with our small group size: it suggests a strong effect.

These results are similar to those reported in the FLAME clinical trial (Chollet et al., 2011), where they saw no effect on infarct volume and some hemorrhagic transformation in patients given 20 mg fluoxetine beginning two days after stroke and continuing for 90 days. Also, we previously saw that female stroke rats just given 5 mg/kg fluoxetine and 20 mg/kg ascorbic acid 20-26 hours after stroke and continued for 30 days, had a roughly 11% motor recovery, as assessed by Montoya Staircase. This roughly matched the recovery seen in the FLAME clinical trial using the Fugl Meyer Assessment score when stroke patients were given only 20 mg fluoxetine daily (A. M. Corbett et al., 2015). Although our dose was twice that given in the FLAME trial.

Table 8. One-way-ANOVA with Dunnett's multiple comparisons test.

Dunnett's Multiple Comparisons Test	Mean Control	Mean Test	Mean Diff.	95% CI of diff.	Significance
Control vs. 6-12hrs	8.035	7.626	0.4092	-2.518 to 3.337	No
Control vs. 20-26hrs	8.035	4.782	3.253	0.1746 to 6.331	Yes *p*=0.0366
Control vs. 48-54hrs	8.035	8.202	-0.1671	-3.245 to 2.911	No

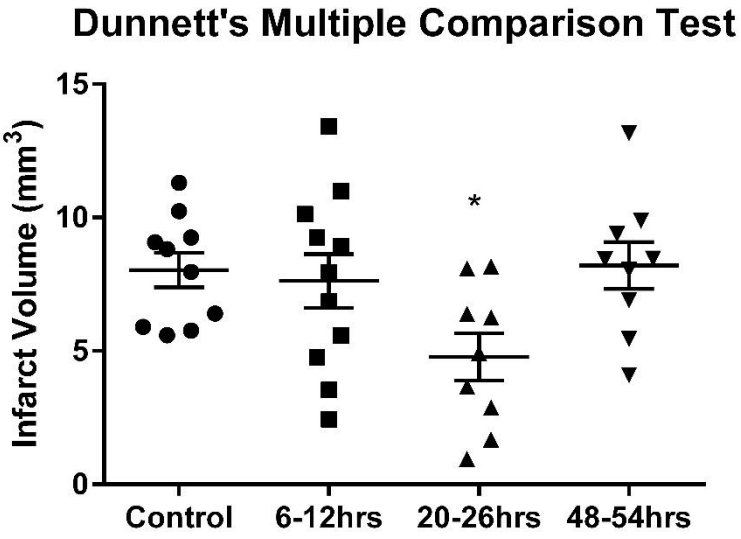

Figure 20. Direct comparison of infarct volumes between all groups treated with fluoxetine and ascorbic acid at different time points following stroke induction indicates that infarct volume varies with the timing of fluoxetine delivery post-stroke. There are no outliers at either end of the range. Each dot represents a single animal in each group. The x-axis displays treatment groups at different time points, and the y-axis shows the infarct volume in mm^3. The broad horizontal bar indicates the group mean and the error bars represent SEM. *p = 0.0366 using one-way ANOVA with Dunnett's multiple comparisons.

These results are consistent with previous findings in our lab on female rats. The methods are similar to previous work with few exceptions: 1) in the previous work we examined infarct volumes on day 91 after stroke induction and rats were not on simvastatin before the surgery; 2) we added a new time-point (48-54 hours) of drug administration after stroke, to match the earliest time point for fluoxetine delivery in human clinical trials.

Figure 21. Representative images showing H&E stained coronal brain sections with infarcts in male rats. (A). Control (simvastatin only) administered 7 days pre-stroke and 7 days post-stroke shows large infarct volume with hemorrhagic transformation. (B). Infarct size was unchanged if fluoxetine and ascorbic acid was administered 6-12 hours after stroke and had a highest relative risk of hemorrhagic transformation. (C). Significant reduction of both infarct volume and hemorrhagic transformation when fluoxetine and ascorbic acid combination was administered 20-26 hours after stroke surgery. (D). The panel shows same infarct size when drug combination was delayed 48-54 hours; a possible bleeding (hemorrhagic transformation) is marked with an arrowhead. Scale bar is 500 micrometers.

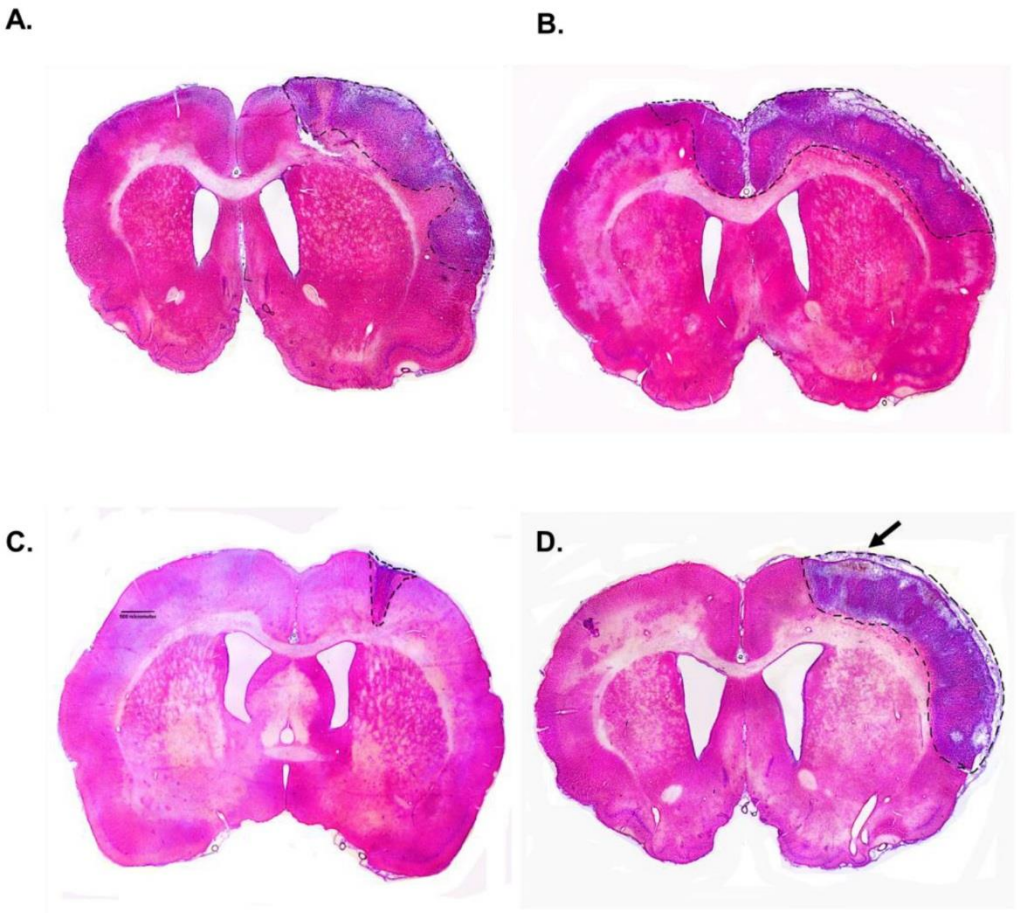

3.1.2 To improve the sensitivity of the Forelimb Asymmetry test by refining wall touches into a more specified parameter that correlates better with functional tests from Montoya staircase**.**

Forelimb Asymmetry analysis is routinely used in small rodents to predict functional motor deficits caused by focal ischemic stroke; however, we found that results of this test are not as sensitive as the Montoya Staircase test. The aim of this part is to refine the forelimb asymmetry analysis to strengthen the sensitivity of the assessment. A traditional Forelimb Asymmetry test, which counts all wall contacts, fails to detect consistent functional deficits where the Montoya Staircase has identified a functional deficit. Understanding that the hand movements in the two tests are different, with the Montoya Staircase using finer motor control for grasping, I nevertheless wanted to determine if some of the wall touches in the Forelimb Asymmetry test could be considered "abnormal" when compared with pre-stroke functional analysis, and if the sensitivity of the test would be increased if abnormal touches were not counted. In this study in particular, I investigated whether counting only palmar pads pressed to the wall rather than any attempt to touch the cylinder wall (e.g. by fingertips) would allow a better correlation with Montoya staircase results. This section deals with the functional data from the male rat groups shown in Table 7 and also some female rats who were given 5 mg/kg fluoxetine, 1 mg/kg simvastatin and 20 mg/kg ascorbic acid beginning 20-26 hours post-stroke compared to a vehicle control group.

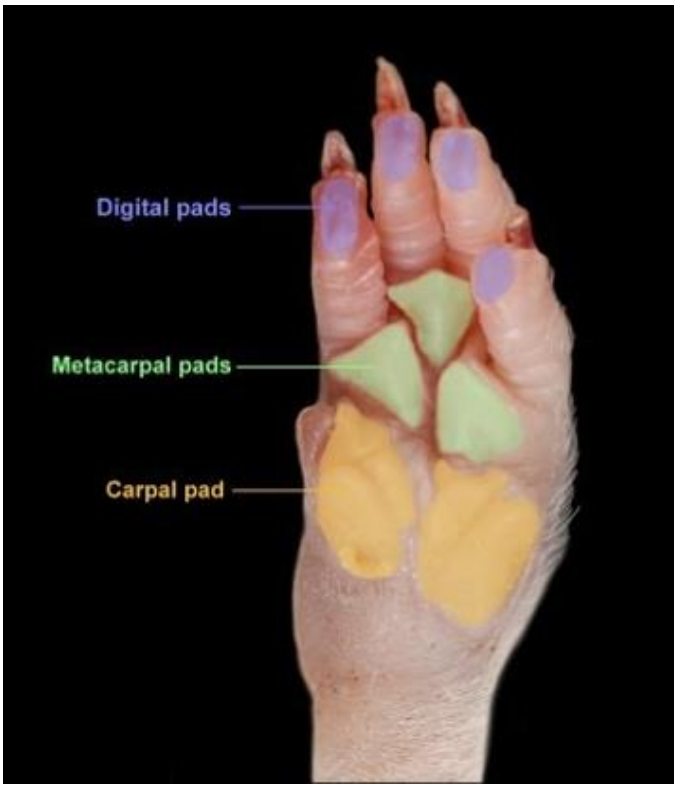

Figure 22. Rat's left forelimb shows palmar pads and fingertips.

To evaluate if any touches to the wall were abnormal after the stroke, I needed to determine if the normal rat pre-stroke ever touched the wall of the cylinder with only its fingertips or if it instead used its palm pressed to the wall (see Figure 23 for different types of wall touches). These data are detailed in Table 9, showing that there were no touches to the wall using only fingertips with pre-stroke animals: this type of touching only occurred after the stroke induction. This type of wall touch could then be considered abnormal, as confirmed by the Fisher's exact test in Table 9.

Figure 23. Forelimb Asymmetry analysis. (A). A post-stroke animal rearing and placing the palmar pads on the wall, which indicates its use for body support. (B). Post-stroke animal leaning on enclosing wall using right (ipsilateral) forepaw while attempting to touch the wall by the left (contralateral) fingertips.

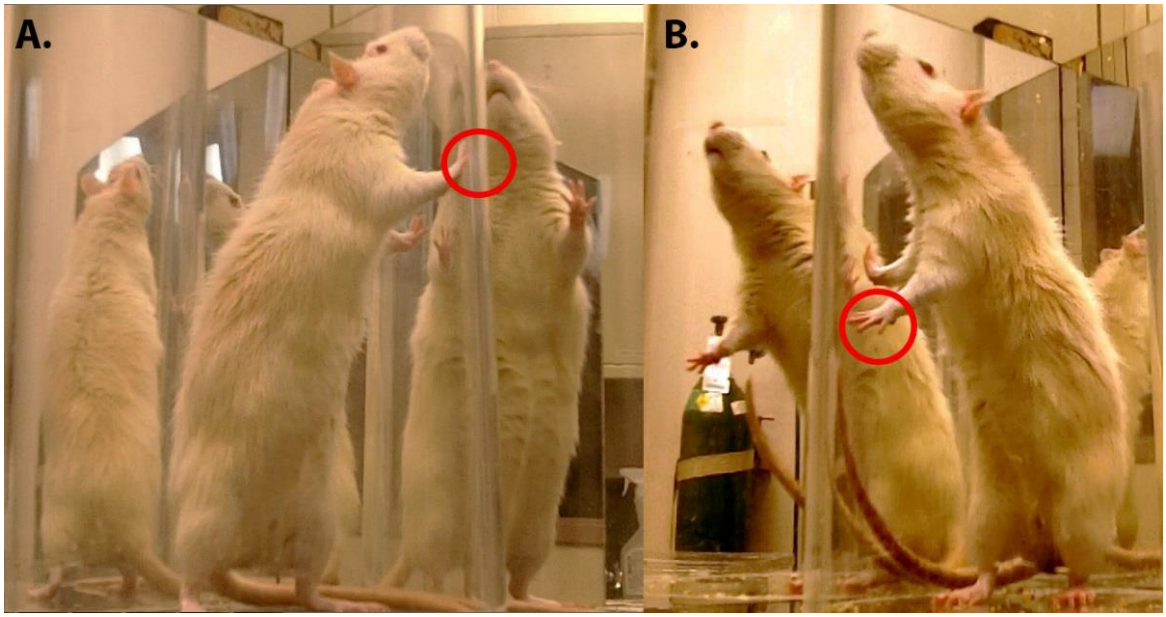

Rat ID	Forelimb Asymmetry Assessment (Pre-Stroke)				Forelimb Asymmetry Assessment (Post-Stroke Day 4)			
	Palmar Pads		Fingertips		Palmar Pads		Fingertips	
	L	R	L	R	L	R	L	R
901	66	61	0	0	10	36	3	3
902	42	37	0	0	31	103	18	3
903	58	54	0	0	25	85	7	1
904	26	26	0	0	1	17	3	1
905	30	33	0	0	4	19	12	0
906	70	73	0	0	9	83	29	0
907	45	42	0	0	20	63	16	0
909	35	33	0	0	23	34	5	0
910	50	35	0	0	23	33	0	0
911	27	30	0	0	118	55	10	0
912	31	35	0	0	7	30	7	0
913	32	36	0	0	2	18	10	0
915	23	25	0	0	24	33	0	0
916	74	84	0	0	27	40	5	0
917	54	46	0	0	0	63	17	0
919	69	72	0	0	18	39	5	0
921	52	55	0	0	29	36	3	0
922	59	32	0	0	29	53	20	0
923	57	61	0	0	10	49	20	0
925	15	15	0	0	2	6	3	1
927	34	33	0	0	6	47	16	0
928	23	25	0	0	0	29	18	0
929	24	22	0	0	10	23	7	0
931	23	33	0	0	2	7	3	0
932	13	13	0	0	0	4	3	0
935	20	14	0	0	3	15	9	0
937	8	13	0	0	5	9	1	0
938	36	37	0	0	0	17	5	0
939	24	30	0	0	0	30	6	0
940	39	42	0	0	0	40	14	0
941	6	6	0	0	3	6	2	0
943	19	26	0	0	0	17	5	0
944	26	27	0	0	9	6	0	0
945	23	25	0	0	3	21	3	0
946	16	13	0	0	9	7	0	0
947	23	29	0	0	0	2	0	0
950	31	32	0	0	0	24	14	0
951	19	20	0	0	3	13	1	0
953	13	27	0	0	5	26	2	0

Table 9. Number of contacts made by animal's left and right forepaws pre-stroke compared to post-stroke. Evaluating the number of wall contacts made by each animal before and after stroke surgery indicates that attempts to touch the wall with fingertips only occur after stroke surgery, which strongly indicates they are abnormal.

Table 10. This contingency table shows animals that made fingertip contacts to the wall vs. the ones that did not (before/after stroke surgery), indicated that fingertip contacts were only made after injury, so there is high statistical probability that they are abnormal.

	Pre-Stroke	**Post-Stroke**	**Total**
Fingertip touches	0	34	34
No fingertip touches	39	5	44
Total	39	39	78
p-value	< 0.0001 (Fishers exact test)		

To refine wall touches, the numbers of ipsilateral and contralateral contacts made by the animal were first quantified before surgery to establish the baseline, then four days after stroke surgery to evaluate the functional deficit. We looked at the percentage of touches to the wall by right or left paw post-stroke and divided that by their pre-stroke performance rates. When the quotient is 1, the animal had fully regained pre-stroke function, and when the quotient is less than 1, the animal had a functional deficit in that limb. In this modified analysis, I focused on the contralateral side performance by counting any touch to the wall, whether by the palm or the fingertips and compared the percentage of deficit obtained from this quantification method to the percentage of deficit obtained when counting touches made by animal palm (fingertip touches are not included). This refined approach indicates that counting only the numbers of contacts made by palmar pads

is a more sensitive behavioral analysis of functional deficit than including amounts of touches made by both palmar pads and fingertips.

A paired *t*-test with Welch's correction for unequal variances was used for statistical comparison of the percentage of the contralateral deficit before and after stroke using the two methods of counting. Figure 24 (B) showed a reduced functional deficit and improved motor recovery when fingertips touches were included in the analysis, which gave us reduced sensitivity in the assay. Counting only the palmar touches, however gave us contralateral functional deficits that were consistent with the contralateral functional deficits seen in the Montoya Staircase case on Post-stroke days 3, 4, and 5 (Panel A). Again, although these tests use different muscles, this seemed to be a good initial indication that evaluating the Forelimb Asymmetry response with palmar touches only was an improvement.

In Table 11, Forelimb Asymmetry % contralateral deficit, calculated with either palmar touches (middle column) or palmar and fingertip touches (final column) were compared to the contralateral % deficit in Montoya Staircase. The female rats were included to determine if there were any sex differences in the response. In Figure 25 we separated the male rats and in Figure 26 we separated the female rats to perform a linear regression and a correlation analysis to determine which Forelimb Asymmetry method of wall

Figure 24. Percentage of the contralateral deficit in Montoya Staircase analysis versus Forelimb Asymmetry analysis using two methods of counting the wall touches. (A). Quantifying only palm touches in cylinder test shows a similar level of contralateral deficit correlating with Montoya staircase results (p = 0.573, paired t-test with Welch's correction for unequal variances). (B). including fingertips touches with palm contacts (in the same animal) does not accurately reflect the functional deficit that showed by Montoya staircase results (p =0.0001). Each dot represents a single animal. The x-axis displays functional tests (Montoya Staircase vs. forelimb asymmetry (Palm only, A); or palm and fingertips, B). The y-axis shows the percentage of contralateral deficit (%) in each rat measured by different analyses. The broad horizontal bar indicates the group mean and the error bars represent SEM.

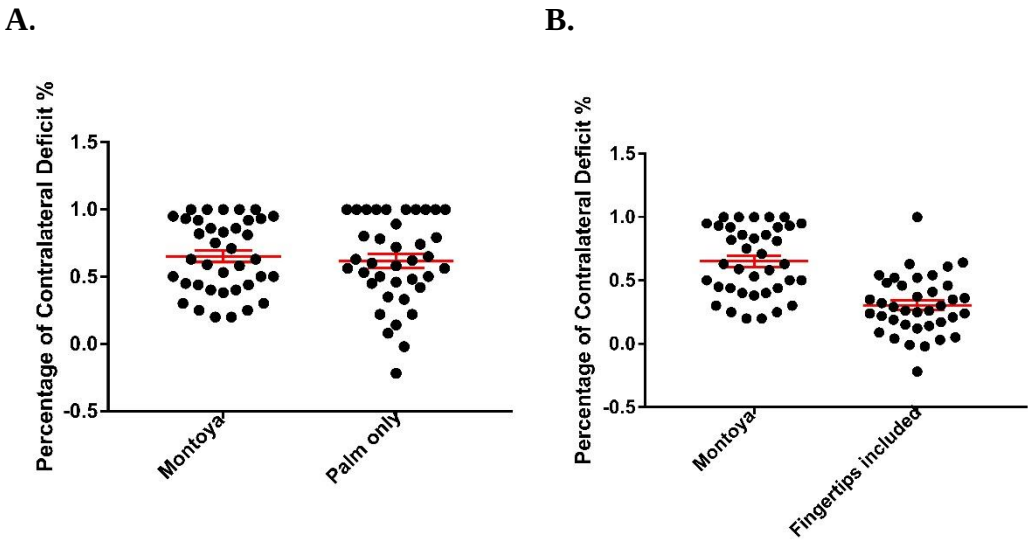

Table 11. Comparison of percentage of contralateral deficit measured by Montoya Staircase versus Forelimb Asymmetry (palmar pads contacts and fingertip attempts to hit the cylinder wall). Only animals that showed 20% deficit on the contralateral side of Montoya staircase analysis were included.

Rat's ID/Gender	Percentage of Contralateral Deficit		
	Montoya Staircase (%)	Forelimb Asymmetry (Palm touches %)	Forelimb Asymmetry (Palm and fingertip touches %)
901F	0.20	0.58	0.52
902F	0.93	0.56	0.41
903F	0.92	0.56	0.48
904F	0.58	0.89	0.64
905F	0.93	0.63	0.04
906F	0.95	0.80	0.36
907F	1.00	0.53	0.30
909F	0.50	0.22	0.12
910F	1.00	0.22	0.22
911F	0.75	0.48	0.29
912F	0.95	0.60	0.32
913F	0.92	0.79	0.15
915F	0.83	1.00	0.35
916F	0.30	0.14	0.05
917F	1.00	1.00	0.61
919F	0.59	0.35	0.24
921F	0.50	0.08	0.03
922F	1.00	0.45	0.26
923F	0.82	0.65	0.21
925M	0.25	0.50	0.17
927M	0.63	0.78	0.37
928M	0.40	1.00	0.26
929M	0.38	0.42	0.19
931M	0.53	0.46	-0.01
932M	0.30	1.00	0.14
935M	0.50	0.72	0.24
937M	0.00	0.06	-0.05
938M	1.00	1.00	0.54
939M	0.25	1.00	0.63
940M	0.81	1.00	0.46
941M	0.44	0.33	0.09
943M	0.71	1.00	0.46
944M	0.86	-0.22	-0.22
945M	0.45	0.74	0.54
946M	0.20	-0.02	-0.02
947M	0.63	1.00	1.00
950M	0.86	1.00	0.25
951M	0.44	0.62	0.52
953M	0.40	0.50	0.35

Figure 25. Linear regression between Montoya staircase deficit and the Forelimb Asymmetry wall touches (palm versus palm + fingertips) in male Sprague-Dawley rats. Comparing the overall average deficit measured by the two methods shows a similar correlation between results of Montoya staircase and Forelimb Asymmetry using the two counting methods of wall contacts. The Y intercept or elevation was significantly different between the two lines (p = 0.0008). In a correlation analysis of this data, the R-squared value for male Montoya staircase vs. Forelimb Asymmetry palm only is R^2= 0.1582 with a p-value of 0.0820, and the R-squared value Montoya staircase vs. Forelimb Asymmetry that analyzed using both palm and fingertip touches is R^2= 0.1021 with a p-value of 0.6279.

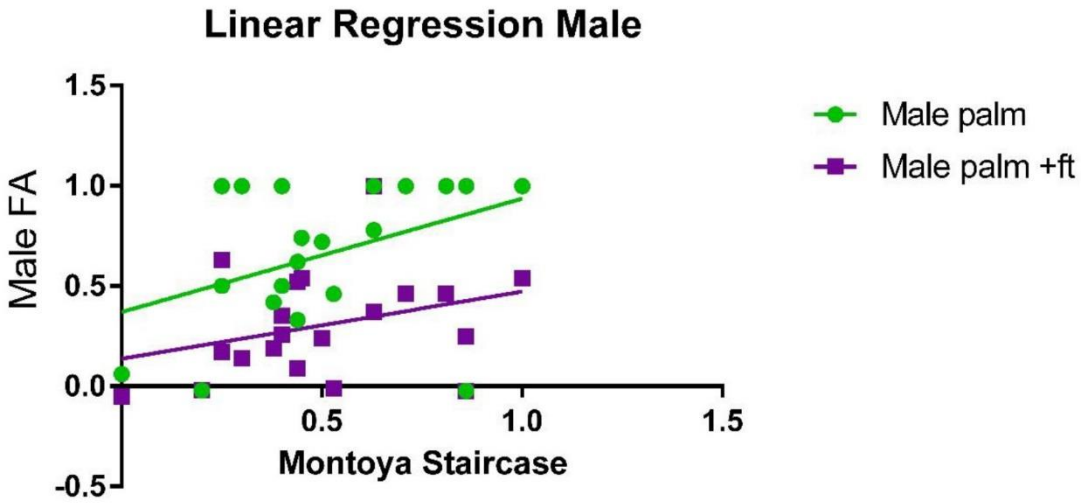

touching correlated better with the Montoya Staircase Analysis. In Female rats, we saw a 10 fold better correlation between the palmar touches and the Montoya staircase percent contralateral deficit. We did see a better correlation with the palmar touches in the male

Figure 26. Linear regression between Montoya staircase deficit and the Forelimb Asymmetry wall touch (palm versus palm + fingertips) deficits in female Sprague-Dawley rats. The elevations or y-intercepts were found to be significantly different (*p*=0.0011). Correlation analysis of these data showed a better correlation between results of Montoya staircase and Forelimb Asymmetry when only palm touches were counted. The R-squared value (R^2= 0.1674; *p* = 0.082) was about 10 fold more than R-squared value when Forelimb Asymmetry was analyzed using both palm and fingertip touches (R^2= 0.01413; *p* = .6279).

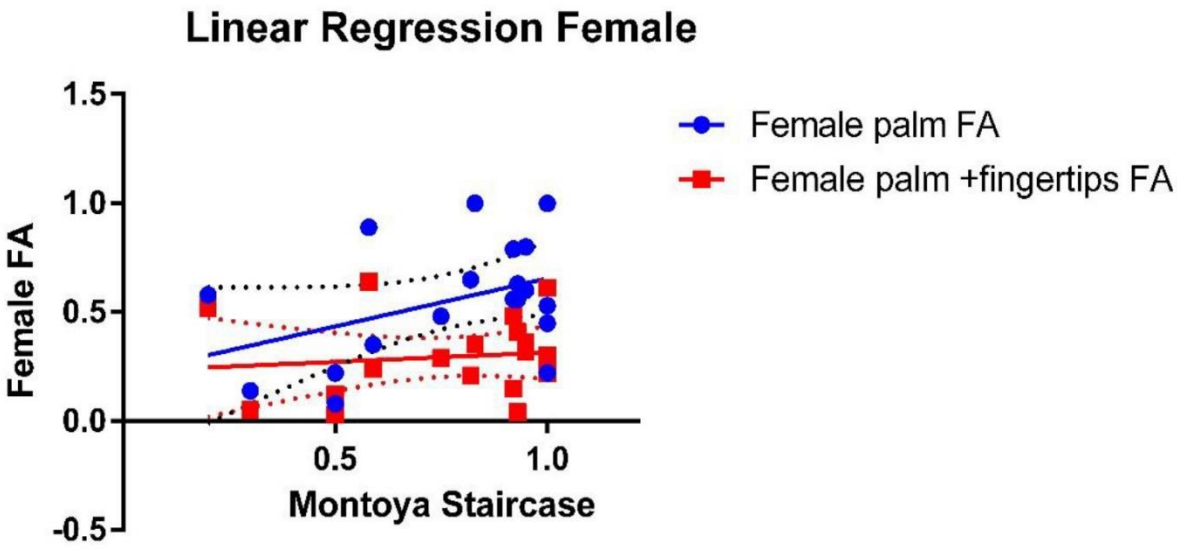

rats as well, and the *p*-value for the R square correlation (0.0824) was remarkably similar to that for the female rat using palm touches (*p*-value of 0.082). In each case, the *p*-value for the R square correlation using the palms and fingertips was much higher (*p* = 0.6279) for males and females (*p* = 0.167). Again, since the muscles used for grasping are different from the muscles used for pressing your hand against a wall, we did not expect a high correlation: the value we obtained seems reasonable in this case.

3.2 Specific Aim II

To investigate the impact of moderate rehabilitation with the impaired arm on functional recovery with and without post-stroke drug treatment.

Adult female Sprague-Dawley rats (10-12 month old) underwent a cerebral ischemic stroke induced by endothelin-1 and were then treated daily using a drug combination of 5 mg/kg fluoxetine and 1 mg/kg simvastatin or a vehicle control beginning 6-12 hours after stroke induction and continued for a total of 91 days. On post-stroke day eight, the rats were subjected to voluntary physical rehabilitation every other day for five and half weeks (a total of 19 days rehabilitation), except when the animals were on restricted diet for Montoya Staircase (fasted overnight, 85% of their *ad libitum* feed for 2 days). The animal groups in this study are laid out in Table 12. We performed Montoya Staircase to evaluate functional recovery on post stroke days 3-5, 28-30, 58-60 and 88-90. All animals were euthanized on post-stroke day 91.

Table 12. Treatment Groups and Rehabilitation for Female Sprague Dawley rats (10-12 month)

Group	Treatment	Rehabilitation	Duration of Treatment
Group I (N= 14)	Vehicle Control	No	90 days
Group II (N=14)	Vehicle Control	Yes	90 days
Group III (N=14)	5 mg/kg fluoxetine + 1mg/kg simvastatin	No	90 days
Group IV (N=18)	5 mg/kg fluoxetine + 1mg/kg simvastatin	Yes	90 days

In pre-stroke training, rats retrieved between 16-18 pellets per forelimb by the end of training. In the rehabilitation assigned group, there was a significant difference

(p=0.002) in the performance of right and left forepaws. More pellets were retrieved using right forepaws (ANOVA; Tukey post-hoc test) as shown in Figure 27.

Evaluating the post-stroke baseline functional deficit (Figure 28) indicates statistically significant functional deficit (p<0.001) in post-stroke contralateral sides of both rehabilitation and non-rehabilitation animals (approximately 55% and 66% functional deficit, respectively) compared to the ipsilateral side, but no significant difference between rehabilitation and non-rehabilitation baseline deficits for contralateral function. The ipsilateral side baseline deficit (26%) of the non-rehabilitation group was found to be significantly different from the rehabilitation group (3%) (p<0.001). This may have been caused by slight differences in the depth of endothelin-1 injection in the stroke induction surgeries, causing the infarct to extend into the corpus callosum.

By examining the influence of physical rehabilitation on contralateral functional recovery (Figure 29), we noticed that the percentage of contralateral functional recovery (26%) in the control rehabilitation group is enhanced compared to the non-rehabilitation group (8.6%), (p =0.014); however, there was no difference in the percentage of contralateral functional recovery between the fluoxetine & simvastatin (FS) rehabilitation group and the FS non-rehabilitation group, where both are showing 34% contralateral recovery (p = 0.98). We did note that the drug plus rehabilitation group reached its 34% recovery in 30 days, while the drug only group took the entire 90 days to reach 34% recovery, showing a steady increase each month. Overall, there is a significant difference between drug-treated groups and control groups (p =0.037) and a significant difference between non-rehabilitation FS group and non-rehabilitation control group (p =0.014) as analyzed with two-way ANOVA.

Both control and drug non-rehabilitation groups show about 23% of ipsilateral functional recovery, which was statistically significant ($p<0.05$) compared to the ipsilateral functional recovery in control and drug rehabilitation groups (~-0.1%) (Figure 30). Of course, the rehabilitation groups did not show an ipsilateral deficit in their baseline deficit following stroke surgery (see Figure 28), so it is not surprising there was no recovery.

Overall, these results suggest that the post-stroke drug combination may allow for functional motor recovery in individuals for whom physical rehabilitation may not be available.

Figure 27. Montoya Staircase Pre-stroke Training. The y-axis depicts the number of pellets retrieved in each group using contralateral (blue bar) or ipsilateral (red bar) forelimb before stroke induction. The x-axis shows the rehabilitation assigned group vs. non-rehabilitation. The graph indicates a significant difference (two-way ANOVA, *p*=0.002; Tukey post-hoc test) between ipsilateral and contralateral forepaw performance among the rehabilitation group, but not the non-rehabilitation group.

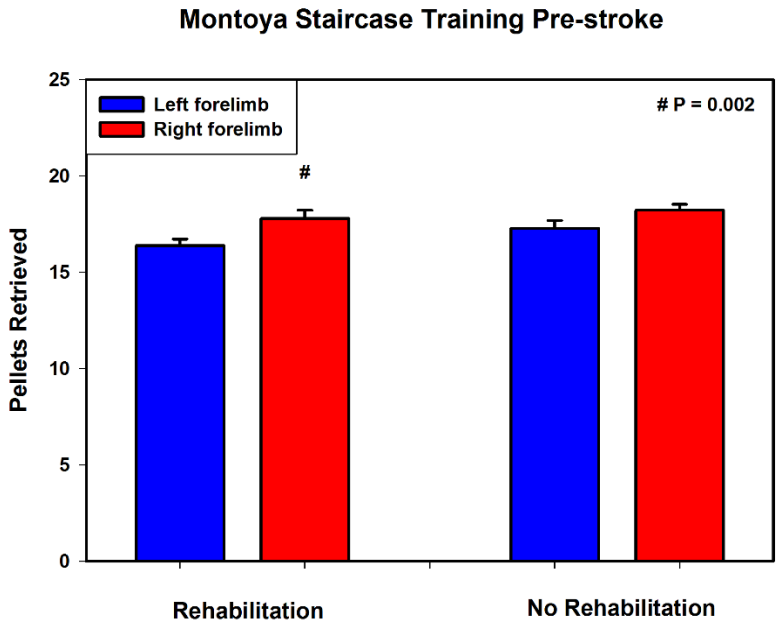

Figure 28. Montoya Staircase Post-Stroke Baseline Functional Deficit. The y-axis depicts functional deficit in contralateral (blue bar) or ipsilateral (red bar) forelimb. The x-axis shows the rehabilitation assigned group vs. non-rehabilitation. The graph indicates a significant functional deficit (p<0.001) in post-stroke contralateral sides of both rehabilitation and non-rehabilitation groups compared to ipsilateral sides. The non-rehabilitation group was significantly different from the rehabilitation group (p<0.001).

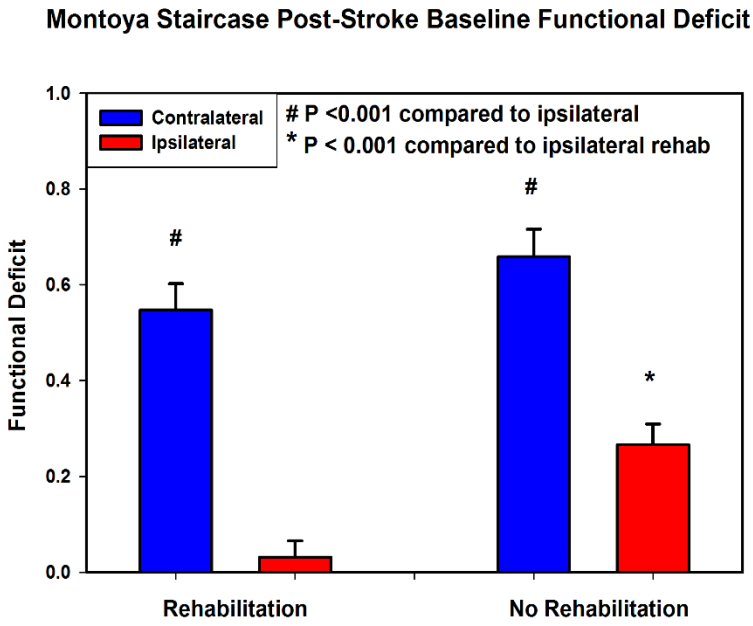

Figure 29. Effect of Physical Rehabilitation on Contralateral Functional Recovery. Yellow bars denote control groups, and green bars denote FS drug treated groups. Rehabilitation groups are indicated by hatched bars, and non-rehabilitation groups are indicated by solid bars. The graph depicts significant difference between drug-treated groups and control groups (p =0.037), and a significant difference between non-rehabilitation FS group (solid green bar) and non-rehabilitation control group (solid yellow bar) (p =0.014).

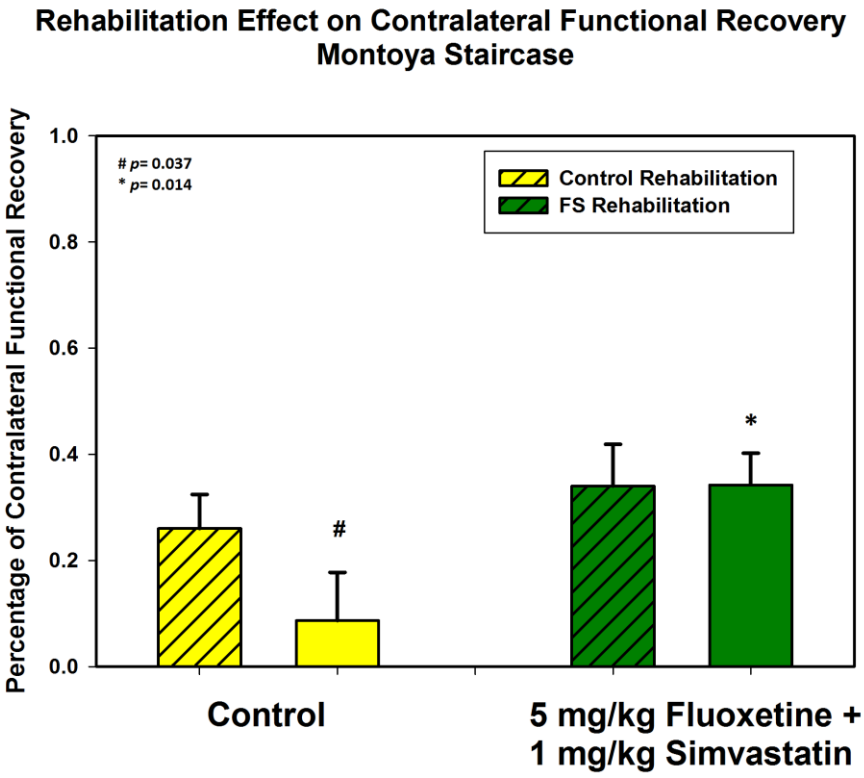

Figure 30. Effect of Physical Rehabilitation on Ipsilateral Functional Recovery. Both control and drug non-rehabilitation groups show about 23% of ipsilateral functional recovery, which was statistically significant (p<0.05) compared to the ipsilateral functional recovery in control and drug rehabilitation groups. The baseline ipsilateral functional deficit in the non-rehabilitation group explains the apparent significant recovery when comparing to rehabilitation group that did not show as much ipsilateral deficit at the baseline (Figure 30).

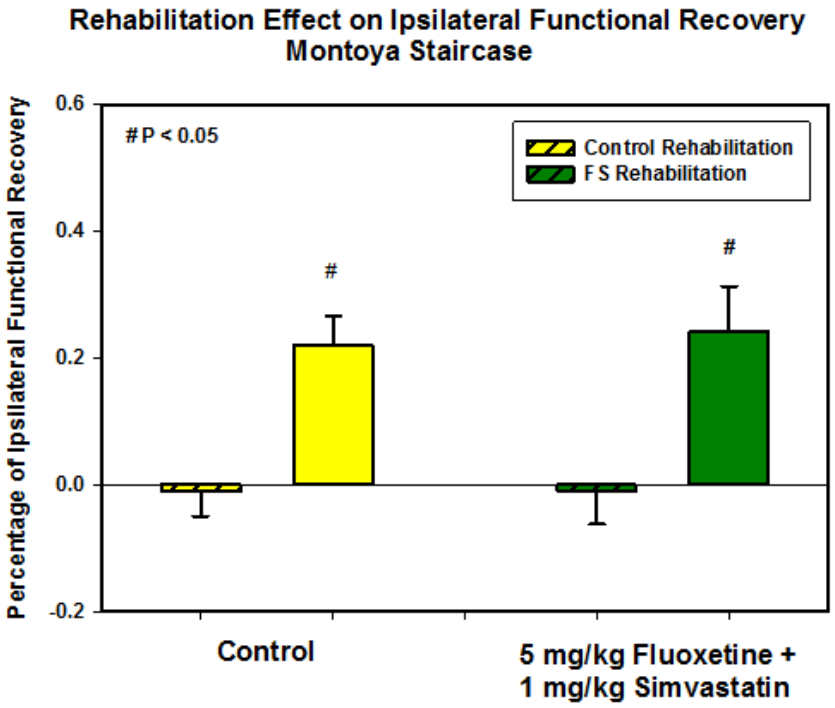

3.3 Specific Aim III

To explore sex-dependent changes in gene expression of inflammation and polarization markers expressed by microglia in the peri-infarct zone in response to combination drug treatment. Neurotrophic factors and synaptic plasticity genes will also be examined in male rats.

The animal groups used in this study are shown in Table 13, with each male group having an N of 6 pre-stroke and each female group having an N of 6 pre-stroke. All animals except the control group, were on simvastatin beginning 7 days pre-stroke and continued daily throughout the study. The functional tests used are shown in the table and were analyzed in the Specific Aim 1. Animals were euthanized on post-stroke day 7, perfused with phosphate-buffered saline, then the brain dissected, blocked and quick frozen in isopentene and dry ice. Peri-infarct region was excised on the cryostat, mRNA prepared,

Table 13. Male and Female Sprague-Dawley rats: Control group received the vehicle. Simvastatin and FSA groups were on 1mg/kg Simvastatin for seven days before stroke induction and continued for six days post-stroke, then euthanized. PSD refers to Post-Stroke Day. All treatment started at 20-26 hours after stroke. There was no Female Simvastatin only group.

Group	Oral Dose	Montoya Staircase	Forelimb Asymmetry	Euthanasia
Male and Female Control Group (N= 6)	Vehicle	PSD 3-5	PSD 4	PSD 7
Male Simvastatin Group (N= 6)	1 mg/kg Simvastatin	PSD 3-5	PSD 4	PSD 7
Male and Female FSA Group (N= 6)	5 mg/kg fluoxetine + 1 mg/kg simvastatin + 20 mg/kg Vit C	PSD 3-5	PSD 4	PSD 7

and reverse transcribed to cDNA with the Qiagen First Strand Kit. cDNA was then applied to custom and purchased micro-array real time PCR microarray plates for analysis of gene

expression differences. All samples in data analysis passed the quality control tests for PCR array reproducibility, reverse transcription efficiency, and genomic DNA contamination test. Hypoxanthine phosphoribosyl transferase-1 (*Hprt1*) and lactate dehydrogenase A (*Ldha*) have been chosen from the housekeeping gene panel for normalization. Other HK genes such as *Ppih*, *Actb* and *Nono*, were not included since they show small variations between the plates.

Data were analyzed, and statistical significance was assessed by using the online software at (http://pcrdataanalysis.sabiosciences.com/pcr/arrayanalysis.php). This online tool does statistical analysis by calculating the *p*-values and fold changes using a Student's *t*-test (two-tail distribution and equal variances between the two samples) based on the Livak method in which, Ct value of the target gene normalized to Ct value of the reference gene in each experiment to obtain ΔCt. Then ΔCt of the Test Sample normalized to ΔCt of the Control Sample to obtain ΔΔCt. The Fold Changes in expression is calculated as 2^-ΔΔCt, and the Fold Regulation is the negative inverse of the fold change.

3.3.1 Results of Profiling Microglia Markers in FSA treated Male Rats vs. Control

RT^2 PCR analysis data was presented as fold-change and fold regulations, where fold-change $2^{\wedge(-\text{ Delta Delta Ct})}$ is the normalized gene expression $2^{\wedge(-\text{ Delta Ct})}$ in the Test Sample divided the normalized gene expression $2^{\wedge(-\text{ Delta Ct})}$ in the Control Sample.

Fold-Regulation represents fold-change results in a biologically meaningful way. Fold-change values greater than 1 indicate a positive or an up-regulation, and the fold-regulation is equal to the fold-change. Fold-change values less than 1 indicate a negative or down-regulation, and the fold-regulation is the negative inverse of the fold-change. The

lists of genes that are presented in result tables were chosen based on fold upregulation >2 or fold down-regulation <-2. Data was sorted by lowest to highest *p*-value. The full lists of all genes including the ones that did not show a significant change are shown in Apendix VII with fold-change and fold-regulation values greater than 2 are indicated in red; fold-change values less than 0.5 and fold-regulation values less than -2 are indicated in blue.

Table 14 represents significantly up-regulated genes in the FSA treatment group versus control in male Sprague-Dawely rats. Signal Transducer and Activator of Transcription *Stat4* and Chemokine (C-C motif) ligand 11 *Ccl11* show fold regulation of 3.74 and 2.08 (p= 0.0323 and 0.0413, respectively). STAT4 protein is involved in both classic and alternative immune responses; it binds to specific regions of DNA to promote T cell activation and proliferation as well as helps in cytokine production. The molecular mechanisms by which STAT4 modulates the immune system are unclear (Wurster, Tanaka, & Grusby, 2000). Chemokine (C-C motif) ligand 11 *Ccl11* is associated with aging in mice and humans (Villeda et al., 2011). Brain-derived neurotrophic factor *Bdnf* was highly

Table 14. Genes up-regulated in FSA treated male rats vs. control group with a fold regulation >2. *Ccl11* and *Stat4* are associated with M1 type microglia, and *Bdnf* is associated with M2a and M2c type microglia.

Up-regulated Genes	Description	Role of the gene	*p*-value	Fold Change	Fold Regulation
Ccl11	Chemokine (C-C motif) ligand 11	M1 marker	0.0323	3.74	3.74
Stat4	Signal transducer and activator of transcription 4	M1 marker	0.0413	2.08	2.08
Bdnf	Brain-derived neurotrophic factor	M2a and M2c marker / growth factor	0.089	3.85	3.85

upregulated in male FSA treated animals (fold regulation 3.85) with a trend toward significance (p =0.089) compared to control group. BDNF has been found to regulate neuronal activity and enhance neurogenesis (Zigova, Pencea, Wiegand, & Luskin, 1998) and we believe this growth factor is contributing to both our functional recovery and smaller infarct size. Our findings on the down-regulated genes in FSA-treated male rats and the corresponding fold regulation and *p*-values are summarized below in Table 15. The only gene that was down-regulated and shows trend towards significance (p=0.094) is the inducible nitric oxide synthase 2 (*Nos2*). This gene is associated with inflammatory M1 microglia and is believed to cause most of the damage following stroke.

Table 15. Down-regulated genes in FSA treated male rats with a fold regulation ≤-2.0

Down-regulated Genes	**Description**	**Role of the gene**	***p*-value**	**Fold Change**	**Fold Regulation**
Nos2	Nitric oxide synthase 2, inducible	M1 marker	0.094	0.50	-2.0

We used the protein-protein interaction (PPI) information reported in STRING software (version 10.0) to predict interactions between genes in certain pathways. We first examined the interaction of the highly up-/down-regulated genes with tightly stringent approach, followed by a loose stringent approach. The networks were identified from a list of pathways based on the count of gene involved and a False Discovery Rate (FDR) threshold less than 0.05. Complete lists of differentially expressed genes are provided in Appendix VII.

3.3.2 Analysis of Protein-Protein Interaction (PPI) in Microglia Markers: Upregulated Microglia Genes in FSA-treated Male Rats vs. Control

PPI Analysis: Network does not have significantly more interactions than expected. This means that current set of proteins is either rather small (i.e. less than 5 proteins or so) or that it is essentially a random collection of proteins that are not very well connected (see Figure 31). This does not necessarily mean that it is not a biologically meaningful selection

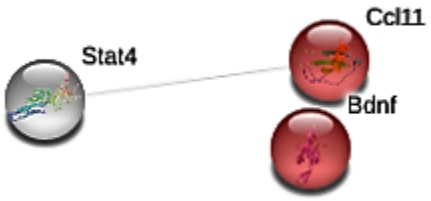

Figure 31. Predicted protein-protein interaction network (PPI) of the up-regulated genes in male FSA treatment group created by STRING 10.0 (tight stringency) (Threshold: 0.4, medium confidence).

of proteins, it could simply be that these proteins have not been studied very much and that their interactions might not yet be known to STRING. All genes that belong to same pathway are represented in red highlighted nodes.

Both *Ccl11* and *Stat4* are M1 microglia biomarkers that are involved in chronic inflammatory response. *Bdnf* gene, however, is an M2 biomarker and essential contributor in neurogenesis. The large nodes suggest that some 3D structure is known or predicted. The very thin line between *Ccl11* and *Stat4* indicates weak interactions between the two molecules.

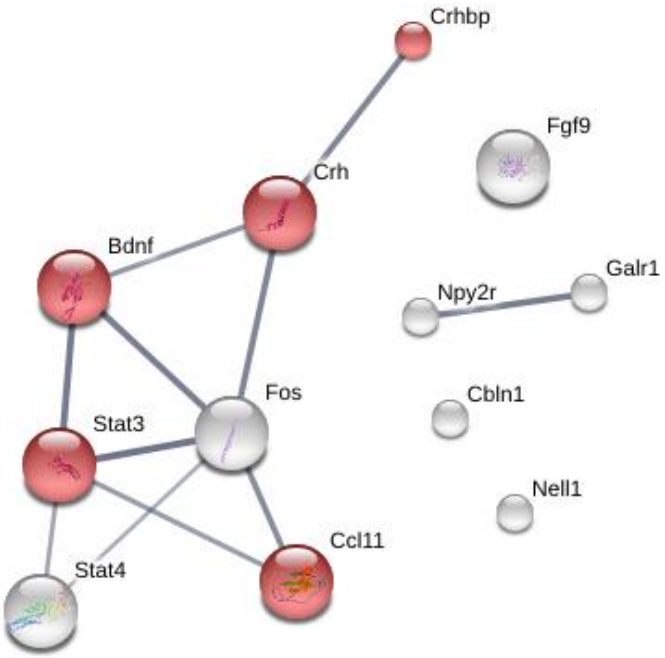

Figure 32. Predicted protein-protein interaction network (PPI) of up-regulated genes in male FSA treatment group (loose stringency) shows 5 genes involved in inflammatory response and positive regulation of cell communication. (Threshold: 0.4, medium confidence).

In Figure 32, we examined protein-protein interaction of the upregulated genes in Male FSA versus control with loose stringency. Here we see growth factors or their receptors up-regulated (*Bdnf*, *Fgf9* and *Npy2r*) with upregulation of *Stat3*, a M2 microglial marker. The network shows interaction between *Stat4*, *Ccl11* (M1 markers) and *Stat3* (M2 marker) because these shifts are fluid rather than absolute, retaining some markers as the shift

occurs. We begin to see interactions between the neuropeptide Y receptor 2 and Gal receptor1, and also see some signs of stress (upregulated corticotropin-releasing hormone releasing hormone and its binding protein), but the binding protein may actually be reducing the stress effect by preventing *Crh* binding to its receptor.

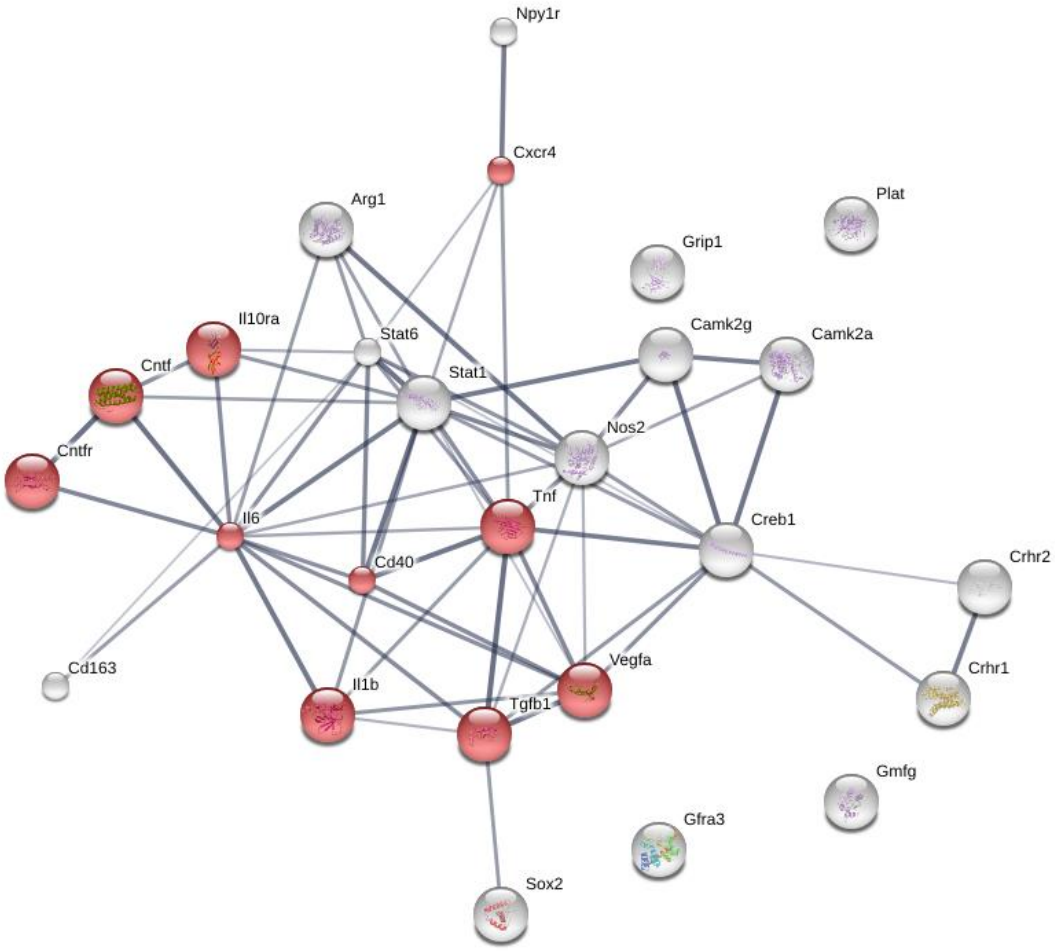

Figure 33. Predicted protein-protein interaction network (PPI) of down-regulated genes in male FSA treatment group (loose stringency) shows a large count of genes involved in cytokine-cytokine receptor interaction. (Threshold: 0.4, medium confidence).

In Figure 33, we see a general downregulation of inflammatory factors (*Cd40, Il6, Stat1, Nos2, Tnf*) but we also see some beginning downregulation of some anti-inflammatory factors (*Tgfb, Il10ra, Arg1*(M2 microglia marker)). We see downregulation of *Crh* receptors and downregulation of some growth factors and neuroplasticity markers.

3.3.3 Results of Profiling Microglia Markers in FSA treated Female vs. Control

Table 16. Up-regulated genes with fold regulation >2 in female rats treated with FSA vs. control.

Up-regulated Genes	Description	Role of the gene	*p*-value	Fold Change	Fold Regulation
Sox2	SRY (sex determining region Y)-box 2	transcription factor	0.047	2.5115	2.5115
Crhr1	Corticotropin releasing hormone receptor 1	receptor in rat microglia	0.103	2.4755	2.4755
Camk2g	Calcium/calmodulin-dependent protein kinase II gamma	CREB cofactor	0.125	2.1039	2.1039
Crh	Corticotropin releasing hormone	Neuropeptide involved in microglia activation	0.147	2.3538	2.3538
Crhbp	Corticotropin releasing hormone binding protein	Neuropeptide	0.215	2.2195	2.2195
Cbln1	Cerebellin 1 precursor	Neuronal apoptosis	0.310	2.0208	2.0208
Nell1	NEL-like 1	Apoptotic factor	0.412	2.1142	2.1142

Table 16 show a significant upregulation of *Sox2* in female rats, which is a transcription factor important for maintaining self-renewal of undifferentiated embryonic stem cells. *Sox2* plays a vital role in maintenance of neural stem cells. Other upregulated

genes that show trend toward significance are *Crhr1, Camk2g, Crh, Crhbp, Cbln1* and *Nell1*.

Crhr1 gene encodes corticotropin releasing hormone receptor-1 (CRH-R1). Both *in vitro* studies on embryonic rat microglia culture (W. Wang, Ji, Riopelle, & Dow, 2002), and in *vivo* studies (Stevens et al., 2003) found that CRH-R1 and CRH-R2 receptors are expressed on microglia in rodent's brain with CRH-R1 being the predominant receptor expressed in rat brain microglia. These findings suggest that microglia may play a role in mediating effects of corticotropin releasing hormone in brain under normal and pathological conditions.

Table 17 indicates a reasonable trend of down-regulation of Arginase *Arg1*, which is an M2a and M2c biomarker that involved in cellular response to hydrogen peroxide, tissue remodeling, response to toxic substance and response to wounding (Kolluru, Bir, & Kevil, 2012).

Table 17. Down-regulated genes in female rats treated with FSA

Down-regulated Genes	Description	Role of the gene	*p*-value	Fold Change	Fold Regulation
Arg1	Arginase	M2a, M2c marker	0.155	0.3795	-2.6353

3.3.4 Analysis of Protein-Protein Interaction (PPI) in Microglia Markers:
Up-regulated Microglia Genes in FSA-treated Female Rats vs. Control

PPI Analysis: The network has significantly more interactions than expected. Proteins have more interactions among themselves than what would be expected for a random set of proteins of similar size, drawn from the genome. Such an enrichment indicates that the proteins are at least partially biologically connected, as a group.

For tight clustering using only the upregulated genes from Table 16, the predicted graph shows the highest number of genes are involved in two networks consisting of 6 and 4 genes. These networks are: single-organism cellular process and regulation of synapse structure or activity (Figure 34 A and B).

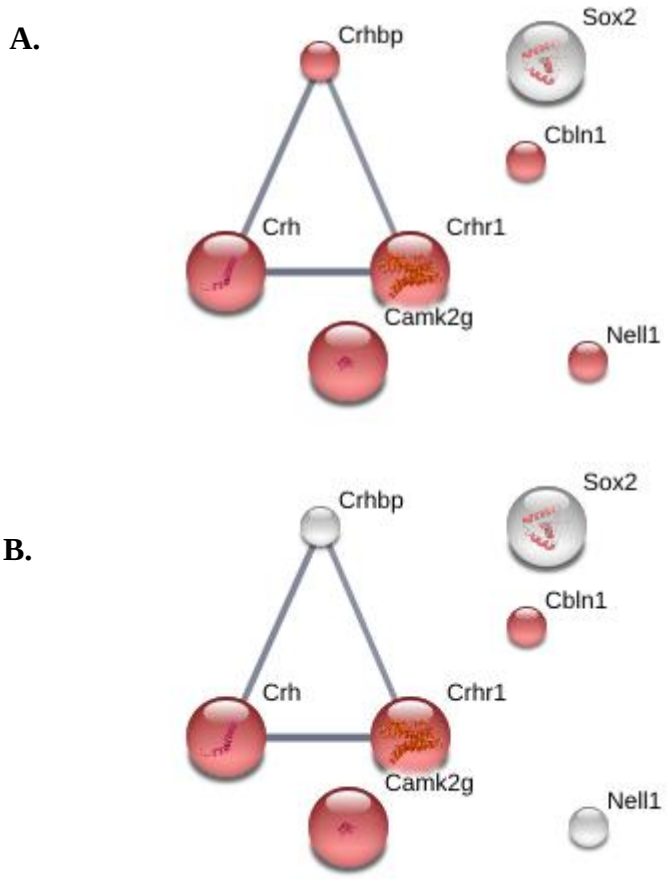

Figure 34. PPI analysis of up-regulated genes in female FSA treatment group (tight stringency). (A). Genes involved in single-organism cellular process. (B). Genes play role in regulation of synapse structure or activity. (Threshold: 0.4, medium confidence).

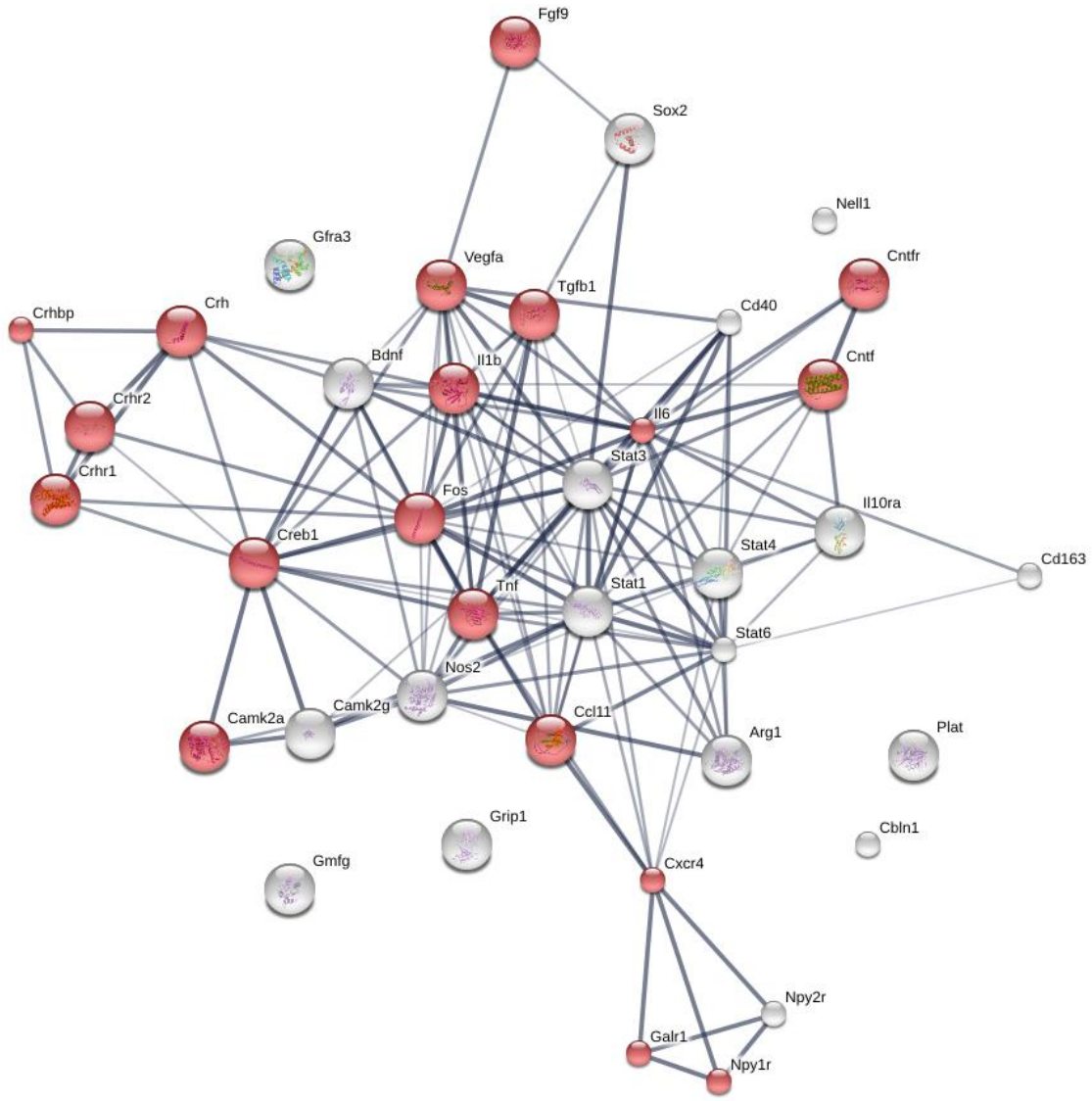

Figure 35. PPI analysis of up-regulated genes in female FSA treatment group (loose stringency) shows 19 microglia genes are involved in positive regulation of cell communication.

In Figure 35, we see interactions that may have occurred if we had used a higher N in our gene analysis to obtain lower p values. We see a stress network (Crh receptors and binding protein) connected to synaptic plasticity network (*Creb1, Camk2a, Camk2g, Bdnf)* and also see more growth factors upregulated. This network is strikingly more complex than that seen in male rats with the same drug treatment.

3.3.5 Results of Profiling Microglia Markers in Simvastatin-treated Male Rats vs. Control

Testing samples from male rats pre-treated with simvastatin for 7 days before stroke surgery, and 6 days after stroke induction shows that Chemokine (C-C motif) ligand 11 (*Ccl11),* which is associated with M1 microglia, is significantly up-regulated as seen in FSA treated male rats but not FSA treated females. In addition, both cerebellin 1 precursor and Brain-derived neurotrophic factor were highly expressed.

Table 18. Up-regulated genes in male rats treated with simvastatin compared to control.

Up-regulated Genes	Description	Role of the gene	*p*-value	Fold Change	Fold Regulation
Ccl11	Chemokine (C-C motif) ligand 11	M1 marker	0.022319	2.3405	2.3405
Cbln1	Cerebellin 1 precursor	Regulates synapse function	0.185183	2.0057	2.0057
Bdnf	Brain-derived neurotrophic factor	M2a and M2c marker/ growth factor	0.200537	3.0055	3.0055

In contrast to FSA treated males, none of the genes in simvastatin treatment group was significantly down-regulated to -2. This suggests a possible essential role of fluoxetine as an anti-inflammatory agent inhibiting the inducible nitric oxide synthase 2 (*Nos2*), which associated with inflammatory M1 microglia.

3.3.6 Analysis of Protein-Protein Interaction (PPI) in Microglia Markers: Up-regulated Microglia Genes in Simvastatin-treated Male Rats vs. Control

PPI Analysis: As seen in FSA male groups, network does not have significantly more interactions than expected. Although the upregulated genes are not directly connected to each other, the STRING system proposed that all of these genes are involved in positive regulation of cellular component biogenesis and both *Bdnf* and *Cbln1* contribute to positive regulation of synapse assembly.

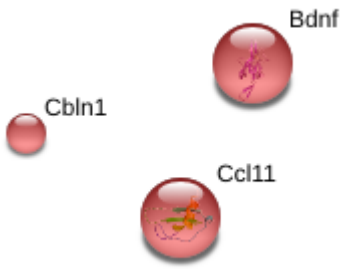

Figure 36. PPI analysis of up-regulated genes in male simvastatin treatment group. (Tight stringency) (Threshold: 0.4, medium confidence).

Figure 36 shows the protein-protein interaction analysis with loose stringency to both upregulated and down-regulated genes displays 16 up-regulated genes that are connected in positive regulation of signal transduction. We see upregulation of growth factors and their receptors (*Bdnf*, *Cntf*, receptors for neuropeptide Y) and synaptic plasticity

genes. Interestingly, we see association of the Stat genes that are associated with the different M1 and M2 microglial subtypes, as well as other associated markers, again suggesting a fluid transition from one microglial subtype to another. These genes seem to be predominately anti-inflammatory. On the other hand, three of the down-regulated genes (*Vegfa*, *Nos2* and *il6*) appear to be involved in hypoxia-inducible factor (HIF-1) signaling pathway that mediates the cellular oxygen signaling pathway, and plays a multifaceted role of HIF-1 in outcomes of ischemic stroke (Kalakech et al., 2013), (Sharp, Bergeron, & Bernaudin, 2001) .

A.

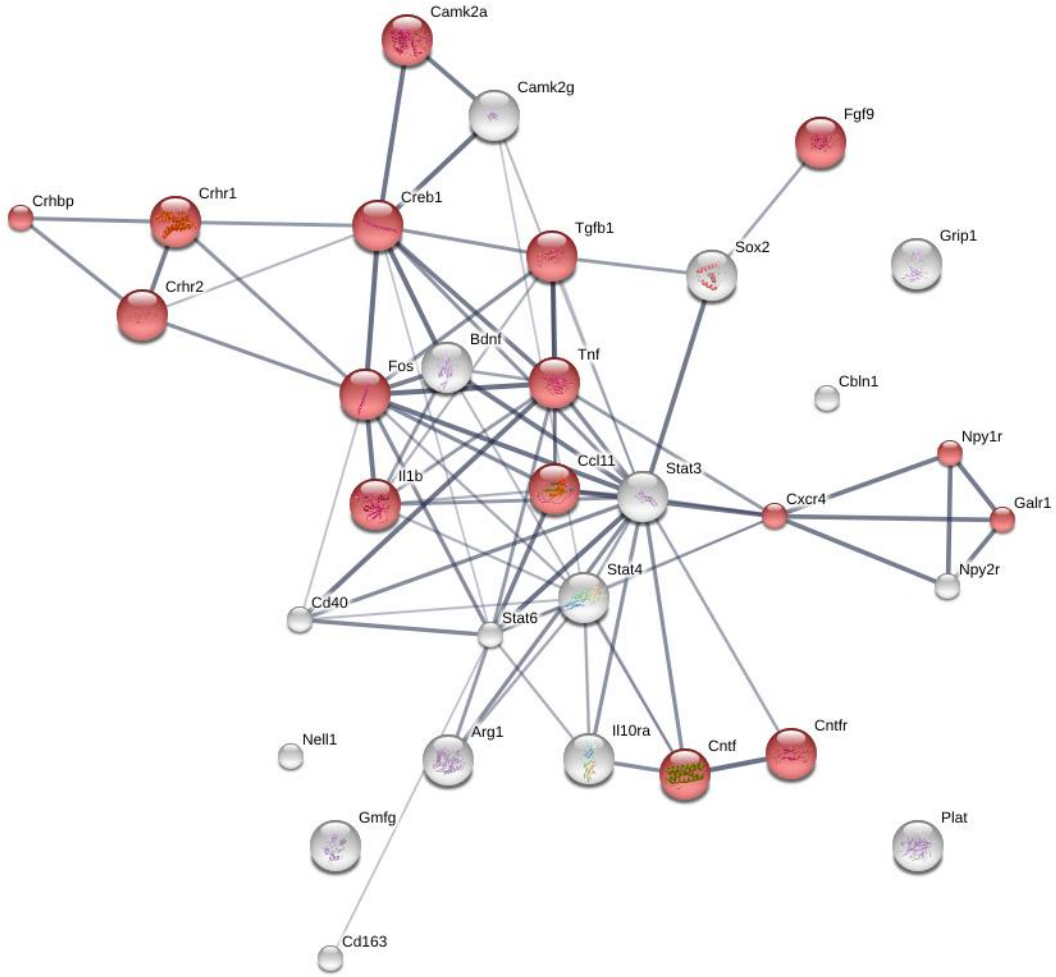

B.

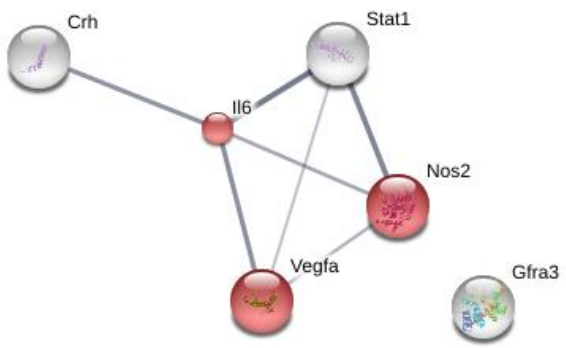

Figure 37. PPI analysis of up-regulated genes in male simvastatin treatment group (A); and down-regulated genes (B) (loose stringency). (Threshold: 0.4, medium confidence).

3.3.7 Comparing the Expression of Microglia Markers in FSA treated Female Rats to FSA treated Males

Examining changes in gene expression patterns in female rats in relation to same age male rats that received same drug combination treatment (used as control in this analysis) showed a tendency towards statistical significance in the expression of a potent neurotrophic factor, GDNF family receptor alpha 3 (*Gfra3)*, with a 6 fold increase. This protein play key role in the control of neuron survival and differentiation. Other up-regulated genes in response to the FSA treatment in female rats are: cluster of differentiation (*Cd163* gene), which is an M2 microglia marker that is expressed when microglia is recruited to sites of ischemia (Cherry, Olschowka, & O'Banion, 2014). CD163 protein functions in hemoglobin scavenging (Kowal et al., 2011), and it has been used in experimental studies to identify M2 microglia in rat traumatic brain injury (Z. Zhang, Zhang, Wu, & Schluesener, 2012). Moreover, multiple pro-inflammatory biomarkers of M1 microglia appear to be up-regulated in females compared than male rats, which include *Il1b, Nos2, Tnf, Stat1, il10ra* and *Il6* cytokines.

Although there was no significant difference in gene expression between the two tested genders, this pattern of response to the drug treatment in female rats may promote future studies to build on these findings and determine whether the two genders are significantly different from one another. Significant variation could be seen after increasing the number of experimental animals.

Gene regulation pattern in female FSA treated animals vs. male FSA treated animal is represented in Table 19.

Table 19. Up-regulated genes in female FSA treated group compared to male FSA treated rats.

Up-regulated Genes	Description	Role of the gene	*p*-value	Fold Change	Fold Regulation
Gfra3	GDNF family receptor alpha 3	Neurogenesis	0.084574	5.8624	5.8624
Cd163	CD163 molecule	Cytokine	0.089223	3.0674	3.0674
Cntf	Ciliary neurotrophic factor	Neurotrophic factor/ Cell differentiation	0.105728	2.2289	2.2289
Il1b	Interleukin 1 beta	Cytokine	0.150449	3.2735	3.2735
Nos2	Nitric oxide synthase 2, inducible	M1 marker	0.174178	2.371	2.371
Tnf	Tumor necrosis factor	Cytokine / M1 marker	0.273191	3.012	3.012
Tgfb1	Transforming growth factor, beta 1	Growth factor	0.295521	2.6995	2.6995
Cxcr4	Chemokine (C-X-C motif) receptor 4	Cytokine / M1 marker	0.346437	3.4937	3.4937
Stat1	Signal transducer and activator of transcription 1	M1 marker	0.352873	2.3304	2.3304
il10ra	Interleukin 10 receptor, alpha	Cytokine / M1 marker	0.464164	2.0297	2.0297
Cd40	CD40 molecule, TNF receptor superfamily member 5	Apoptotic factor	0.487533	2.4509	2.4509
Gmfg	Glia maturation factor, gamma	Growth factor	0.582022	2.2929	2.2929
Il6	Interleukin 6	Cytokine	0.639032	2.3906	2.3906

3.3.8 Analysis of Protein-Protein Interaction (PPI) in Microglia Markers: Up-regulated Microglia Genes in Female FSA vs. Male FSA Group

PPI Analysis: Network has significantly more interactions than expected. Figure 38 shows six genes in the tight stringency analysis appear to influence positive regulation of response to external stimulus. These are the neurotrophic factor ciliary neurotrophic factor (*Cntf),* M1 microglia markers; interleukin 1 beta (*Ilb),* Tumor necrosis factor (*Tnf),* Interleukin 6 (*Il6)* and Chemokine (C-X-C motif) receptor 4 *(Cxcr4)* (red highlighted nodes in Figure 38). In the loose stringency prediction, half of all upregulated genes are involved in signal transduction and cell communication (Figure 39).

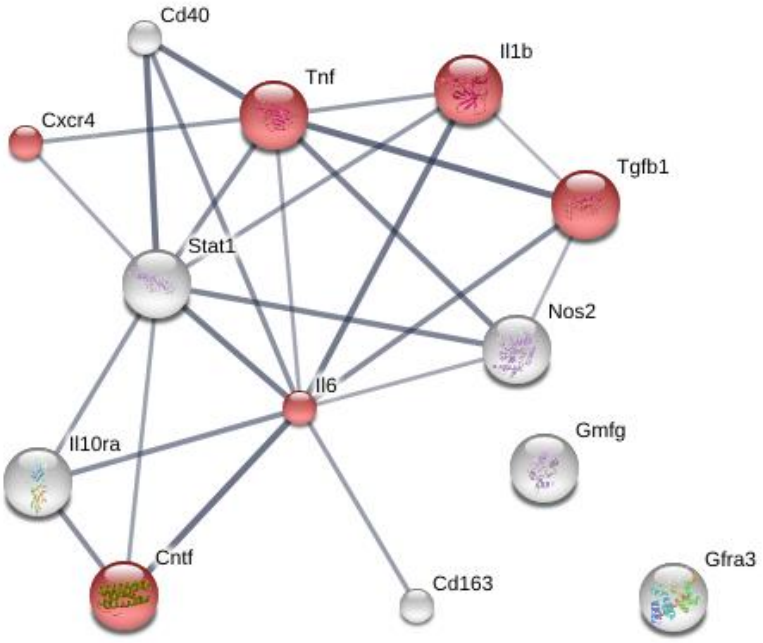

Figure 38. PPI analysis of up-regulated genes in female FSA treatment group compared to male FSA group (tight stringency). (Threshold: 0.4, medium confidence).

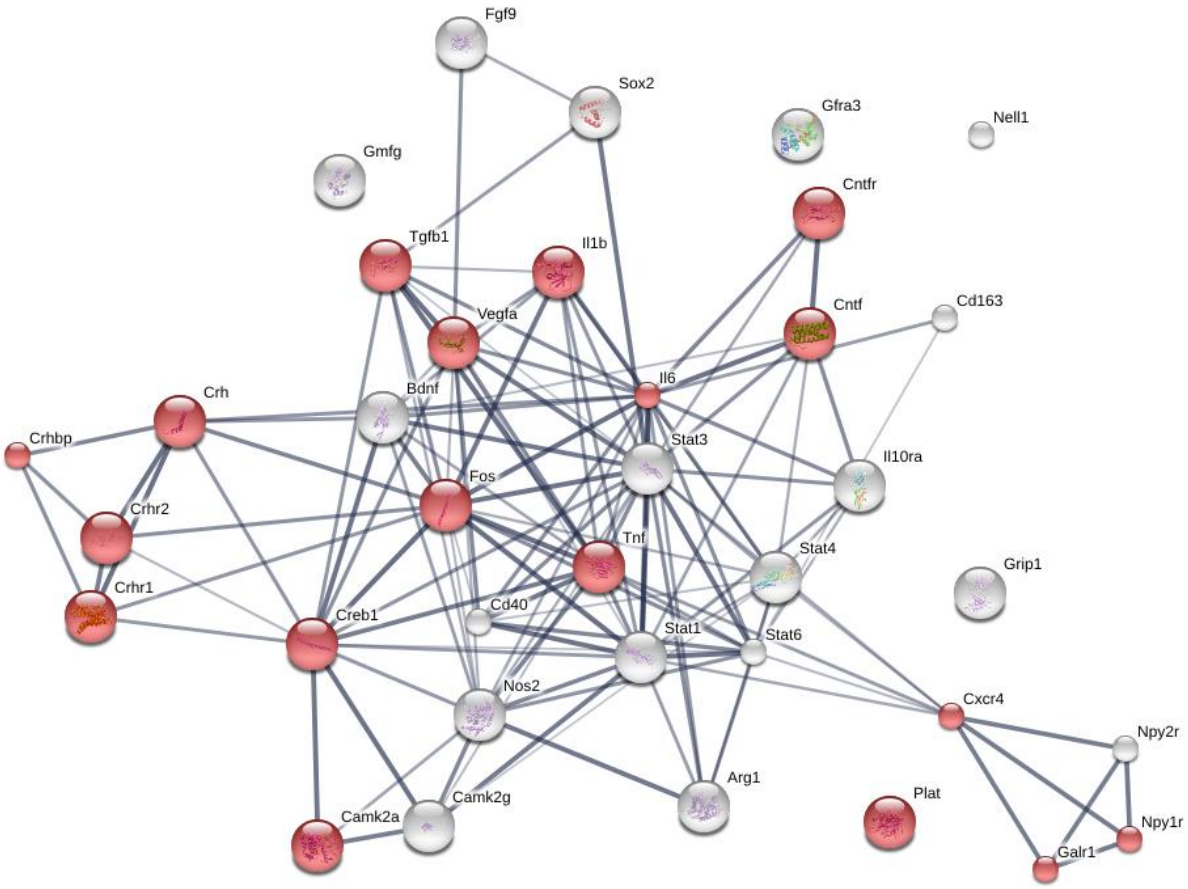

Figure 39. PPI analysis of up-regulated genes in female FSA treatment group compared to male FSA group (loose stringency). Graph indicates that (Threshold: 0.4, medium confidence).

3.3.9 Comparing the Expression of Microglia Markers in Female Control against Male Control Group

Profiling gene expression in female control group against male control (Table 20) shows that *Sox2* is the only significant down-regulated gene with a *p*-value 0.046. A group of 10 other genes were down-regulated with at least a -2 fold regulation. This may indicate a sex-dependent difference in gene expression pattern in response to endothelin induced stroke. The down-regulated genes are presented in the table below and their predicted interactions are demonstrated in Figures 40 and 41.

Table 20. Down-regulated genes in control female rats compared to control male rats.

Down-regulated Genes	Description	Role of the gene	*p*-value	Fold Change	Fold Regulation
Sox2	SRY (sex determining region Y)-box 2	Transcription factor	0.046	0.403	-2.4814
Cntfr	Ciliary neurotrophic factor	Neurotrophic factor/ Cell differentiation	0.074	0.4995	-2.0022
Camk2g	Calcium/calmodulin-dependent protein kinase II gamma	CREB cofactor	0.130	0.4639	-2.1558
Fgf9	Fibroblast growth factor 9	Cell differentiation	0.1307	0.4431	-2.2566
Npy2r	Neuropeptide Y receptor Y2	Neuropeptide	0.151	0.4974	-2.0105
Crhr1	Corticotropin releasing hormone receptor 1	CRH receptor	0.172	0.4365	-2.2911
Npy1r	Neuropeptide Y receptor Y1	Neuropeptide	0.268	0.4962	-2.0152
Cbln1	Cerebellin 1 precursor		0.286	0.4205	-2.3784
Arg1	Arginase	M2 marker	0.343	2.6161	2.6161
Camk2a	Calcium/calmodulin-dependent protein kinase II alpha	Synaptic plasticity	0.415	0.4426	-2.2593
Nell1	NEL-like 1	Apoptotic factor	0.443	0.4082	-2.4496

3.3.10 Analysis of Protein-Protein Interaction (PPI) in Microglia Markers: Down-regulated Microglia Genes in Female Control vs. Male Control Group

PPI Analysis: The network has significantly more interactions than expected. In Figure 40, regulation of synapse structure or activity is the only predicted biological pathway in which 4 genes are involved. These genes are (*Crhr1, Camk2a, Camk2g* and *Cbln1)*. Under-expression of these important genes in control untreated female rats when compared to control males worth further investigation. The loose stringency analysis in Figure 41 shows that genes are primarily involved in signal transduction and cellular response to endogenous stimulus and cell differentiation.

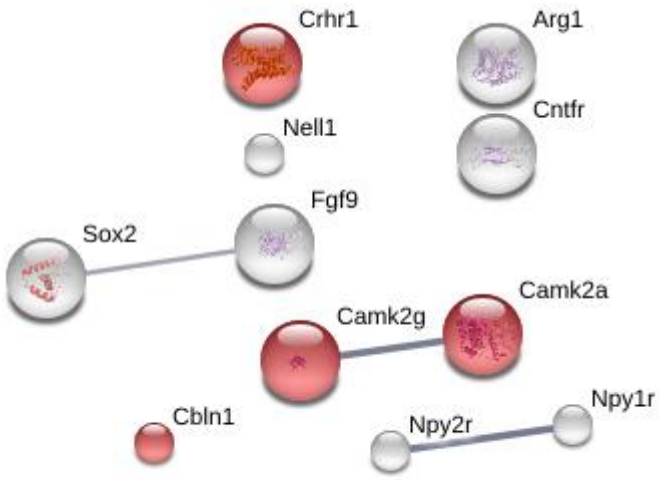

Figure 40. PPI analysis of down-regulated genes in female control group compared to male control group (tight stringency). (Threshold: 0.4, medium confidence).

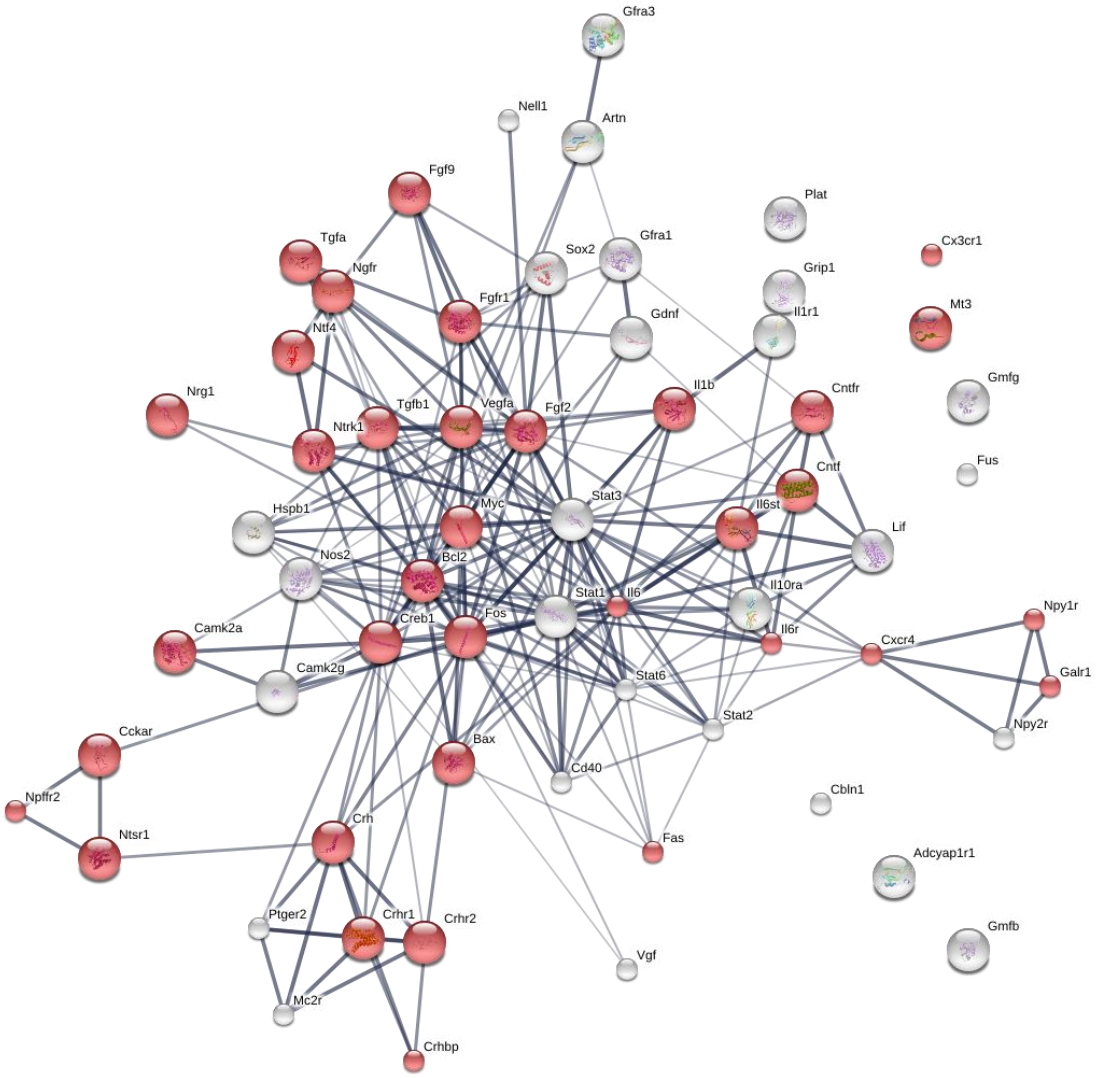

Figure 41. PPI analysis of down-regulated genes in female control group compared to male control group (loose stringency). (Threshold: 0.4, medium confidence).

3.3.11 Results for Neurotrophic Gene Profiling in Male Rats

Gene analysis of neurotrophic factors and their receptors shows upregulation of multiple growth factors and their receptors in Table 22 and downregulation of genes in Table 23. Male (10-12 months) Sprague-Dawley rats that were treated with FSA for 7 days after stroke and were compared to vehicle control in this gene expression analysis according to the groups are listed in Table 22.

Table 21. Treatment groups for genetic analysis of neurotrophic factors

RT-qPCR Array	Control Group	FSA Group
Neurotrophins and Receptors	N=6	N=5

In Table 23, one of the markedly up-regulated genes is orexin (also known as hypocretin *HcRt)* with a trend towards significance in FSA treated group of male Sprague-Dawley rats. This was similar to previous results in female rats using this same microarray plate. In the current study on male FSA treated vs. control, orexin (*HcRt*) shows about 10 fold of increase (9.92). Our previous work on female rats (10-12 month) treated with the same dose of FSA for 10 days after stroke showed that *HcRt* was upregulated to 2.06 fold. Another experiment in our lab on female 10-12 month rats using fluoxetine and simvastatin (FS) without ascorbic acid for 10 days treatment indicates that orexin receptors *Hctr1 and Hctr2* are up-regulated to 2.07 and 2.93, respectively ($p < 0.05$). This suggests that males and females may require different drug combinations for optimal recovery after stroke.

A summary of the main orexinergic pathways and receptor mRNA distribution in the rat brain is illustrated in Figure 42. Note particularly that the orexin receptors are in the

cortex itself, and are thought to increase Bdnf when activated. In human stroke patients, decrease in orexin in the blood following stroke has been observed. This upregulation of receptors that we see may help counter the drop of orexin in this region, helping more of the cortex survive. Other potential players in the possible neuroprotective role of the drug combination are listed below in Table 22 and Table 23.

Table 22. Neurotrophic Factors and Receptors: Gene profiling in male Sprague-Dawley rats shows up-regulated genes in FSA treated group vs. control group.

Up-regulated Genes	Description	Role of the gene	*p*-value	Fold Change	Fold Regulation
Nr1i2	Nuclear receptor subfamily 1, group I, member 2	Transcription factor	0.039	3.77	3.77
HcRt	Orexin/Hypocretin	Neuropeptide	0.128	9.92	9.92
Grpr	Gastrin releasing peptide receptor	Neuropeptide	0.132	2.24	2.24
Bdnf	Brain-derived neurotrophic factor	M2a and M2c marker/ growth factor	0.275	3.97	3.97

Table 23. Neurotrophic Factors and Receptors: Gene profiling in male Sprague-Dawley rats shows down-regulated genes in FSA treated group vs. control group.

Downregulated Genes	Description	Role of the gene	*p*-value	Fold Change	Fold Regulation
Fas	Fas (TNF receptor superfamily, member 6)	Apoptotic factor	0.031	0.40	-2.47
Il1b	Interleukin 1 beta	M1 marker	0.032	0.38	-2.57
Il10	Interleukin 10	M1 marker	0.059	0.45	-2.21
Lif	Leukemia inhibitory factor	Cytokine	0.149	0.28	-3.52
Hspb1	Heat shock protein 1	Apoptotic factor	0.160	0.35	-2.79
Il6	Interleukin 6	M1 marker	0.210	0.36	-2.74
Cxcr4	Chemokine (C-X-C motif) receptor 4	Cytokine	0.260	0.43	-2.27
Myc	Myelocytomatosis oncogene	Apoptotic factor	0.490	0.49	-2.03

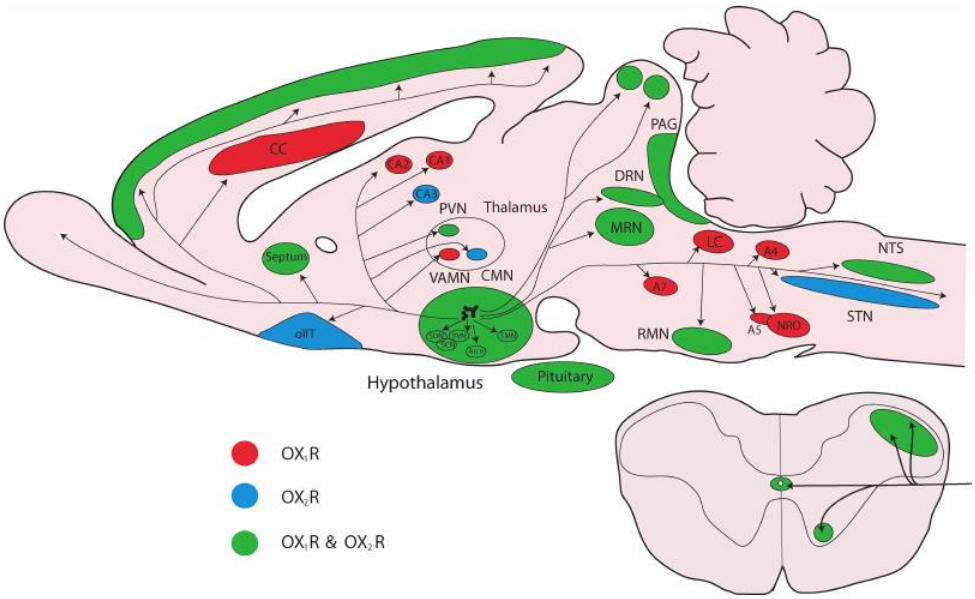

Figure 42. The schematic diagram illustrates the majority of orexinergic pathways and locations in brain. The level of expression varies between areas. CA1–3 = areas of hippocampus; CC = cingulate cortex; CMN = centromedial nucleus; DRN = dorsal raphe; LC = locus coeruleus; MRN = median raphe nucleus; NST = nucleus of solitary tract; olfB = olfactory bulb; olfT = olfactory tubercle; PVN = paraventricular nucleus; NRM = nucleus raphe magnus; RO = nucleus raphe obscurus; SCN = suprachiasmatic nucleus; SON = supraoptic nucleus; STN = spinal trigeminal nucleus; TMN = tuberomamillary nucleus; VAMN = ventral anteromedial nuclei. Adapted from The Hypothalamic Orexinergic System: Pain and Primary Headaches (Holland & Goadsby, 2007).

3.3.12 Analysis of Protein-Protein Interaction (PPI) within Neurotrophic Genes in Male Rats

PPI Analysis: The tight stringency analysis of upregulated genes for Male FSA versus control is shown in Figure 43. The network does not have significantly more interactions than expected. This could be explained by the small number of interacting proteins or because it is essentially a random collection of proteins that are not very well connected. Again, this does not necessarily mean that it is not a biologically meaningful selection of proteins, it could be that these proteins have not been studied very much and that their interactions might not yet be known to STRING.

The loose stringency analysis of the upregulated genes in Figure 45 indicates that the upregulated *HcRt* and *Bdnf* genes networked through the neuropeptide Y receptors.

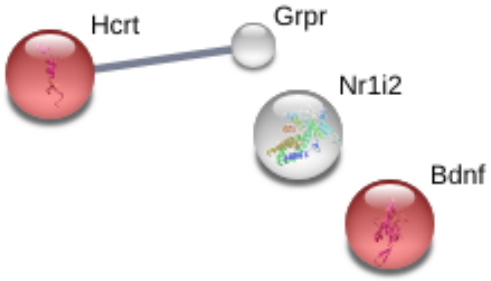

Figure 43. PPI analysis of up-regulated neurotrophic genes in male FSA group compared to male control group (tight stringency). (Threshold: 0.4, medium confidence).

On the other hand, PPI prediction shows that down-regulated neurotrophic factors are part of regulatory pathway of programmed cell death (Figure 44, A) and inflammatory immune response process (Figure 44, B). Loose stringency (Figure 46) showed more network connections

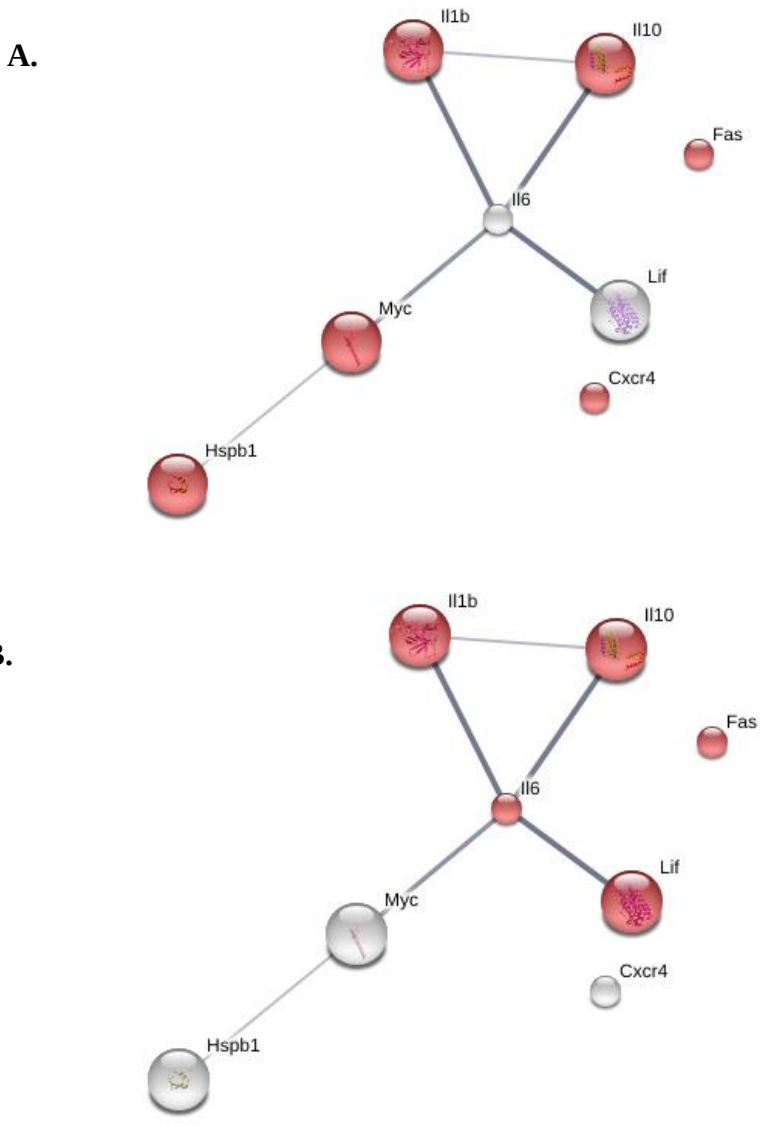

Figure 44. PPI analysis of down-regulated neurotrophic genes in male FSA group compared to male control group (tight stringency). A. Genes that involved in regulation of apoptosis; B. Genes that involved in immune response. (Threshold: 0.4, medium confidence).

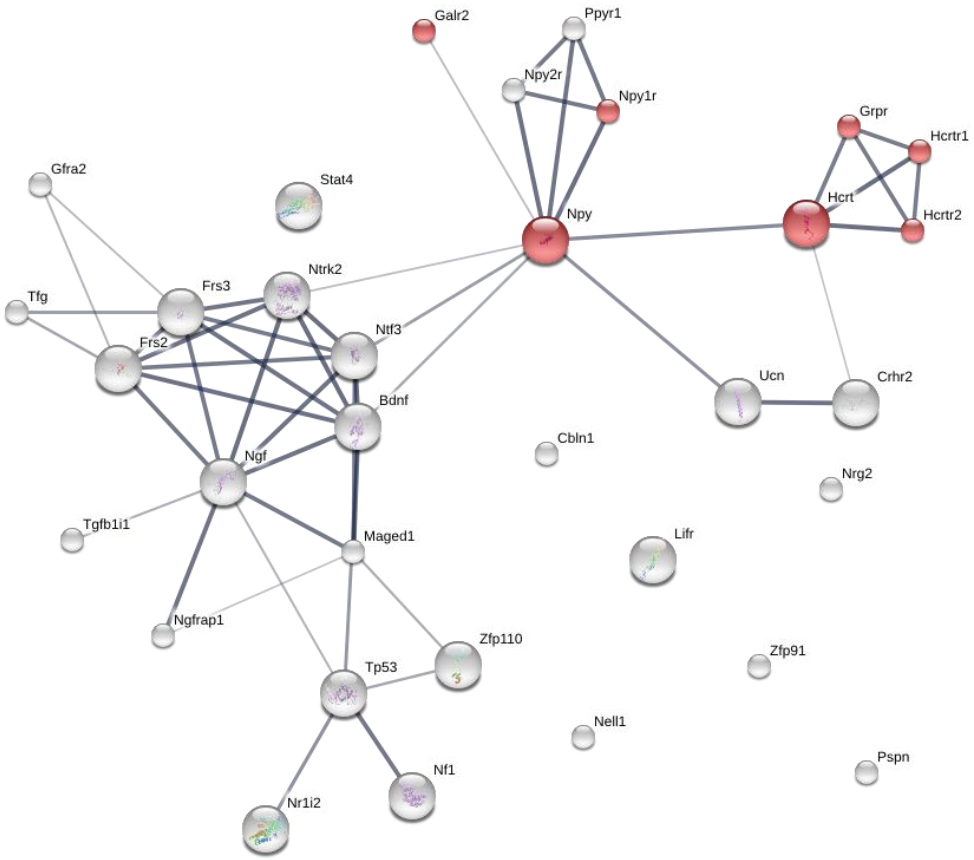

Figure 45. PPI analysis of up-regulated neurotrophic genes in male FSA group compared to male control group (loose stringency). (Threshold: 0.4, medium confidence).

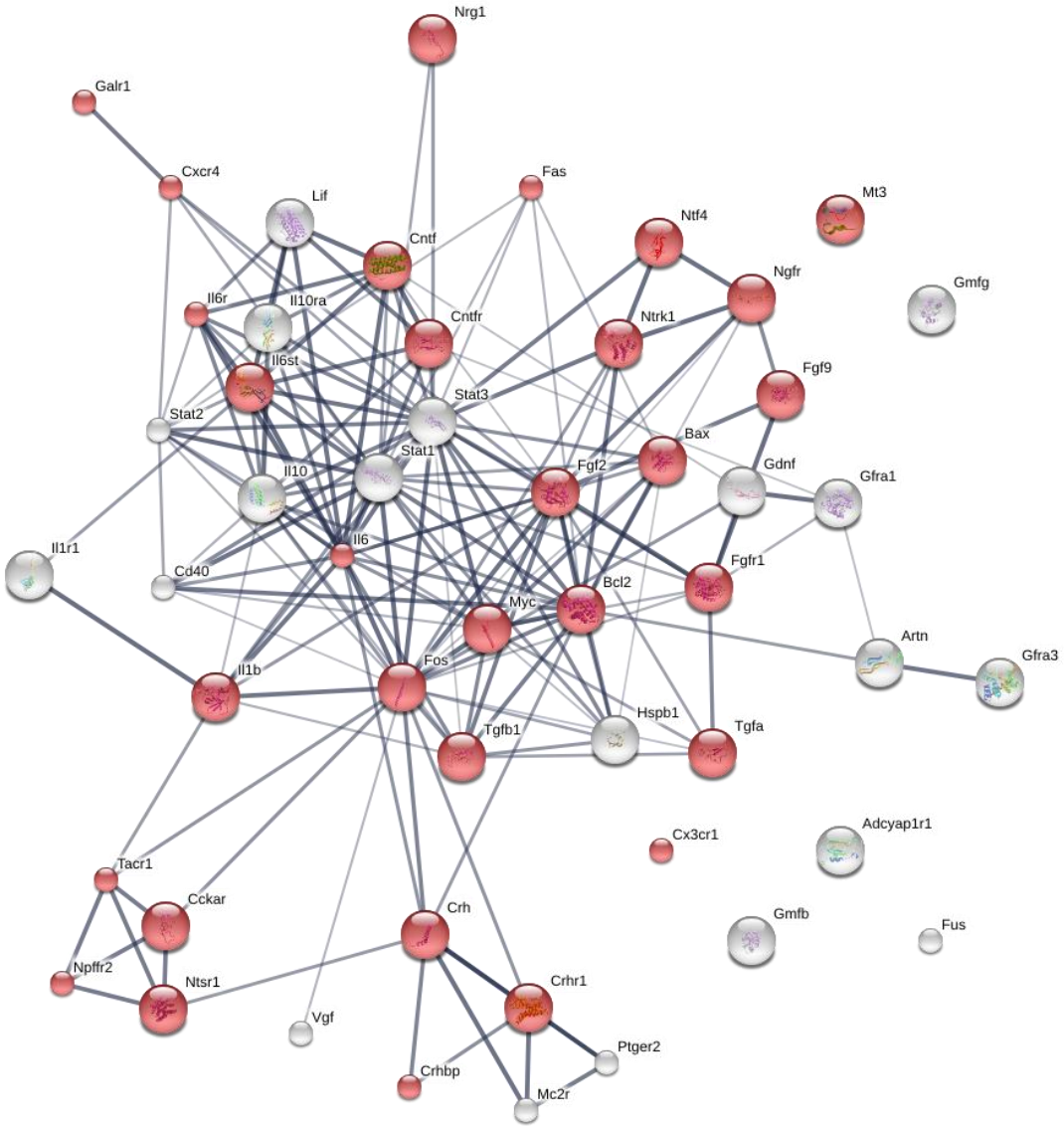

Figure 46. PPI analysis of down-regulated neurotrophic genes in male FSA group compared to male control group (loose stringency). (Threshold: 0.4, medium confidence).

3.3.13 Results for Synaptic Plasticity Gene Profiling in Male Rats

Table 24 shows the number of animals used in RT-qPCR analysis of synaptic plasticity gene upregulation in male (10-12 months) Sprague-Dawley rats that treated with FSA for 7 days after stroke were compared to vehicle control.

Table 24. Treatment groups for genetic analysis of synaptic plasticity factors

RT-qPCR Array	Control Group	FSA Group
Synaptic Plasticity	N=6	N=5

Profiling of synaptic plasticity genes of FSA-treated male animals in Table 25 (upregulated genes) shows increase in a cell adhesion gene, Protocadherin 8 (*Pcdh8)* that may be confirmed by increasing number of animals. The results of profiling synaptic plasticity genes were uploaded to STRING program and investigated for any protein-protein interactions under loose and stringent clustering settings.

Table 25. Synaptic Plasticity Gene Profiling in Male Sprague-Dawley rats: Table shows up-regulated gene in FSA treated group vs. Control group.

Up-regulated Genes	Description	Role of the gene	*p*-value	Fold Change	Fold Regulation
Pcdh8	Protocadherin 8	Cell adhesion	0.218854	2.851	2.851

Table 25 shows the downregulated genes in Male FSA treated group versus control when using the Synaptic Plasticity RT PCR microarray plate. Interestingly, we see downregulation of matrix metallopeptidase 9, which is thought to be involved is

hemorrhagic transformation after stroke. The FSA treated rats had a lower relative risk of hemorrhagic transfomation compared to controls.

Table 26. Synaptic Plasticity Gene Profiling in Male Sprague-Dawley rats: Table shows down-regulated genes in FSA treated group vs. Control group.

Down-regulated Genes	Description	Role of the gene	*p*-value	Fold Change	Fold Regulation
Mmp9	Matrix metallopeptidase 9	Immediate-Early Response Gene	0.177072	0.4552	-2.1968
Cebpd	CCAAT/enhancer binding protein (C/EBP), delta	Immediate-Early Response Gene	0.186163	0.3841	-2.6035
Igf1	Insulin-like growth factor 1	Long Term Depression (LTD)	0.401632	0.4222	-2.3683

3.3.14 Analysis of Protein-Protein Interaction (PPI) within Synaptic Plasticity Genes in Male Rats

PPI Analysis: In Figure 47, the network does not have significantly more interactions than expected due to the number of tested genes or the lack of information about their interactions. The PPI prediction suggests that two of the down-regulated genes, *Igf1* and *Mmp9*, are involved in transcriptional misregulation in cancer, but *Mmp9* is also associated with damage in stroke. As shown in a previous study on adult male mice (J. Y. Lee et al., 2012), fluoxetine in the drug combination appears to down-regulate matrix metalloprotease gene (*Mmp9*) which responsible for degrading the extracellular matrix proteins and involved in blood-brain-barrier damage after ischemic stroke.

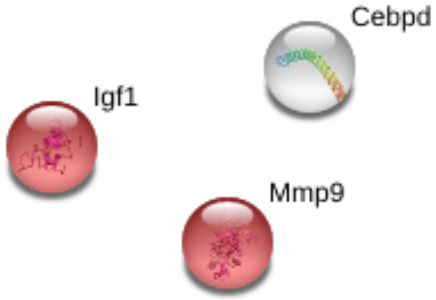

Figure 47. PPI analysis of down-regulated synaptic plasticity genes in male FSA group compared to male control group (tight stringency).

The backbone network in Figure 48 (loose stringency of upregulated genes) consists of 29 nodes of which 20 genes (red nodes) are involved in positive regulation of cellular process with medium to high interactions. Upregulating of these genes reveals a

positive role of the FSA drug combination in synaptic plasticity in male rats as seen before in females. These genes in a different network pattern are involved in learning, neurogenesis, protein binding, and regulation of apoptotic process, cell communication, and signal transduction, cellular response to stimulus and cellular components of neuron projections.

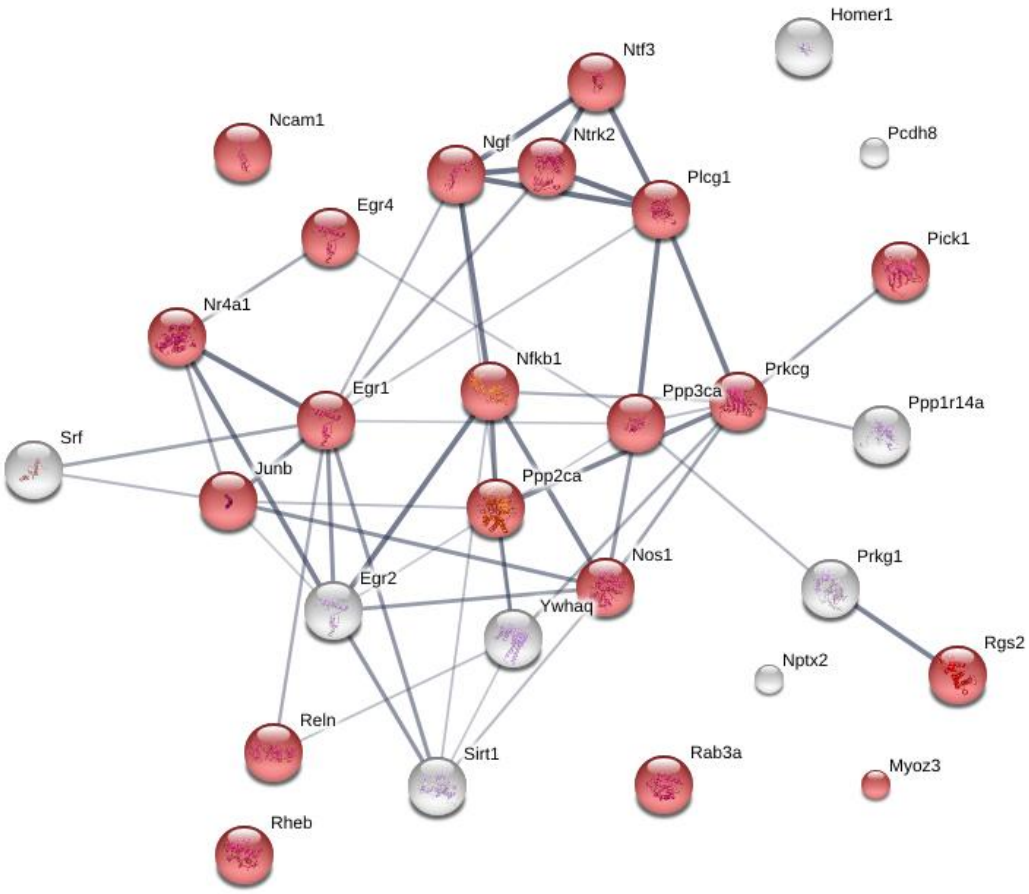

Figure 48. PPI analysis of up-regulated synaptic plasticity genes in male FSA group compared to male control group (loose stringency). The 3D structure of the majority of the clustered proteins is known from the literature.

One interesting gene family network in the down-regulated genes (although they are not significant), is their clustering in glutamatergic synapse pathway representing the metabotropic glutamate receptors. This includes *Grm1, Grm2, Grm3, Grm5, and Grm8*. Glutamate is a key excitatory neurotransmitter that thought to mediate neuronal damage after cerebral ischemia by acting upon these receptors (J. M. Lee, Grabb, Zipfel, & Choi, 2000).

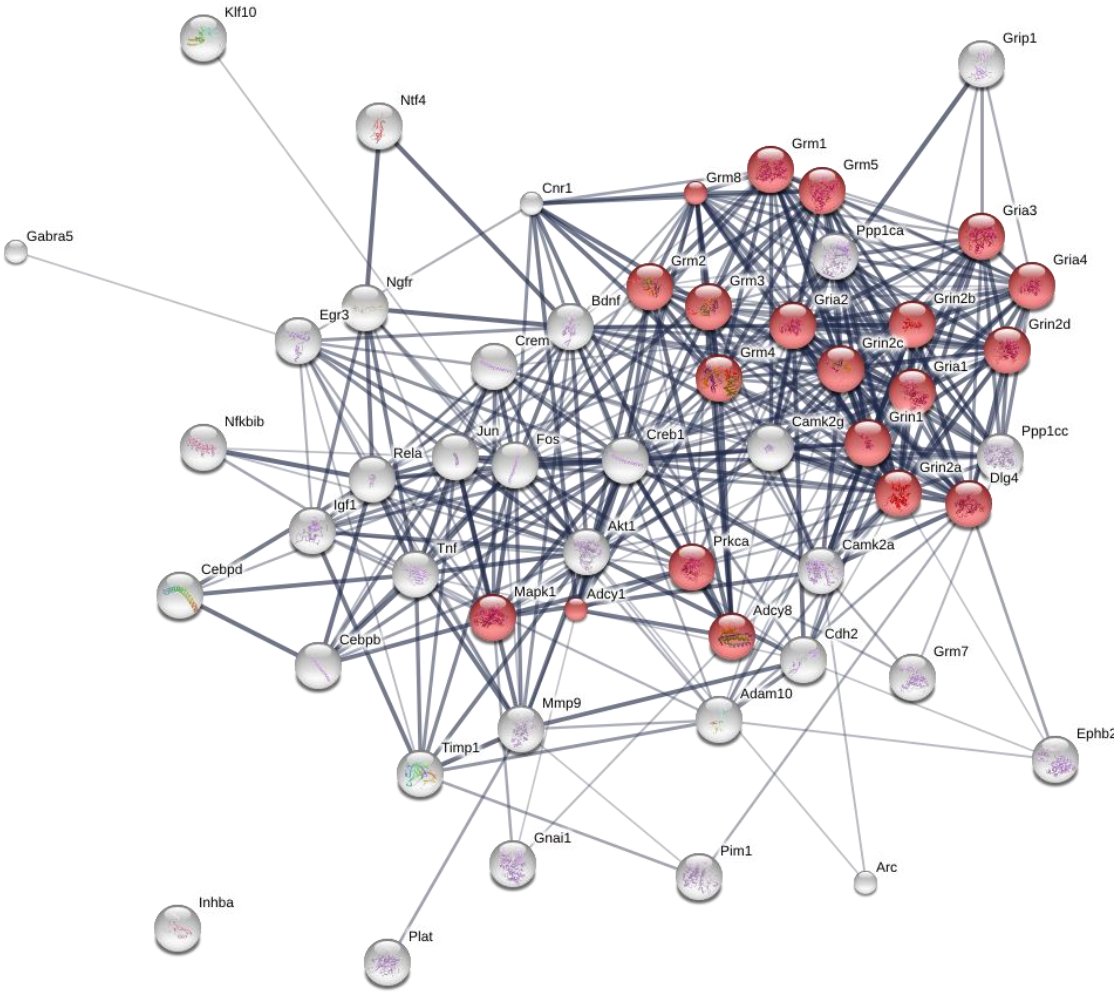

Figure 49. PPI analysis of down-regulated synaptic plasticity genes in male FSA group compared to male control group (loose stringency).

CHAPTER IV
DISCUSSION

Stroke is a cerebrovascular accident that occurs when the normal blood supply to the brain is interrupted. With the limited availability of pharmacologic therapy to treat stroke and the increase in number of people having stroke along with the cost of treatment that is projected to more than double by 2030, there remains a pressing need for finding an appropriate post-stroke drug or drug combination that can prevent long-term disability and save lives.

Preclinical stroke research

Despite the remarkable investments in advancing translational research; numerous pre-clinical stroke studies failed in translating their outcomes into human clinical trials. Some reasons that explain this failure are related to poor experimental design in which inappropriate animal models employed did not sufficiently simulate the clinical condition in humans. The lack of efficient methodologies and accurate data analysis, blinding and randomization of experimental data are essential factors that contribute to this unsuccessful translation. Also, publication bias and funding resources could hugely influence the reliability of studies. We considered a combination of innovative approaches to closely mirror what happens in the clinic and bridge the gap between the two sides of translational research. By optimizing the pre-clinical studies design, we aimed at developing the most

appropriate animal model and methodologies to increase the translational capability of the stroke model.

Pre-clinical studies in other laboratories have looked at fluoxetine administration in animals after stroke induction, or traumatic brain injury, and many have failed to see any positive effect of the fluoxetine (Couillard-Despres et al., 2009; Y. Wang et al., 2011; Windle & Corbett, 2005). In several of these studies, neurogenesis is examined primarily in the dentate gyrus, with only cursory examination of neurogenesis in lateral ventricles that are very posterior in the brain (to the side of the hippocampus). Also, the delivery method for fluoxetine is one which would induce stress in the animal (surgical implantation of an osmotic pump delivering fluoxetine, daily intraperitoneal injections of fluoxetine, oral gavage of fluoxetine, etc.). We have seen increases in neurogenesis in older (10-12 month) rats in the subventricular zone (SVZ) of the anterior lateral ventricles in the presence of fluoxetine when it is given with voluntary oral administration, thus eliminating any stress with the administration of the drug. We also see functional recovery, which correlates well with what is being observed in clinical trials of the drug in stroke patients (Chollet et al., 2011; Gaillard & Mir, 2011) or traumatic brain injury patients (Horsfield et al., 2002). Since stress has an inhibitory effect on neurogenesis and fluoxetine can induce neurogenesis (Dwivedi, Rizavi, & Pandey, 2006; Hitoshi et al., 2007), we believe that care must be taken to eliminate stress when administering the fluoxetine to animal models of disease, which our drug delivery system accomplishes (A. Corbett et al., 2012).

Animal models are designed to provide therapeutic relevance to human research, however, there is an ongoing disconnect between animal studies and human clinical trials that can be mainly attributed to either employing improper animal age or sex preference.

Gender bias exists in animal stroke models, in which male models are usually employed in pre-clinical studies (Dietz, 2006). Consistency with using methods that have been shown to induce deficits in an animal model similar to human stroke patients and using a reliable method of drug delivery and suitable functional evaluation techniques are fundamental factors of sound pre-clinical research. In addition, randomization and blinding of the experimenter to treatment conditions are crucial to eliminate bias.

Since the majority of pre-clinical stroke studies conducted on young rats, they often show spontaneous recovery after focal ischemia. To better correlate with the human stroke population, animal models need to be middle-aged or older. We use adult male and female Sprague-Dawley rats at 10-12 months of age as an animal model of stroke because of their age correlates with middle age human, and their blood vessel collateralization is similar to the human population. We are assessing differences between females and males, as diversity in the response to stroke is clinically relevant. Moreover, we suggest further experimentation in a variety of species such as rabbits and guinea pigs and even larger animal models to confirm any findings.

Appropriate Timing of Drug Administration

Fluoxetine, simvastatin and ascorbic acid combination that was developed in our lab might be a potential therapeutic intervention to complement the limited availability of thrombolytic therapy rt-PA, and improve functional motor recovery after ischemic stroke. Given the results of a previous study in our lab on adult (10-12 month) female Sprague-Dawley rats (Balch et al., 2015), it appears that delivering fluoxetine 20-26 hours after stroke induction not only promotes functional motor recovery but also reduces the infarct volume significantly compared to giving the fluoxetine within 6-12 hours of stroke

induction. Moreover, administrating the fluoxetine early (6-12hrs) led to developing a secondary hemorrhagic stroke in female rats.

The current work has emphasized the importance of timing in the delivery of the fluoxetine to a male rat model of ischemic stroke already on simvastatin. Studying the effect of fluoxetine in an animal model of stroke where the rats were already on statins, 7days before stroke induction, correlates better with what is seen during clinical trials with fluoxetine, as almost a third of the clinical trial patient are on statins. The finding of this study in adult (10-12 month) male Sparague-Dawley rats suggests that functional outcome might be substantially enhanced by administering fluoxetine within 20-26 hours of a stroke rather than having the first delivery at 48-54 hours after stroke. Findings of this study are similar to those of females and showed signs of hemorrhagic transformation at both the early time point of drug administratinon (6-12 hrs), and delayed time (48-54 hrs) following stroke. However, any hemorrhagic transformation in male rats were in the reperfusion injury region, extending from the original site of injection and no isolated hemorrhagic infarcts were seen in the males, in direct contrast to the females.

Refining the Functional Assessment of Stroke

Finding appropriate tests to assess functional outcome in preclinical studies of stroke is imperative. Due to the range of different deficits that accompany stroke, a variety of functional tests that are sensitive to the extent of damage, location of the stroke, and beneficial treatment should be applied. Although there are multiple functional tests, I only covered the most commonly performed functional assessments of motor function in the rodent stroke model (Montoya staircase and forelimb asymmetry test). Montoya staircase is considered more sensitive and able to detect even moderate functional impairments

following stroke, due to the fine motor control involved in grasping and holding onto a small object. The forelimb asymmetry analysis has the advantages over Montoya's test in that no pre-training of the animals is required, and no expensive apparatus is needed. However, a more accurate approach is required to adequately assess functional deficit and recovery using this cylinder test. Behavioral studies traditionally count every touch made by the animal to the wall. I analyzed pre-stroke versus post-stroke wall touches and found that fingertip touches to the wall were only seen post-stroke, so are likely to be abnormal touching seen only after injury. In my approach, I calculated the percentage of deficit obtained from counting palm touches versus palm and fingertip touches and compared the outcome to the results obtained from Montoya staircase analysis. The results showed that in female rats there was a slightly better correlation between the results of Montoya staircase and the forelimb asymmetry analyses when only palm touches were counted. These findings might provide evidence of an increased sensitivity of the Forelimb Asymmetry test through the use of the modified counting method (palm only counted as a normal touch), which needs further confirmation with a larger number of experimental animals. By evaluating the available functional assessments in clinical trials, the outcomes of both Forelimb Asymmetry test and Montoya Staircase can be translated over to human clinical trial studies, with similarities in both the Fugl-Meyer Assessment and the Modified Rankin Score.

Infarct Volumes in Female Sprague-Dawley Rats

The previous work in our lab to evaluate infarct volume in 10-12 month female Sprague-Dawley rats were conducted by using a Cresyl Violet (Nissl) stain, in which slides of coronal sections of the brain were stained, cleared and dehydrated using a series of timed

washes. After the stained tissue was dry, cover slips were placed over the tissue using a permanent mordant DPX (Balch, 2014).

Table 27. Female treatment groups with different times of drug delivery. Combined medications (5 mg/kg fluoxetine and 1 mg/kg simvastatin) were orally administered either beginning 6-12 hours or 20-26 hours after stroke induction and continued daily for 90 days. Infarct volumes were assessed at post-stroke day 91 using Nissl stained coronal brain sections (representative sections shown in Figure 50).

Group	Oral Dose	Montoya Staircase	Forelimb Asymmetry	Euthanasia
6-12 hrs. Control (N=8)	None	PSD 3-5	PSD 4	PSD 91
6-12 hrs. FS (N=11)	1 mg/kg statin 5 mg/kg fluoxetine	PSD 3-5	PSD 4	PSD 91
20-26 hrs. Control (N=8)	None	PSD 3-5	PSD 4	PSD 91
20-26 hrs. FS (N=6)	1 mg/kg statin 5 mg/kg fluoxetine	PSD 3-5	PSD 4	PSD 91

In Figure 50, I put together the montages for the Nissl stained brain sections (representative figures) used in this publication in which I was a co-first author (Balch et al., 2015). This work showed some similar changes to that seen in my work on the male rats. In particular, notice that in panel A and C, which are control animals for 6-12 hour and 20-26 hour administration respectively, you can clearly see the injection site for the endothelin at the top of the cortex, and to the right of this site there is extensive damage which is likely caused by reperfusion injury. Inflammatory microglia are thought to be

involved in both making the blood brain barrier permeable after stroke and allowing infiltration of peripheral macrophages and lymphocytes, which cause most of the damage in reperfusion injury. Note that in Panels B and D, where drug treatment with fluoxetine and simvastatin has occurred, we do not see the extensive reperfusion damage associated with the injection site, although the 6-12 hour drug administration rats do have evidence of secondary bleeding.

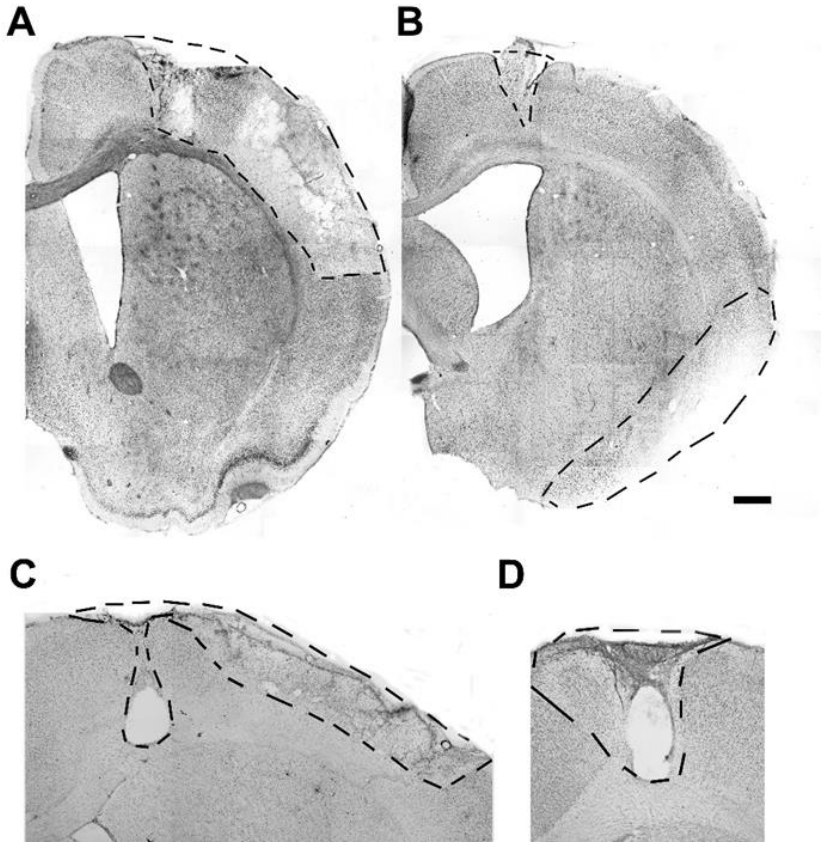

Figure 50: Representative Nissl stained coronal sections showing infarcts from female stroke rats (control versus fluoxetine, simvastatin treated) at two different administration time-points. These rats received fluoxetine (5 mg/kg) and simvastatin (1 mg/kg) at either 6-12 hours after stroke (Panel B) or 20-26 hours after stroke (Panel D). Control rats are in panels A and C for 6-12 hours after stroke and 20-26 hours after stroke respectively. The

lower infarct on Panel B, with fluoxetine and simvastatin given after 6-12 hours, represents a secondary hemorrhagic infarct, totally dissociated from the original infarct site: these were only seen in female rats, although male rats did show hemorrhagic transformation within the reperfusion injury. Rats were euthanized 90 days post-stroke. The scale bar indicates 500 micrometers.

Figure 51. Infarct volumes vary with timing of fluoxetine and simvastatin delivery after ischemic stroke. (A). in delayed drug delivery time (20-26 hrs. post-stroke), a strong trend of volume reduction was seen using *t*-test with Welch's correction for the drug group, but missed a significant difference (3 ± 0.3447 mm^3 SEM, $p = 0.0563$). (B). Infarct volumes in early drug delivery time (6-12 hrs. post-stroke) showed no statistical difference ($p=0.1347$) when compared to vehicle control using *t*-test with Welch's correction for the drug group. (C). Direct comparison of infarct volumes between early and delayed treatment groups that indicates significant difference using *t*-test with Welch's correction (15.4 ± 4.260 mm^3 SEM, $p = 0.0157$), with the earlier delivery time producing a much larger infarct. Each dot represents an animal in each group. The x-axis displays treatment groups, and the y-axis shows the infarct volume in mm^3. The broad horizontal bar indicates the group mean and the error bars represent SEM, with individual infarct volumes given by closed symbols clustered around means.

Impact of Physical Rehabilitation on Motor Recovery

Another limitation for a successful translation between experimental studies and clinical research is the usefulness of the rehabilitation procedure and time. Appropriate and adequate physical rehabilitation is essential to ensuring effective improvement of post-stroke motor recovery in a rodent model. To obtain reliable data, the chosen method of physical rehabilitation we utilized was performed with minimum stress and anxiety to the animals. Our findings indicate that the drug combination (fluoxetine and simvastatin) treatment in female Sprague-Dawley rats achieved slightly greater motor functional recovery in rehabilitated animals compared to rehabilitated vehicle-treated animals. Rehabilitation did not improve the overall functional recovery seen in the drug treated animals, but it did seem to speed the overall recovery, with drug combination only providing a slower steady progression. This drug treatment, however, may provide adequate recovery for human stroke patients who cannot participate in physical rehabilitation.

The Anti-inflammatory Role of the Drug Combination

The combination therapy of fluoxetine and simvastatin reveals promising signs of a neuroprotective role in inflammation through inducing anti-inflammatory markers and suppressing the pro-inflammatory ones. Studies have shown that activated microglia can act as a double-edged sword to detrimentally intensify neurotoxicity when inflammatory markers are high (Levesque et al., 2010), (Harry & Kraft, 2008), or potentially promoting neuronal regeneration and recovery when they are changed into M2 type microglia (Diestel et al., 2010), (McPherson, Kraft, & Harry, 2011). These contradictory effects come from diverse experimental sets of *in vitro* and *in vivo* models that vary in terms of the activation

stimulus, timing of microglial activation, sex and age of animals (Luo & Chen, 2012). Our preliminary data has indicated that at post-stroke day 7, the microglia is primarily in the M2 form, however, as a recent review of neuroinflammation indicates that microglia undergoes a broad range of morphological transformations in a time-dependent fashion (Fumagalli, Perego, Pischiutta, Zanier, & De Simoni, 2015), microglia express M1 markers in the very early phases after injury followed by recruitment of macrophages and expression of M2 markers by both myeloid populations. The peak of M2 marker expression rapidly disappears and is followed by another upregulation of M1 markers that persists longer. The cells also undergo morphological changes from sprouting ramified cells soon after brain injury to non-branching phenotype followed by phagocytic ameboid shape few days after the initial brain insult (Xiang, Haroutunian, Ho, Purohit, & Pasinetti, 2006).

Our customized array contains microglia markers to pro-inflammatory M1 and anti-inflammatory M2 subtypes that have been discussed in literature; however, we do not know whether these markers are sufficient to distinguish between the different types of microglia in our animal models. There are some troubling signs, like up-regulation of some markers and down-regulation of other markers for the same microglial subtype, which require further investigation. As it has been previously reported, after focal cerebral ischemia, microglia are activated rapidly in response to brain damage and their proliferation peaks within 2 to 3 days of ischemia onset (Lalancette-Hebert, Gowing, Simard, Weng, & Kriz, 2007). We might miss the opportunity to explore the early stage changes in microglia activity by delaying the evaluation of microglia markers to post-stroke day 7. In future studies, we will need to test an earlier time point, perhaps 48 to 72 hours post-stroke to see any potential differences in the M1 and M2 microglial subtypes.

There is a possibility that expression of microglia markers may vary with animal's age and sex. Our findings indicate variable effects of the drug combination on gene expression by microglial subtypes in male and female animals. For example; treating male rats with the combination drug significantly led to significant up-regulation of two pro-inflammatory markers of M1 microglia, *Ccl11* and *Stat4*, while also showing reduced expression of a tryptophan metabolism effector molecule *Nos2,* which is another M1 pro-inflammatory marker. Female rats, on the other hand, show a different pattern of response to drug treatment; the significant up-regulation of the sex determining region Y-box 2 (*Sox2*) gene in female rats may provide a sign of a sex-dependent role of the drug on microglial gene upregulation. The SOX2 transcription factor is critical for maintaining self-renewal of embryonic and neural stem cells (Rizzino, 2009). The drug combination exhibits a trend of up-regulation of the anti-inflammatory marker of M2a and M2c microglia, *Bdnf*, with a 3.85 fold change in male rats; whereas when female rats treated with the same combination drug the fold change of *Bdnf* was 1.99. These findings suggest a possible sex-dependent effect of the medicine that needs to be confirmed by increasing the number of tested animals.

Interestingly, prior and post-treatment of male Sprague-Dawley rats with simvastatin only demonstrates that simvastatin by itself has no inhibitory effect on pro-inflammatory cytokines as fluoxetine does. This outcome proposes a vital role of fluoxetine in the FSA drug combination in down-regulating the pro-inflammatory genes.

Effects of the Drug Combination on Neurotrophic Factors and Synaptic Plasticity

Our results imply a positive effect of the drug combination in stimulating neurotrophic factors and synaptic plasticity genes. The sex-specific pattern of gene

expression varies between male and female rats receiving the same dose of fluoxetine, simvastatin, and ascorbic acid treatment at the same time.

An interesting finding in neurotrophic factors expression profile indicates remarkable upregulation of orexin/hypocretin (HCRT) protein in male drug treatment group of rats, with a trend toward significance (9.92 fold regulation). These results were similar to what we have seen before in female rats. Our previous work on adult female rats treated with the same dose of drug combination for 10 days after stroke showed that orexin was upregulated to 2.06 fold, while another experiment that used fluoxetine and simvastatin (FS) only for the same amount of time in adult female rats showed significant upregulation of *Hctr1 (*2.07) *and Hctr2 (*2.93); $p < 0.05$. In light of these findings, endogenous *HcRt* may mediate the neuroprotective effect of the FSA drug combination and contribute to its beneficial role in motor recovery in male rats. The exact mechanisms of action of *HcRt* though are not clear. In Figure 45 of protein-protein interaction network, it appears that the orexin pathway (*Hcrt* and *Hcrtr1 and Hcrtr2*) would work through neuropeptide Y *Npy* and its receptor *Npy1r,* that are known for their significant role in hippocampal learning and memory (Howell et al., 2003), to boost synaptic plasticity.

Further studies are required to elucidate these mechanisms.

Another critical finding was the down-regulation of matrix metalloprotease gene (*Mmp9*) in male rats treated with FSA combination. This gene encodes a protein that is responsible for degrading the extracellular matrix proteins and involved in blood-brain-barrier damage after ischemic stroke. A previous *in vivo* study on adult mice from another laboratory demonstrated an inhibitory role of fluoxetine in *Mmp9* regulation.

A significant down-regulation of the apoptotic gene, *Fas* (TNF receptor superfamily, member 6) in adult male rats treated with FSA in compare to control animals ($p=0.031$) provide preliminary evidence of possible anti-apoptotic role of the drug combination in suppressing this gene that is involved in negative regulation of cell death, apoptotic process and TNF signaling pathway.

Utilizing the STRING software to predict protein-protein interactions and demonstrate how genes cluster in individual pathways, enables a previously unobtainable level of visualization of the regulated genes in the pathophysiology of stroke. The predicted analyses depict gene networks that interact mainly in signal transduction, cell-cell signaling, regulation of multicellular organismal process, cellular response to stimulus, nervous system development, cell differentiation and proliferation, positive regulation of biological process and receptor binding. Up-regulating of these genes in response to FSA drug treatment may indicate a potential role of the drug in inducing neurotrophic factors critical for neurogenesis and motor recovery after stroke.

To better understand mechanisms that promote recovery after ischemic stroke and to evaluate the effect of pharmacologic interventions, future studies should continue to investigate the relationship between molecular data (neurotrophic factors and brain tissue plasticity), histopathological analysis (infarct volume and hemorrhagic transformation) as well as behavioral outcome; with emphasis on investigating early genetic changes in different sexes for their effect long-term functional recovery. These data suggest that different slightly drug treatments for males and females may optimize functional recovery following stroke.

CHAPTER V
CONCLUSIONS AND FUTURE DIRECTIONS

1). Giving Fluoxetine 20-26 hours after stroke induction not only promotes functional motor recovery but also reduces the infarct volume significantly compared to giving the Fluoxetine within 6-12hrs of stroke induction. Waiting for 48hours before giving the treatment did not have any beneficial effect on infarct size.

2). Counting only the numbers of touches made by palmar pads is a more sensitive behavioral analysis of functional deficit than including amounts of contacts made by both palmar pads and fingertips.

3). Rehabilitation speeds recovery post-stroke when there is drug treatment, but we are able to achieve the same level of recovery with our drug treatment without rehabilitation.

4) We see differences in the upregulation and down regulation of genes in female rats compared to male rats following stroke, with better recovery seen with a slightly different drug combination.

5). Gene analysis shows upregulation of neurotrophic factors and synaptic plasticity genes in FSA males, pointing to a possibly important upregulation of orexin receptors, which may play a key role in cortical recovery in both males and females.

6) Preliminary data suggested that at post-stroke day 7, the microglia is primarily in the M2 form, but the control rats also showed the same markers. We will need to test an earlier time point, perhaps post-stroke day 3 to see potential differences in the M1 and M2 microglial subtypes in female and male rats**.**

CHAPTER VI
REFERENCES

AD, F. (Ed.). (2012). *Mucosal macrophages: phenotype and functionality in homeostasis and pathology*.

Adams, H. P., Jr., del Zoppo, G., Alberts, M. J., Bhatt, D. L., Brass, L., Furlan, A., . . . Quality of Care Outcomes in Research Interdisciplinary Working, G. (2007). Guidelines for the early management of adults with ischemic stroke: a guideline from the American Heart Association/American Stroke Association Stroke Council, Clinical Cardiology Council, Cardiovascular Radiology and Intervention Council, and the Atherosclerotic Peripheral Vascular Disease and Quality of Care Outcomes in Research Interdisciplinary Working Groups: the American Academy of Neurology affirms the value of this guideline as an educational tool for neurologists. *Stroke, 38*(5), 1655-1711. doi: 10.1161/STROKEAHA.107.181486

Agus, D. B., Gambhir, S. S., Pardridge, W. M., Spielholz, C., Baselga, J., Vera, J. C., & Golde, D. W. (1997). Vitamin C crosses the blood-brain barrier in the oxidized form through the glucose transporters. *J Clin Invest, 100*(11), 2842-2848. doi: 10.1172/JCI119832

Alberts, A. W. (1990). Lovastatin and simvastatin--inhibitors of HMG CoA reductase and cholesterol biosynthesis. *Cardiology, 77 Suppl 4*, 14-21.

Alfaro, C. L., Lam, Y. W., Simpson, J., & Ereshefsky, L. (2000). CYP2D6 inhibition by fluoxetine, paroxetine, sertraline, and venlafaxine in a crossover study: intraindividual variability and plasma concentration correlations. *J Clin Pharmacol, 40*(1), 58-66.

Alkayed, N. J., Harukuni, I., Kimes, A. S., London, E. D., Traystman, R. J., & Hurn, P. D. (1998). Gender-linked brain injury in experimental stroke. *Stroke, 29*(1), 159-165; discussion 166.

Alper, B. S., Malone-Moses, M., McLellan, J. S., Prasad, K., & Manheimer, E. (2015). Thrombolysis in acute ischaemic stroke: time for a rethink? *BMJ, 350*, h1075. doi: 10.1136/bmj.h1075

Arvidsson, A., Collin, T., Kirik, D., Kokaia, Z., & Lindvall, O. (2002). Neuronal replacement from endogenous precursors in the adult brain after stroke. *Nat Med, 8*(9), 963-970. doi: 10.1038/nm747

Asahi, M., Huang, Z., Thomas, S., Yoshimura, S., Sumii, T., Mori, T., . . . Moskowitz, M. A. (2005). Protective effects of statins involving both eNOS and tPA in focal cerebral ischemia. *J Cereb Blood Flow Metab, 25*(6), 722-729. doi: 10.1038/sj.jcbfm.9600070

Bacigaluppi, M., Comi, G., & Hermann, D. M. (2010). Animal models of ischemic stroke. Part two: modeling cerebral ischemia. *Open Neurol J, 4*, 34-38. doi: 10.2174/1874205X01004020034

Balch, M. H. (2014). *Effects of Delayed Pharmacological Treatment and Limb Rehabilitation on Infarct Size and Functional Recovery After Stroke.* (Master of Science (MS)), Wright State University, OhioLink. (wright1408630500)

Balch, M. H., Ragas, M. A., Wright, D., Hensley, A., Reynolds, K., Kerr, B., & Corbett, A. M. (2015). Appropriate Timing of Fluoxetine and Statin Delivery Reduces the Risk of Secondary Bleeding in Ischemic Stroke Rats. *Journal of Neurology and Neuroscience*.

Barlow, C., & Targum, S. D. (2007). Hippocampal Neurogenesis: Can it be a Marker for New Antidepressants? *Psychiatry (Edgmont), 4*(5), 18-20.

Bath, P. M., Macleod, M. R., & Green, A. R. (2009). Emulating multicentre clinical stroke trials: a new paradigm for studying novel interventions in experimental models of stroke. *Int J Stroke, 4*(6), 471-479. doi: 10.1111/j.1747-4949.2009.00386.x

Beery, A. K., & Zucker, I. (2011). Sex bias in neuroscience and biomedical research. *Neurosci Biobehav Rev, 35*(3), 565-572. doi: 10.1016/j.neubiorev.2010.07.002

Bejot, Y., Prigent-Tessier, A., Cachia, C., Giroud, M., Mossiat, C., Bertrand, N., . . . Marie, C. (2011). Time-dependent contribution of non neuronal cells to BDNF production after ischemic stroke in rats. *Neurochem Int, 58*(1), 102-111. doi: 10.1016/j.neuint.2010.10.019

Benfield, P., Heel, R. C., & Lewis, S. P. (1986). Fluoxetine. A review of its pharmacodynamic and pharmacokinetic properties, and therapeutic efficacy in depressive illness. *Drugs, 32*(6), 481-508.

Biernaskie, J., & Corbett, D. (2001). Enriched rehabilitative training promotes improved forelimb motor function and enhanced dendritic growth after focal ischemic injury. *J Neurosci, 21*(14), 5272-5280.

Blanco, M., Nombela, F., Castellanos, M., Rodriguez-Yanez, M., Garcia-Gil, M., Leira, R., . . . Castillo, J. (2007). Statin treatment withdrawal in ischemic stroke: a controlled randomized study. *Neurology, 69*(9), 904-910. doi: 10.1212/01.wnl.0000269789.09277.47

Bland, S. T., Schallert, T., Strong, R., Aronowski, J., Grotta, J. C., & Feeney, D. M. (2000). Early exclusive use of the affected forelimb after moderate transient focal ischemia in rats : functional and anatomic outcome. *Stroke, 31*(5), 1144-1152.

Bonita, R., & Beaglehole, R. (1988). Recovery of motor function after stroke. *Stroke, 19*(12), 1497-1500.

Cao, L., Wei, D., Reid, B., Zhao, S., Pu, J., Pan, T., . . . Zhao, M. (2013). Endogenous electric currents might guide rostral migration of neuroblasts. *EMBO Rep, 14*(2), 184-190. doi: 10.1038/embor.2012.215

Carmichael, S. T. (2005). Rodent models of focal stroke: size, mechanism, and purpose. *NeuroRx, 2*(3), 396-409. doi: 10.1602/neurorx.2.3.396

Casals, J. B., Pieri, N. C., Feitosa, M. L., Ercolin, A. C., Roballo, K. C., Barreto, R. S., . . . Ambrosio, C. E. (2011). The use of animal models for stroke research: a review. *Comp Med, 61*(4), 305-313.

Chen, G. C., Lu, D. B., Pang, Z., & Liu, Q. F. (2013). Vitamin C intake, circulating vitamin C and risk of stroke: a meta-analysis of prospective studies. *J Am Heart Assoc, 2*(6), e000329. doi: 10.1161/JAHA.113.000329

Chen, J., Zhang, C., Jiang, H., Li, Y., Zhang, L., Robin, A., . . . Chopp, M. (2005). Atorvastatin induction of VEGF and BDNF promotes brain plasticity after stroke in mice. *J Cereb Blood Flow Metab, 25*(2), 281-290. doi: 10.1038/sj.jcbfm.9600034

Chen, Y., & Johnson, A. G. (1993). In vivo activation of macrophages by prolactin from young and aging mice. *Int J Immunopharmacol, 15*(1), 39-45.

Cherry, J. D., Olschowka, J. A., & O'Banion, M. K. (2014). Neuroinflammation and M2 microglia: the good, the bad, and the inflamed. *J Neuroinflammation, 11*, 98. doi: 10.1186/1742-2094-11-98

Chhabra, N. (2014). Immediate treatment of Acute MI. *Clinical Cases Biochemistry.* Retrieved 07/20/2016, 2016, from http://usmle.biochemistryformedics.com/immediate-treatment-of-acute-mi/

Chollet, F., Tardy, J., Albucher, J. F., Thalamas, C., Berard, E., Lamy, C., . . . Loubinoux, I. (2011). Fluoxetine for motor recovery after acute ischaemic stroke (FLAME): a randomised placebo-controlled trial. *Lancet Neurol, 10*(2), 123-130. doi: 10.1016/S1474-4422(10)70314-8

Corbett, A., McGowin, A., Sieber, S., Flannery, T., & Sibbitt, B. (2012). A method for reliable voluntary oral administration of a fixed dosage (mg/kg) of chronic daily medication to rats. *Lab Anim, 46*(4), 318-324. doi: 10.1258/la.2012.012018

Corbett, A. M., Sieber, S., Wyatt, N., Lizzi, J., Flannery, T., Sibbit, B., & Sanghvi, S. (2015). Increasing neurogenesis with fluoxetine, simvastatin and ascorbic Acid leads to functional recovery in ischemic stroke. *Recent Pat Drug Deliv Formul, 9*(2), 158-166.

Couillard-Despres, S., Wuertinger, C., Kandasamy, M., Caioni, M., Stadler, K., Aigner, R., . . . Aigner, L. (2009). Ageing abolishes the effects of fluoxetine on neurogenesis. *Mol Psychiatry, 14*(9), 856-864. doi: mp2008147 [pii]

10.1038/mp.2008.147

Dahlqvist, P., Zhao, L., Johansson, I. M., Mattsson, B., Johansson, B. B., Seckl, J. R., & Olsson, T. (1999). Environmental enrichment alters nerve growth factor-induced gene A and glucocorticoid receptor messenger RNA expression after middle cerebral artery occlusion in rats. *Neuroscience, 93*(2), 527-535.

Dam, M., Tonin, P., De Boni, A., Pizzolato, G., Casson, S., Ermani, M., . . . Battistin, L. (1996). Effects of fluoxetine and maprotiline on functional recovery in poststroke hemiplegic patients undergoing rehabilitation therapy. *Stroke, 27*(7), 1211-1214.

de Lecea, L., Kilduff, T. S., Peyron, C., Gao, X., Foye, P. E., Danielson, P. E., . . . Sutcliffe, J. G. (1998). The hypocretins: hypothalamus-specific peptides with neuroexcitatory activity. *Proc Natl Acad Sci U S A, 95*(1), 322-327.

Dean, S. L., Knutson, J. F., Krebs-Kraft, D. L., & McCarthy, M. M. (2012). Prostaglandin E2 is an endogenous modulator of cerebellar development and complex behavior during a sensitive postnatal period. *Eur J Neurosci, 35*(8), 1218-1229. doi: 10.1111/j.1460-9568.2012.08032.x

del Zoppo, G. J., & Hallenbeck, J. M. (2000). Advances in the vascular pathophysiology of ischemic stroke. *Thromb Res, 98*(3), 73-81.

del Zoppo, G. J., & Milner, R. (2006). Integrin-matrix interactions in the cerebral microvasculature. *Arterioscler Thromb Vasc Biol, 26*(9), 1966-1975. doi: 10.1161/01.ATV.0000232525.65682.a2

Del Zoppo, G. J., Saver, J. L., Jauch, E. C., Adams, H. P., Jr., & American Heart Association Stroke, C. (2009). Expansion of the time window for treatment of acute ischemic stroke with intravenous tissue plasminogen activator: a science advisory from the American Heart Association/American Stroke Association. *Stroke, 40*(8), 2945-2948. doi: 10.1161/STROKEAHA.109.192535

Diestel, A., Troeller, S., Billecke, N., Sauer, I. M., Berger, F., & Schmitt, K. R. (2010). Mechanisms of hypothermia-induced cell protection mediated by microglial cells in vitro. *Eur J Neurosci, 31*(5), 779-787. doi: 10.1111/j.1460-9568.2010.07128.x

Dietz, V. (2006). Good clinical practice in neurorehabilitation. *Lancet Neurol, 5*(5), 377-378. doi: 10.1016/S1474-4422(06)70420-3

Dirnagl, U. (2006). Bench to bedside: the quest for quality in experimental stroke research. *J Cereb Blood Flow Metab, 26*(12), 1465-1478. doi: 10.1038/sj.jcbfm.9600298

Dittmar, M., Spruss, T., Schuierer, G., & Horn, M. (2003). External carotid artery territory ischemia impairs outcome in the endovascular filament model of middle cerebral artery occlusion in rats. *Stroke, 34*(9), 2252-2257. doi: 10.1161/01.STR.0000083625.54851.9A

Duncan, P. W., Goldstein, L. B., Horner, R. D., Landsman, P. B., Samsa, G. P., & Matchar, D. B. (1994). Similar motor recovery of upper and lower extremities after stroke. *Stroke, 25*(6), 1181-1188.

Duncan, P. W., Jorgensen, H. S., & Wade, D. T. (2000). Outcome measures in acute stroke trials: a systematic review and some recommendations to improve practice. *Stroke, 31*(6), 1429-1438.

Dwivedi, Y., Rizavi, H. S., & Pandey, G. N. (2006). Antidepressants reverse corticosterone-mediated decrease in brain-derived neurotrophic factor expression: differential regulation of specific exons by antidepressants and corticosterone. *Neuroscience, 139*(3), 1017-1029. doi: S0306-4522(06)00059-5 [pii]

10.1016/j.neuroscience.2005.12.058

Elder, G. A., De Gasperi, R., & Gama Sosa, M. A. (2006). Research update: neurogenesis in adult brain and neuropsychiatric disorders. *Mt Sinai J Med, 73*(7), 931-940.

Eriksson, P. S., Perfilieva, E., Bjork-Eriksson, T., Alborn, A. M., Nordborg, C., Peterson, D. A., & Gage, F. H. (1998). Neurogenesis in the adult human hippocampus. *Nat Med, 4*(11), 1313-1317. doi: 10.1038/3305

Estrada, C., & Murillo-Carretero, M. (2005). Nitric oxide and adult neurogenesis in health and disease. *Neuroscientist, 11*(4), 294-307. doi: 10.1177/1073858404273850

Faralli, A., Bigoni, M., Mauro, A., Rossi, F., & Carulli, D. (2013). Noninvasive strategies to promote functional recovery after stroke. *Neural Plast, 2013*, 854597. doi: 10.1155/2013/854597

Feigenson, J. S., McDowell, F. H., Meese, P., McCarthy, M. L., & Greenberg, S. D. (1977). Factors influencing outcome and length of stay in a stroke rehabilitation unit. Part 1. Analysis of 248 unscreened patients--medical and functional prognostic indicators. *Stroke, 8*(6), 651-656.

Fugl-Meyer, A. R., Jaasko, L., Leyman, I., Olsson, S., & Steglind, S. (1975). The post-stroke hemiplegic patient. 1. a method for evaluation of physical performance. *Scand J Rehabil Med, 7*(1), 13-31.

Fumagalli, S., Perego, C., Pischiutta, F., Zanier, E. R., & De Simoni, M. G. (2015). The ischemic environment drives microglia and macrophage function. *Front Neurol, 6*, 81. doi: 10.3389/fneur.2015.00081

Gaillard, R., & Mir, O. (2011). Fluoxetine and motor recovery after ischaemic stroke. *Lancet Neurol, 10*(6), 499; author reply 500-491. doi: 10.1016/S1474-4422(11)70111-9

Germann, P. G., & Ockert, D. (1994). Granulomatous inflammation of the oropharyngeal cavity as a possible cause for unexpected high mortality in a Fischer 344 rat carcinogenicity study. *Lab Anim Sci, 44*(4), 338-343.

Ginsberg, M. D., & Busto, R. (1989). Rodent models of cerebral ischemia. *Stroke, 20*(12), 1627-1642.

Goldkuhl, R., Carlsson, H. E., Hau, J., & Abelson, K. S. (2008). Effect of subcutaneous injection and oral voluntary ingestion of buprenorphine on post-operative serum corticosterone levels in male rats. *Eur Surg Res, 41*(3), 272-278. doi: 10.1159/000142372

Gore-Felton, C., Somlai, A. M., Benotsch, E. G., Kelly, J. A., Ostrovski, D., & Kozlov, A. (2003). The influence of gender on factors associated with HIV transmission risk among young Russian injection drug users. *Am J Drug Alcohol Abuse, 29*(4), 881-894.

Gotto, A. M., Jr. (1997). Results of recent large cholesterol-lowering trials and implications for clinical management. *Am J Cardiol, 79*(12), 1663-1666.

Greenberg, D. A., & Jin, K. (2005). From angiogenesis to neuropathology. *Nature, 438*(7070), 954-959. doi: 10.1038/nature04481

Harada, S., Fujita-Hamabe, W., & Tokuyama, S. (2011). Effect of orexin-A on post-ischemic glucose intolerance and neuronal damage. *J Pharmacol Sci, 115*(2), 155-163.

Harry, G. J., & Kraft, A. D. (2008). Neuroinflammation and microglia: considerations and approaches for neurotoxicity assessment. *Expert Opin Drug Metab Toxicol, 4*(10), 1265-1277. doi: 10.1517/17425255.4.10.1265

Hawkins, R. A., O'Kane, R. L., Simpson, I. A., & Vina, J. R. (2006). Structure of the blood-brain barrier and its role in the transport of amino acids. *J Nutr, 136*(1 Suppl), 218S-226S.

Hayes, S. H., & Carroll, S. R. (1986). Early intervention care in the acute stroke patient. *Arch Phys Med Rehabil, 67*(5), 319-321.

Heffner, R. S., & Masterton, R. B. (1983). The role of the corticospinal tract in the evolution of human digital dexterity. *Brain Behav Evol, 23*(3-4), 165-183.

Hernandez-Perera, O., Perez-Sala, D., Navarro-Antolin, J., Sanchez-Pascuala, R., Hernandez, G., Diaz, C., & Lamas, S. (1998). Effects of the 3-hydroxy-3-methylglutaryl-CoA reductase inhibitors, atorvastatin and simvastatin, on the expression of endothelin-1 and endothelial nitric oxide synthase in vascular endothelial cells. *J Clin Invest, 101*(12), 2711-2719. doi: 10.1172/JCI1500

Hitoshi, S., Maruta, N., Higashi, M., Kumar, A., Kato, N., & Ikenaka, K. (2007). Antidepressant drugs reverse the loss of adult neural stem cells following chronic stress. *J Neurosci Res, 85*(16), 3574-3585. doi: 10.1002/jnr.21455

Hoehn, B. D., Palmer, T. D., & Steinberg, G. K. (2005). Neurogenesis in rats after focal cerebral ischemia is enhanced by indomethacin. *Stroke, 36*(12), 2718-2724. doi: 10.1161/01.STR.0000190020.30282.cc

Holland, P., & Goadsby, P. J. (2007). The hypothalamic orexinergic system: pain and primary headaches. *Headache, 47*(6), 951-962. doi: 10.1111/j.1526-4610.2007.00842.x

Hornig, D. (1975). Distribution of ascorbic acid, metabolites and analogues in man and animals. *Ann N Y Acad Sci, 258*, 103-118.

Horsfield, S. A., Rosse, R. B., Tomasino, V., Schwartz, B. L., Mastropaolo, J., & Deutsch, S. I. (2002). Fluoxetine's effects on cognitive performance in patients with traumatic brain injury. *Int J Psychiatry Med, 32*(4), 337-344.

Hossmann, K. A. (2006). Pathophysiology and therapy of experimental stroke. *Cell Mol Neurobiol, 26*(7-8), 1057-1083. doi: 10.1007/s10571-006-9008-1

Howell, O. W., Scharfman, H. E., Herzog, H., Sundstrom, L. E., Beck-Sickinger, A., & Gray, W. P. (2003). Neuropeptide Y is neuroproliferative for post-natal hippocampal precursor cells. *J Neurochem, 86*(3), 646-659.

Howells, D. W., Porritt, M. J., Rewell, S. S., O'Collins, V., Sena, E. S., van der Worp, H. B., . . . Macleod, M. R. (2010). Different strokes for different folks: the rich diversity of animal models of focal cerebral ischemia. *J Cereb Blood Flow Metab, 30*(8), 1412-1431. doi: 10.1038/jcbfm.2010.66

Hu, X., Li, P., Guo, Y., Wang, H., Leak, R. K., Chen, S., . . . Chen, J. (2012). Microglia/macrophage polarization dynamics reveal novel mechanism of injury

expansion after focal cerebral ischemia. *Stroke, 43*(11), 3063-3070. doi: 10.1161/STROKEAHA.112.659656

Huang, A., Vita, J. A., Venema, R. C., & Keaney, J. F., Jr. (2000). Ascorbic acid enhances endothelial nitric-oxide synthase activity by increasing intracellular tetrahydrobiopterin. *J Biol Chem, 275*(23), 17399-17406. doi: 10.1074/jbc.M002248200

Iadecola, C., & Anrather, J. (2011). The immunology of stroke: from mechanisms to translation. *Nat Med, 17*(7), 796-808. doi: 10.1038/nm.2399

Jakubs, K., Nanobashvili, A., Bonde, S., Ekdahl, C. T., Kokaia, Z., Kokaia, M., & Lindvall, O. (2006). Environment matters: synaptic properties of neurons born in the epileptic adult brain develop to reduce excitability. *Neuron, 52*(6), 1047-1059. doi: 10.1016/j.neuron.2006.11.004

Janssen, H., Bernhardt, J., Collier, J. M., Sena, E. S., McElduff, P., Attia, J., . . . Spratt, N. J. (2010). An enriched environment improves sensorimotor function post-ischemic stroke. *Neurorehabil Neural Repair, 24*(9), 802-813. doi: 10.1177/1545968310372092

Jin, K., Sun, Y., Xie, L., Childs, J., Mao, X. O., & Greenberg, D. A. (2004). Post-ischemic administration of heparin-binding epidermal growth factor-like growth factor (HB-EGF) reduces infarct size and modifies neurogenesis after focal cerebral ischemia in the rat. *J Cereb Blood Flow Metab, 24*(4), 399-408. doi: 10.1097/00004647-200404000-00005

Joyce, J., Rabe-Hesketh, S., & Wessely, S. (1998). Reviewing the reviews: the example of chronic fatigue syndrome. *JAMA, 280*(3), 264-266.

Kalakech, H., Tamareille, S., Pons, S., Godin-Ribuot, D., Carmeliet, P., Furber, A., . . . Prunier, F. (2013). Role of hypoxia inducible factor-1alpha in remote limb ischemic preconditioning. *J Mol Cell Cardiol, 65*, 98-104. doi: 10.1016/j.yjmcc.2013.10.001

Kawada, H., Takizawa, S., Takanashi, T., Morita, Y., Fujita, J., Fukuda, K., . . . Hotta, T. (2006). Administration of hematopoietic cytokines in the subacute phase after cerebral infarction is effective for functional recovery facilitating proliferation of intrinsic neural stem/progenitor cells and transition of bone marrow-derived

neuronal cells. *Circulation, 113*(5), 701-710. doi: 10.1161/CIRCULATIONAHA.105.563668

Kim, M. K., Park, H. J., Kim, S. R., Choi, Y. K., Shin, H. K., Jeon, J. H., . . . Bae, M. K. (2010). Angiogenic role of orexin-A via the activation of extracellular signal-regulated kinase in endothelial cells. *Biochem Biophys Res Commun, 403*(1), 59-65. doi: 10.1016/j.bbrc.2010.10.115

Kitamura, E., Hamada, J., Kanazawa, N., Yonekura, J., Masuda, R., Sakai, F., & Mochizuki, H. (2010). The effect of orexin-A on the pathological mechanism in the rat focal cerebral ischemia. *Neurosci Res, 68*(2), 154-157. doi: 10.1016/j.neures.2010.06.010

Kleim, J. A., Boychuk, J. A., & Adkins, D. L. (2007). Rat models of upper extremity impairment in stroke. *ILAR J, 48*(4), 374-384.

Kleim, J. A., Jones, T. A., & Schallert, T. (2003). Motor enrichment and the induction of plasticity before or after brain injury. *Neurochem Res, 28*(11), 1757-1769.

Kokaia, Z., Andsberg, G., Yan, Q., & Lindvall, O. (1998). Rapid alterations of BDNF protein levels in the rat brain after focal ischemia: evidence for increased synthesis and anterograde axonal transport. *Exp Neurol, 154*(2), 289-301. doi: 10.1006/exnr.1998.6888

Kolluru, G. K., Bir, S. C., & Kevil, C. G. (2012). Endothelial dysfunction and diabetes: effects on angiogenesis, vascular remodeling, and wound healing. *Int J Vasc Med, 2012*, 918267. doi: 10.1155/2012/918267

Kowal, K., Silver, R., Slawinska, E., Bielecki, M., Chyczewski, L., & Kowal-Bielecka, O. (2011). CD163 and its role in inflammation. *Folia Histochem Cytobiol, 49*(3), 365-374.

Kubera, M., Grygier, B., Arteta, B., Urbanska, K., Basta-Kaim, A., Budziszewska, B., . . . Lason, W. (2009). Age-dependent stimulatory effect of desipramine and fluoxetine pretreatment on metastasis formation by B16F10 melanoma in male C57BL/6 mice. *Pharmacol Rep, 61*(6), 1113-1126.

Lalancette-Hebert, M., Gowing, G., Simard, A., Weng, Y. C., & Kriz, J. (2007). Selective ablation of proliferating microglial cells exacerbates ischemic injury in the brain. *J Neurosci, 27*(10), 2596-2605. doi: 10.1523/JNEUROSCI.5360-06.2007

Lapchak, P. A., & Han, M. K. (2010). Simvastatin improves clinical scores in a rabbit multiple infarct ischemic stroke model: synergism with a ROCK inhibitor but not the thrombolytic tissue plasminogen activator. *Brain Res, 1344*, 217-225. doi: 10.1016/j.brainres.2010.05.035

Laufs, U., Fata, V. L., & Liao, J. K. (1997). Inhibition of 3-hydroxy-3-methylglutaryl (HMG)-CoA reductase blocks hypoxia-mediated down-regulation of endothelial nitric oxide synthase. *J Biol Chem, 272*(50), 31725-31729.

Lee, J. M., Grabb, M. C., Zipfel, G. J., & Choi, D. W. (2000). Brain tissue responses to ischemia. *J Clin Invest, 106*(6), 723-731. doi: 10.1172/JCI11003

Lee, J. Y., Kim, H. S., Choi, H. Y., Oh, T. H., & Yune, T. Y. (2012). Fluoxetine inhibits matrix metalloprotease activation and prevents disruption of blood-spinal cord barrier after spinal cord injury. *Brain, 135*(Pt 8), 2375-2389. doi: 10.1093/brain/aws171

Lees, K. R., Bluhmki, E., von Kummer, R., Brott, T. G., Toni, D., Grotta, J. C., . . . Byrnes, G. (2010). Time to treatment with intravenous alteplase and outcome in stroke: an updated pooled analysis of ECASS, ATLANTIS, NINDS, and EPITHET trials. *Lancet, 375*(9727), 1695-1703. doi: 10.1016/S0140-6736(10)60491-6

Leisman, G., Braun-Benjamin, O., & Melillo, R. (2014). Cognitive-motor interactions of the basal ganglia in development. *Front Syst Neurosci, 8*, 16. doi: 10.3389/fnsys.2014.00016

Leist, M., Ghezzi, P., Grasso, G., Bianchi, R., Villa, P., Fratelli, M., . . . Brines, M. (2004). Derivatives of erythropoietin that are tissue protective but not erythropoietic. *Science, 305*(5681), 239-242. doi: 10.1126/science.1098313

Levesque, S., Wilson, B., Gregoria, V., Thorpe, L. B., Dallas, S., Polikov, V. S., . . . Block, M. L. (2010). Reactive microgliosis: extracellular micro-calpain and microglia-mediated dopaminergic neurotoxicity. *Brain, 133*(Pt 3), 808-821. doi: 10.1093/brain/awp333

Li, K., Futrell, N., Tovar, S., Wang, L. C., Wang, D. Z., & Schultz, L. R. (1996). Gender influences the magnitude of the inflammatory response within embolic cerebral infarcts in young rats. *Stroke, 27*(3), 498-503.

Li, W. L., Cai, H. H., Wang, B., Chen, L., Zhou, Q. G., Luo, C. X., . . . Zhu, D. Y. (2009). Chronic fluoxetine treatment improves ischemia-induced spatial cognitive deficits through increasing hippocampal neurogenesis after stroke. *J Neurosci Res, 87*(1), 112-122. doi: 10.1002/jnr.21829

Liao, J. K., & Laufs, U. (2005). Pleiotropic effects of statins. *Annu Rev Pharmacol Toxicol, 45*, 89-118. doi: 10.1146/annurev.pharmtox.45.120403.095748

Lim, C. M., Kim, S. W., Park, J. Y., Kim, C., Yoon, S. H., & Lee, J. K. (2009). Fluoxetine affords robust neuroprotection in the postischemic brain via its anti-inflammatory effect. *J Neurosci Res, 87*(4), 1037-1045. doi: 10.1002/jnr.21899

Liss, H. (2006). Publication bias in the pulmonary/allergy literature: effect of pharmaceutical company sponsorship. *Isr Med Assoc J, 8*(7), 451-454.

Liu, D., Wang, Z., Liu, S., Wang, F., Zhao, S., & Hao, A. (2011). Anti-inflammatory effects of fluoxetine in lipopolysaccharide(LPS)-stimulated microglial cells. *Neuropharmacology, 61*(4), 592-599. doi: 10.1016/j.neuropharm.2011.04.033

Liu, S. (2009). Dealing with publication bias in translational stroke research. *J Exp Stroke Transl Med, 2*(1), 16-21.

Liu, X., Zhang, J., Sun, D., Fan, Y., Zhou, H., & Fu, B. (2013). Fluoxetine enhances Brain Derived Neurotropic Factor Serum Concentration and Cognition in Patients with Vascular Dementia. *Curr Neurovasc Res*.

Liu, X. F., Fawcett, J. R., Thorne, R. G., DeFor, T. A., & Frey, W. H., 2nd. (2001). Intranasal administration of insulin-like growth factor-I bypasses the blood-brain barrier and protects against focal cerebral ischemic damage. *J Neurol Sci, 187*(1-2), 91-97.

Liu, X. F., Fawcett, J. R., Thorne, R. G., & Frey, W. H., 2nd. (2001). Non-invasive intranasal insulin-like growth factor-I reduces infarct volume and improves neurologic function in rats following middle cerebral artery occlusion. *Neurosci Lett, 308*(2), 91-94.

Livingston-Thomas, J. M., Hume, A. W., Doucette, T. A., & Tasker, R. A. (2013). A novel approach to induction and rehabilitation of deficits in forelimb function in a rat model of ischemic stroke. *Acta Pharmacol Sin, 34*(1), 104-112. doi: 10.1038/aps.2012.106

Livingston-Thomas, J. M., McGuire, E. P., Doucette, T. A., & Tasker, R. A. (2014). Voluntary forced use of the impaired limb following stroke facilitates functional recovery in the rat. *Behav Brain Res, 261*, 210-219. doi: 10.1016/j.bbr.2013.12.032

Lledo, P. M., Alonso, M., & Grubb, M. S. (2006). Adult neurogenesis and functional plasticity in neuronal circuits. *Nat Rev Neurosci, 7*(3), 179-193. doi: 10.1038/nrn1867

Longa, E. Z., Weinstein, P. R., Carlson, S., & Cummins, R. (1989). Reversible middle cerebral artery occlusion without craniectomy in rats. *Stroke, 20*(1), 84-91.

Luo, X. G., & Chen, S. D. (2012). The changing phenotype of microglia from homeostasis to disease. *Transl Neurodegener, 1*(1), 9. doi: 10.1186/2047-9158-1-9

Macrae, I. M. (2011). Preclinical stroke research--advantages and disadvantages of the most common rodent models of focal ischaemia. *Br J Pharmacol, 164*(4), 1062-1078. doi: 10.1111/j.1476-5381.2011.01398.x

Malberg, J. E., Eisch, A. J., Nestler, E. J., & Duman, R. S. (2000). Chronic antidepressant treatment increases neurogenesis in adult rat hippocampus. *J Neurosci, 20*(24), 9104-9110.

Mang, C. S., Campbell, K. L., Ross, C. J., & Boyd, L. A. (2013). Promoting neuroplasticity for motor rehabilitation after stroke: considering the effects of aerobic exercise and genetic variation on brain-derived neurotrophic factor. *Phys Ther, 93*(12), 1707-1716. doi: 10.2522/ptj.20130053

Mantovani, A., Sica, A., Sozzani, S., Allavena, P., Vecchi, A., & Locati, M. (2004). The chemokine system in diverse forms of macrophage activation and polarization. *Trends Immunol, 25*(12), 677-686. doi: 10.1016/j.it.2004.09.015

Marlier, Q., Verteneuil, S., Vandenbosch, R., & Malgrange, B. (2015). Mechanisms and Functional Significance of Stroke-Induced Neurogenesis. *Front Neurosci, 9*, 458. doi: 10.3389/fnins.2015.00458

McPherson, C. A., Kraft, A. D., & Harry, G. J. (2011). Injury-induced neurogenesis: consideration of resident microglia as supportive of neural progenitor cells. *Neurotox Res, 19*(2), 341-352. doi: 10.1007/s12640-010-9199-6

Mead, G. E., Hsieh, C. F., Lee, R., Kutlubaev, M., Claxton, A., Hankey, G. J., & Hackett, M. (2013). Selective serotonin reuptake inhibitors for stroke recovery: a systematic

review and meta-analysis. *Stroke, 44*(3), 844-850. doi: 10.1161/STROKEAHA.112.673947

Mecca, A. P., O'Connor, T. E., Katovich, M. J., & Sumners, C. (2009). Candesartan pretreatment is cerebroprotective in a rat model of endothelin-1-induced middle cerebral artery occlusion. *Exp Physiol, 94*(8), 937-946. doi: 10.1113/expphysiol.2009.047936

Meijer, M. K., Spruijt, B. M., van Zutphen, L. F., & Baumans, V. (2006). Effect of restraint and injection methods on heart rate and body temperature in mice. *Lab Anim, 40*(4), 382-391. doi: 10.1258/002367706778476370

Miller, D. J., Simpson, J. R., & Silver, B. (2011). Safety of thrombolysis in acute ischemic stroke: a review of complications, risk factors, and newer technologies. *Neurohospitalist, 1*(3), 138-147. doi: 10.1177/1941875211408731

Montoya, C. P., Campbell-Hope, L. J., Pemberton, K. D., & Dunnett, S. B. (1991). The "staircase test": a measure of independent forelimb reaching and grasping abilities in rats. *J Neurosci Methods, 36*(2-3), 219-228.

Mozaffarian, D., Benjamin, E. J., Go, A. S., Arnett, D. K., Blaha, M. J., Cushman, M., . . . Stroke Statistics, S. (2016). Heart Disease and Stroke Statistics-2016 Update: A Report From the American Heart Association. *Circulation, 133*(4), e38-e360. doi: 10.1161/CIR.0000000000000350

Nijland, R., Kwakkel, G., Bakers, J., & van Wegen, E. (2011). Constraint-induced movement therapy for the upper paretic limb in acute or sub-acute stroke: a systematic review. *Int J Stroke, 6*(5), 425-433. doi: 10.1111/j.1747-4949.2011.00646.x

Ohab, J. J., & Carmichael, S. T. (2008). Poststroke neurogenesis: emerging principles of migration and localization of immature neurons. *Neuroscientist, 14*(4), 369-380. doi: 10.1177/1073858407309545

Ouellet, D., Hsu, A., Qian, J., Lamm, J. E., Cavanaugh, J. H., Leonard, J. M., & Granneman, G. R. (1998). Effect of fluoxetine on pharmacokinetics of ritonavir. *Antimicrob Agents Chemother, 42*(12), 3107-3112.

Parent, J. M., Vexler, Z. S., Gong, C., Derugin, N., & Ferriero, D. M. (2002). Rat forebrain neurogenesis and striatal neuron replacement after focal stroke. *Ann Neurol, 52*(6), 802-813. doi: 10.1002/ana.10393

Patel, N., Rao, V. A., Heilman-Espinoza, E. R., Lai, R., Quesada, R. A., & Flint, A. C. (2012). Simple and reliable determination of the modified rankin scale score in neurosurgical and neurological patients: the mRS-9Q. *Neurosurgery, 71*(5), 971-975; discussion 975. doi: 10.1227/NEU.0b013e31826a8a56

Pedersen, T. R. (2010). Pleiotropic effects of statins: evidence against benefits beyond LDL-cholesterol lowering. *Am J Cardiovasc Drugs, 10 Suppl 1*, 10-17. doi: 10.2165/1158822-S0-000000000-00000

Perlis, R. H., Perlis, C. S., Wu, Y., Hwang, C., Joseph, M., & Nierenberg, A. A. (2005). Industry sponsorship and financial conflict of interest in the reporting of clinical trials in psychiatry. *Am J Psychiatry, 162*(10), 1957-1960. doi: 10.1176/appi.ajp.162.10.1957

Polan, M. L., Daniele, A., & Kuo, A. (1988). Gonadal steroids modulate human monocyte interleukin-1 (IL-1) activity. *Fertil Steril, 49*(6), 964-968.

Qu, H. L., Zhao, M., Zhao, S. S., Xiao, T., Song, C. G., Cao, Y. P., . . . Zhao, C. S. (2015). Forced limb-use enhanced neurogenesis and behavioral recovery after stroke in the aged rats. *Neuroscience, 286*, 316-324. doi: 10.1016/j.neuroscience.2014.11.040

Rabadi, M. H., & Kristal, B. S. (2007). Effect of vitamin C supplementation on stroke recovery: a case-control study. *Clin Interv Aging, 2*(1), 147-151.

Ragas, M. A., Balch, M., Hensley, A., Reynolds, K., Wright, D., Kerr, B., & Corbett, A. M. (2015). Stroke Physical Rehabilitation: Impact on Motor Functional Recovery in Drug Treated versus Vehicle Treated Rats. *Stroke, 46*.

Randomised trial of cholesterol lowering in 4444 patients with coronary heart disease: the Scandinavian Simvastatin Survival Study (4S). (1994). *Lancet, 344*(8934), 1383-1389.

Rankin, J. (1957). Cerebral vascular accidents in patients over the age of 60. III. Diagnosis and treatment. *Scott Med J, 2*(6), 254-268.

Rickhag, M., Wieloch, T., Gido, G., Elmer, E., Krogh, M., Murray, J., . . . Nikolich, K. (2006). Comprehensive regional and temporal gene expression profiling of the rat

brain during the first 24 h after experimental stroke identifies dynamic ischemia-induced gene expression patterns, and reveals a biphasic activation of genes in surviving tissue. *J Neurochem, 96*(1), 14-29. doi: 10.1111/j.1471-4159.2005.03508.x

Risedal, A., Zeng, J., & Johansson, B. B. (1999). Early training may exacerbate brain damage after focal brain ischemia in the rat. *J Cereb Blood Flow Metab, 19*(9), 997-1003. doi: 10.1097/00004647-199909000-00007

Rizzino, A. (2009). Sox2 and Oct-3/4: a versatile pair of master regulators that orchestrate the self-renewal and pluripotency of embryonic stem cells. *Wiley Interdiscip Rev Syst Biol Med, 1*(2), 228-236. doi: 10.1002/wsbm.12

Rodriguez-Yanez, M., Agulla, J., Rodriguez-Gonzalez, R., Sobrino, T., & Castillo, J. (2008). Statins and stroke. *Ther Adv Cardiovasc Dis, 2*(3), 157-166. doi: 10.1177/1753944708091776

Rosamond, W., Flegal, K., Furie, K., Go, A., Greenlund, K., Haase, N., . . . Stroke Statistics, S. (2008). Heart disease and stroke statistics--2008 update: a report from the American Heart Association Statistics Committee and Stroke Statistics Subcommittee. *Circulation, 117*(4), e25-146. doi: 10.1161/CIRCULATIONAHA.107.187998

Rosell, A., & Lo, E. H. (2008). Multiphasic roles for matrix metalloproteinases after stroke. *Curr Opin Pharmacol, 8*(1), 82-89. doi: 10.1016/j.coph.2007.12.001

Rowntree, S., & Kolb, B. (1997). Blockade of basic fibroblast growth factor retards recovery from motor cortex injury in rats. *Eur J Neurosci, 9*(11), 2432-2441.

Sacrey, L. A., Alaverdashvili, M., & Whishaw, I. Q. (2009). Similar hand shaping in reaching-for-food (skilled reaching) in rats and humans provides evidence of homology in release, collection, and manipulation movements. *Behav Brain Res, 204*(1), 153-161. doi: 10.1016/j.bbr.2009.05.035

Sahay, A., & Hen, R. (2007). Adult hippocampal neurogenesis in depression. *Nat Neurosci, 10*(9), 1110-1115. doi: 10.1038/nn1969

Sakurai, T., Amemiya, A., Ishii, M., Matsuzaki, I., Chemelli, R. M., Tanaka, H., . . . Yanagisawa, M. (1998). Orexins and orexin receptors: a family of hypothalamic

neuropeptides and G protein-coupled receptors that regulate feeding behavior. *Cell, 92*(4), 573-585.

Sanchez, C. A., Rodriguez, E., Varela, E., Zapata, E., Paez, A., Masso, F. A., . . . Loopez-Marure, R. (2008). Statin-induced inhibition of MCF-7 breast cancer cell proliferation is related to cell cycle arrest and apoptotic and necrotic cell death mediated by an enhanced oxidative stress. *Cancer Invest, 26*(7), 698-707. doi: 10.1080/07357900701874658

Sargeant, T. J., Miller, J. H., & Day, D. J. (2008). Opioidergic regulation of astroglial/neuronal proliferation: where are we now? *J Neurochem, 107*(4), 883-897. doi: 10.1111/j.1471-4159.2008.05671.x

Sasaki, Y., Sasaki, M., Kataoka-Sasaki, Y., Nakazaki, M., Nagahama, H., Suzuki, J., . . . Honmou, O. (2016). Synergic Effects of Rehabilitation and Intravenous Infusion of Mesenchymal Stem Cells After Stroke in Rats. *Phys Ther*. doi: 10.2522/ptj.20150504

Saver, J. L. (2006). Time is brain--quantified. *Stroke, 37*(1), 263-266. doi: 10.1161/01.STR.0000196957.55928.ab

Schaar, K. L., Brenneman, M. M., & Savitz, S. I. (2010). Functional assessments in the rodent stroke model. *Exp Transl Stroke Med, 2*(1), 13. doi: 10.1186/2040-7378-2-13

Schabitz, W. R., Berger, C., Kollmar, R., Seitz, M., Tanay, E., Kiessling, M., . . . Sommer, C. (2004). Effect of brain-derived neurotrophic factor treatment and forced arm use on functional motor recovery after small cortical ischemia. *Stroke, 35*(4), 992-997. doi: 10.1161/01.STR.0000119754.85848.0D

Schabitz, W. R., Steigleder, T., Cooper-Kuhn, C. M., Schwab, S., Sommer, C., Schneider, A., & Kuhn, H. G. (2007). Intravenous brain-derived neurotrophic factor enhances poststroke sensorimotor recovery and stimulates neurogenesis. *Stroke, 38*(7), 2165-2172. doi: 10.1161/STROKEAHA.106.477331

Schallert, T., Fleming, S. M., Leasure, J. L., Tillerson, J. L., & Bland, S. T. (2000). CNS plasticity and assessment of forelimb sensorimotor outcome in unilateral rat models of stroke, cortical ablation, parkinsonism and spinal cord injury. *Neuropharmacology, 39*(5), 777-787.

Scheitz, J. F., Seiffge, D. J., Tutuncu, S., Gensicke, H., Audebert, H. J., Bonati, L. H., . . . Nolte, C. H. (2014). Dose-related effects of statins on symptomatic intracerebral hemorrhage and outcome after thrombolysis for ischemic stroke. *Stroke, 45*(2), 509-514. doi: 10.1161/STROKEAHA.113.002751

Schneider, A., Kruger, C., Steigleder, T., Weber, D., Pitzer, C., Laage, R., . . . Schabitz, W. R. (2005). The hematopoietic factor G-CSF is a neuronal ligand that counteracts programmed cell death and drives neurogenesis. *J Clin Invest, 115*(8), 2083-2098. doi: 10.1172/JCI23559

Sharp, F. R., Bergeron, M., & Bernaudin, M. (2001). Hypoxia-inducible factor in brain. *Adv Exp Med Biol, 502*, 273-291.

Siepmann, T., Penzlin, A. I., Kepplinger, J., Illigens, B. M., Weidner, K., Reichmann, H., & Barlinn, K. (2015). Selective serotonin reuptake inhibitors to improve outcome in acute ischemic stroke: possible mechanisms and clinical evidence. *Brain Behav, 5*(10), e00373. doi: 10.1002/brb3.373

Song, J., Kim, E., Kim, C. H., Song, H. T., & Lee, J. E. (2015). The role of orexin in post-stroke inflammation, cognitive decline, and depression. *Mol Brain, 8*, 16. doi: 10.1186/s13041-015-0106-1

Stevens, S. L., Shaw, T. E., Dykhuizen, E., Lessov, N. S., Hill, J. K., Wurst, W., & Stenzel-Poore, M. P. (2003). Reduced cerebral injury in CRH-R1 deficient mice after focal ischemia: a potential link to microglia and atrocytes that express CRH-R1. *J Cereb Blood Flow Metab, 23*(10), 1151-1159. doi: 10.1097/01.WCB.0000086957.72078.D4

Strauss, W. L., Layton, M. E., Hayes, C. E., & Dager, S. R. (1997). 19F magnetic resonance spectroscopy investigation in vivo of acute and steady-state brain fluvoxamine levels in obsessive-compulsive disorder. *Am J Psychiatry, 154*(4), 516-522. doi: 10.1176/ajp.154.4.516

Stroke Therapy Academic Industry, R. (1999). Recommendations for standards regarding preclinical neuroprotective and restorative drug development. *Stroke, 30*(12), 2752-2758.

Su, F., Yi, H., Xu, L., & Zhang, Z. (2015). Fluoxetine and S-citalopram inhibit M1 activation and promote M2 activation of microglia in vitro. *Neuroscience, 294*, 60-68. doi: 10.1016/j.neuroscience.2015.02.028

Szklarczyk, D., Franceschini, A., Kuhn, M., Simonovic, M., Roth, A., Minguez, P., . . . von Mering, C. (2011). The STRING database in 2011: functional interaction networks of proteins, globally integrated and scored. *Nucleic Acids Res, 39*(Database issue), D561-568. doi: 10.1093/nar/gkq973

Szklarczyk, D., Franceschini, A., Wyder, S., Forslund, K., Heller, D., Huerta-Cepas, J., . . . von Mering, C. (2015). STRING v10: protein-protein interaction networks, integrated over the tree of life. *Nucleic Acids Res, 43*(Database issue), D447-452. doi: 10.1093/nar/gku1003

Taub, E., Uswatte, G., Mark, V. W., & Morris, D. M. (2006). The learned nonuse phenomenon: implications for rehabilitation. *Eura Medicophys, 42*(3), 241-256.

Teramoto, T., Qiu, J., Plumier, J. C., & Moskowitz, M. A. (2003). EGF amplifies the replacement of parvalbumin-expressing striatal interneurons after ischemia. *J Clin Invest, 111*(8), 1125-1132. doi: 10.1172/JCI17170

Thelen, K. M., Rentsch, K. M., Gutteck, U., Heverin, M., Olin, M., Andersson, U., . . . Lutjohann, D. (2006). Brain cholesterol synthesis in mice is affected by high dose of simvastatin but not of pravastatin. *J Pharmacol Exp Ther, 316*(3), 1146-1152. doi: 10.1124/jpet.105.094136

Thored, P., Wood, J., Arvidsson, A., Cammenga, J., Kokaia, Z., & Lindvall, O. (2007). Long-term neuroblast migration along blood vessels in an area with transient angiogenesis and increased vascularization after stroke. *Stroke, 38*(11), 3032-3039. doi: 10.1161/STROKEAHA.107.488445

Tissue plasminogen activator for acute ischemic stroke. The National Institute of Neurological Disorders and Stroke rt-PA Stroke Study Group. (1995). *N Engl J Med, 333*(24), 1581-1587. doi: 10.1056/NEJM199512143332401

Toung, T. J., Traystman, R. J., & Hurn, P. D. (1998). Estrogen-mediated neuroprotection after experimental stroke in male rats. *Stroke, 29*(8), 1666-1670.

Trivedi, P., Yu, H., MacNeil, D. J., Van der Ploeg, L. H., & Guan, X. M. (1998). Distribution of orexin receptor mRNA in the rat brain. *FEBS Lett, 438*(1-2), 71-75.

Trombly, C. A., Radomski, M. V., Trexel, C., & Burnet-Smith, S. E. (2002). Occupational therapy and achievement of self-identified goals by adults with acquired brain injury: phase II. *Am J Occup Ther, 56*(5), 489-498.

Tuttolomondo, A., Pecoraro, R., Di Raimondo, D., Arnao, V., Clemente, G., Della Corte, V., . . . Pinto, A. (2013). Stroke subtypes and their possible implication in stroke prevention drug strategies. *Curr Vasc Pharmacol, 11*(6), 824-837.

Villeda, S. A., Luo, J., Mosher, K. I., Zou, B., Britschgi, M., Bieri, G., . . . Wyss-Coray, T. (2011). The ageing systemic milieu negatively regulates neurogenesis and cognitive function. *Nature, 477*(7362), 90-94. doi: 10.1038/nature10357

Viscovich, M., Lykkesfeldt, J., & Poulsen, H. E. (2004). Vitamin C pharmacokinetics of plain and slow release formulations in smokers. *Clin Nutr, 23*(5), 1043-1050. doi: 10.1016/j.clnu.2004.01.007

Wahl, A. S., & Schwab, M. E. (2014). Finding an optimal rehabilitation paradigm after stroke: enhancing fiber growth and training of the brain at the right moment. *Front Hum Neurosci, 8*, 381. doi: 10.3389/fnhum.2014.00381

Walter, J., Keiner, S., Witte, O. W., & Redecker, C. (2011). Age-related effects on hippocampal precursor cell subpopulations and neurogenesis. *Neurobiol Aging, 32*(10), 1906-1914. doi: 10.1016/j.neurobiolaging.2009.11.011

Wang, R. Y., Wang, P. S., & Yang, Y. R. (2003). Effect of age in rats following middle cerebral artery occlusion. *Gerontology, 49*(1), 27-32. doi: 66505

Wang, W., Ji, P., Riopelle, R. J., & Dow, K. E. (2002). Functional expression of corticotropin-releasing hormone (CRH) receptor 1 in cultured rat microglia. *J Neurochem, 80*(2), 287-294.

Wang, Y., Neumann, M., Hansen, K., Hong, S. M., Kim, S., Noble-Haeusslein, L. J., & Liu, J. (2011). Fluoxetine increases hippocampal neurogenesis and induces epigenetic factors but does not improve functional recovery after traumatic brain injury. *J Neurotrauma, 28*(2), 259-268. doi: 10.1089/neu.2010.1648

Warren, J. B. (2012). Antidepressants and the developing nervous system. *Br J Clin Pharmacol, 73*(1), 1-3. doi: 10.1111/j.1365-2125.2011.04107.x

Whishaw, I. Q., Suchowersky, O., Davis, L., Sarna, J., Metz, G. A., & Pellis, S. M. (2002). Impairment of pronation, supination, and body co-ordination in reach-to-grasp

tasks in human Parkinson's disease (PD) reveals homology to deficits in animal models. *Behav Brain Res, 133*(2), 165-176.

Whishaw, I. Q., Whishaw, P., & Gorny, B. (2008). The structure of skilled forelimb reaching in the rat: a movement rating scale. *J Vis Exp*(18). doi: 10.3791/816

Wieloch, T., & Nikolich, K. (2006). Mechanisms of neural plasticity following brain injury. *Curr Opin Neurobiol, 16*(3), 258-264. doi: 10.1016/j.conb.2006.05.011

Williams, K., & Lee, E. (1985). Importance of drug enantiomers in clinical pharmacology. *Drugs, 30*(4), 333-354.

Windle, V., & Corbett, D. (2005). Fluoxetine and recovery of motor function after focal ischemia in rats. *Brain Res, 1044*(1), 25-32. doi: 10.1016/j.brainres.2005.02.060

Windle, V., Szymanska, A., Granter-Button, S., White, C., Buist, R., Peeling, J., & Corbett, D. (2006). An analysis of four different methods of producing focal cerebral ischemia with endothelin-1 in the rat. *Exp Neurol, 201*(2), 324-334. doi: 10.1016/j.expneurol.2006.04.012

Wittenberg, G. F., Chen, R., Ishii, K., Bushara, K. O., Eckloff, S., Croarkin, E., . . . Cohen, L. G. (2003). Constraint-induced therapy in stroke: magnetic-stimulation motor maps and cerebral activation. *Neurorehabil Neural Repair, 17*(1), 48-57.

Wodak, S. J., Pu, S., Vlasblom, J., & Seraphin, B. (2009). Challenges and rewards of interaction proteomics. *Mol Cell Proteomics, 8*(1), 3-18. doi: 10.1074/mcp.R800014-MCP200

Wood, W. G., Eckert, G. P., Igbavboa, U., & Muller, W. E. (2010). Statins and neuroprotection: a prescription to move the field forward. *Ann N Y Acad Sci, 1199*, 69-76. doi: 10.1111/j.1749-6632.2009.05359.x

Wu, H., Lu, D., Jiang, H., Xiong, Y., Qu, C., Li, B., . . . Chopp, M. (2008). Simvastatin-mediated upregulation of VEGF and BDNF, activation of the PI3K/Akt pathway, and increase of neurogenesis are associated with therapeutic improvement after traumatic brain injury. *J Neurotrauma, 25*(2), 130-139. doi: 10.1089/neu.2007.0369

Wurster, A. L., Tanaka, T., & Grusby, M. J. (2000). The biology of Stat4 and Stat6. *Oncogene, 19*(21), 2577-2584. doi: 10.1038/sj.onc.1203485

Xiang, Z., Haroutunian, V., Ho, L., Purohit, D., & Pasinetti, G. M. (2006). Microglia activation in the brain as inflammatory biomarker of Alzheimer's disease neuropathology and clinical dementia. *Dis Markers, 22*(1-2), 95-102.

Xiong, X., White, R. E., Xu, L., Yang, L., Sun, X., Zou, B., . . . Xie, X. S. (2013). Mitigation of murine focal cerebral ischemia by the hypocretin/orexin system is associated with reduced inflammation. *Stroke, 44*(3), 764-770. doi: 10.1161/STROKEAHA.112.681700

Yamada, N., Katsuura, G., Tatsuno, I., Kawahara, S., Ebihara, K., Saito, Y., & Nakao, K. (2009). Orexins increase mRNA expressions of neurotrophin-3 in rat primary cortical neuron cultures. *Neurosci Lett, 450*(2), 132-135. doi: 10.1016/j.neulet.2008.11.028

Yamanaka, A., Tabuchi, S., Tsunematsu, T., Fukazawa, Y., & Tominaga, M. (2010). Orexin directly excites orexin neurons through orexin 2 receptor. *J Neurosci, 30*(38), 12642-12652. doi: 10.1523/JNEUROSCI.2120-10.2010

Yamori, Y., Horie, R., Handa, H., Sato, M., & Fukase, M. (1976). Pathogenetic similarity of strokes in stroke-prone spontaneously hypertensive rats and humans. *Stroke, 7*(1), 46-53.

Yanagita, S., Amemiya, S., Suzuki, S., & Kita, I. (2007). Effects of spontaneous and forced running on activation of hypothalamic corticotropin-releasing hormone neurons in rats. *Life Sci, 80*(4), 356-363. doi: 10.1016/j.lfs.2006.09.027

Yang, D., Han, Y., Zhang, J., Chopp, M., & Seyfried, D. M. (2012). Statins Enhance Expression of Growth Factors and Activate the PI3K/Akt-mediated Signaling Pathway after Experimental Intracerebral Hemorrhage. *World J Neurosci, 2*(2), 74-80. doi: 10.4236/wjns.2012.22011

Yemisci, M., Gursoy-Ozdemir, Y., Vural, A., Can, A., Topalkara, K., & Dalkara, T. (2009). Pericyte contraction induced by oxidative-nitrative stress impairs capillary reflow despite successful opening of an occluded cerebral artery. *Nat Med, 15*(9), 1031-1037. doi: 10.1038/nm.2022

Yuan, L. B., Dong, H. L., Zhang, H. P., Zhao, R. N., Gong, G., Chen, X. M., . . . Xiong, L. (2011). Neuroprotective effect of orexin-A is mediated by an increase of hypoxia-

inducible factor-1 activity in rat. *Anesthesiology, 114*(2), 340-354. doi: 10.1097/ALN.0b013e318206ff6f

Zacco, A., Togo, J., Spence, K., Ellis, A., Lloyd, D., Furlong, S., & Piser, T. (2003). 3-hydroxy-3-methylglutaryl coenzyme A reductase inhibitors protect cortical neurons from excitotoxicity. *J Neurosci, 23*(35), 11104-11111.

Zhang, L., Zhang, Z. G., & Chopp, M. (2012). The neurovascular unit and combination treatment strategies for stroke. *Trends Pharmacol Sci, 33*(8), 415-422. doi: 10.1016/j.tips.2012.04.006

Zhang, Y., Zhang, H., Katiella, K., & Huang, W. (2014). Chemically extracted acellular allogeneic nerve graft combined with ciliary neurotrophic factor promotes sciatic nerve repair. *Neural Regen Res, 9*(14), 1358-1364. doi: 10.4103/1673-5374.137588

Zhang, Z., Zhang, Z. Y., Wu, Y., & Schluesener, H. J. (2012). Lesional accumulation of CD163+ macrophages/microglia in rat traumatic brain injury. *Brain Res, 1461*, 102-110. doi: 10.1016/j.brainres.2012.04.038

Zhang, Z. G., Zhang, L., Jiang, Q., Zhang, R., Davies, K., Powers, C., . . . Chopp, M. (2000). VEGF enhances angiogenesis and promotes blood-brain barrier leakage in the ischemic brain. *J Clin Invest, 106*(7), 829-838. doi: 10.1172/JCI9369

Zhu, M., Wang, J., Liu, M., Du, D., Xia, C., Shen, L., & Zhu, D. (2012). Upregulation of protein phosphatase 2A and NR3A-pleiotropic effect of simvastatin on ischemic stroke rats. *PLoS One, 7*(12), e51552. doi: 10.1371/journal.pone.0051552

Zigova, T., Pencea, V., Wiegand, S. J., & Luskin, M. B. (1998). Intraventricular administration of BDNF increases the number of newly generated neurons in the adult olfactory bulb. *Mol Cell Neurosci, 11*(4), 234-245. doi: 10.1006/mcne.1998.0684

APPENDIX I

FMA-UE PROTOCOL — Rehabilitation Medicine, University of Gothenburg

FUGL-MEYER ASSESSMENT
UPPER EXTREMITY (FMA-UE)
Assessment of sensorimotor function

ID:
Date:
Examiner:

Fugl-Meyer AR, Jaasko L, Leyman I, Olsson S, Steglind S: The post-stroke hemiplegic patient. A method for evaluation of physical performance. Scand J Rehabil Med 1975, 7:13-31.

A. UPPER EXTREMITY, sitting position					
I. Reflex activity			**none**	**can be elicited**	
Flexors: biceps and finger flexors (at least one)			0	2	
Extensors: triceps			0	2	
Subtotal I (max 4)					
II. Volitional movement within synergies, without gravitational help			**none**	**partial**	**full**
Flexor synergy: Hand from contralateral knee to ipsilateral ear. From extensor synergy (shoulder adduction/ internal rotation, elbow extension, forearm pronation) to flexor synergy (shoulder abduction/ external rotation, elbow flexion, forearm supination).	Shoulder	retraction	0	1	2
		elevation	0	1	2
		abduction (90°)	0	1	2
		external rotation	0	1	2
	Elbow	flexion	0	1	2
	Forearm	supination	0	1	2
Extensor synergy: Hand from ipsilateral ear to the contralateral knee	Shoulder	adduction/internal rotation	0	1	2
	Elbow	extension	0	1	2
	Forearm	pronation	0	1	2
Subtotal II (max 18)					
III. Volitional movement mixing synergies, without compensation			**none**	**partial**	**full**
Hand to lumbar spine hand on lap	cannot perform or hand in front of ant-sup iliac spine hand behind ant-sup iliac spine (without compensation) hand to lumbar spine (without compensation)		0	1	2
Shoulder flexion 0°- 90° elbow at 0° pronation-supination 0°	immediate abduction or elbow flexion abduction or elbow flexion during movement flexion 90°, no shoulder abduction or elbow flexion		0	1	2
Pronation-supination elbow at 90° shoulder at 0°	no pronation/supination, starting position impossible limited pronation/supination, maintains starting position full pronation/supination, maintains starting position		0	1	2
Subtotal III (max 6)					
IV. Volitional movement with little or no synergy			**none**	**partial**	**full**
Shoulder abduction 0 - 90° elbow at 0° forearm pronated	immediate supination or elbow flexion supination or elbow flexion during movement abduction 90°, maintains extension and pronation		0	1	2
Shoulder flexion 90° - 180° elbow at 0° pronation-supination 0°	immediate abduction or elbow flexion abduction or elbow flexion during movement flexion 180°, no shoulder abduction or elbow flexion		0	1	2
Pronation/supination elbow at 0° shoulder at 30°- 90° flexion	no pronation/supination, starting position impossible limited pronation/supination, maintains start position full pronation/supination, maintains starting position		0	1	2
Subtotal IV (max 6)					
V. Normal reflex activity assessed only if full score of 6 points is achieved in part IV; compare with the unaffected side			**0 (IV), hyper**	**lively**	**normal**
biceps, triceps, finger flexors	2 of 3 reflexes markedly hyperactive or 0 points in part IV 1 reflex markedly hyperactive or at least 2 reflexes lively maximum of 1 reflex lively, none hyperactive		0	1	2
Subtotal V (max 2)					
Total A (max 36)					

B. WRIST support may be provided at the elbow to take or hold the starting position, no support at wrist, check the passive range of motion prior testing		**none**	**partial**	**full**
Stability at 15° dorsiflexion elbow at 90°, forearm pronated shoulder at 0°	less than 15° active dorsiflexion dorsiflexion 15°, no resistance tolerated maintains dorsiflexion against resistance	0	1	2
Repeated dorsifexion / volar flexion elbow at 90°, forearm pronated shoulder at 0°, slight finger flexion	cannot perform volitionally limited active range of motion full active range of motion, smoothly	0	1	2
Stability at 15° dorsiflexion elbow at 0°, forearm pronated slight shoulder flexion/abduction	less than 15° active dorsiflexion dorsiflexion 15°, no resistance tolerated maintains dorsiflexion against resistance	0	1	2
Repeated dorsifexion / volar flexion elbow at 0°, forearm pronated slight shoulder flexion/abduction	cannot perform volitionally limited active range of motion full active range of motion, smoothly	0	1	2
Circumduction elbow at 90°, forearm pronated shoulder at 0°	cannot perform volitionally jerky movement or incomplete complete and smooth circumduction	0	1	2
	Total B (max 10)			

C. HAND support may be provided at the elbow to keep 90° flexion, no support at the wrist, compare with unaffected hand, the objects are interposed, active grasp		**none**	**partial**	**full**
Mass flexion from full active or passive extension		0	1	2
Mass extension from full active or passive flexion		0	1	2
GRASP				
a. Hook grasp flexion in PIP and DIP (digits II-V), extension in MCP II-V	cannot be performed can hold position but weak maintains position against resistance	0	1	2
b. Thumb adduction 1-st CMC, MCP, IP at 0°, scrap of paper between thumb and 2-nd MCP joint	cannot be performed can hold paper but not against tug can hold paper against a tug	0	1	2
c. Pincer grasp, opposition pulpa of the thumb against the pulpa of 2-nd finger, pencil, tug upward	cannot be performed can hold pencil but not against tug can hold pencil against a tug	0	1	2
d. Cylinder grasp cylinder shaped object (small can) tug upward, opposition of thumb and fingers	cannot be performed can hold cylinder but not against tug can hold cylinder against a tug	0	1	2
e. Spherical grasp fingers in abduction/flexion, thumb opposed, tennis ball, tug away	cannot be performed can hold ball but not against tug can hold ball against a tug	0	1	2
	Total C (max 14)			

D. COORDINATION/SPEED, sitting, after one trial with both arms, eyes closed, tip of the index finger from knee to nose, 5 times as fast as possible		**marked**	**slight**	**none**
Tremor	at least 1 completed movement	0	1	2
Dysmetria at least 1 completed movement	pronounced or unsystematic slight and systematic no dysmetria	0	1	2
		≥ 6s	**2 - 5s**	**< 2s**
Time start and end with the hand on the knee	at least 6 seconds slower than unaffected side 2-5 seconds slower than unaffected side less than 2 seconds difference	0	1	2
	Total D (max 6)			

TOTAL A-D (max 66)	

H. SENSATION, upper extremity eyes closed, compared with the unaffected side		**anesthesia**	**hypoesthesia or dysesthesia**	**normal**
Light touch	upper arm, forearm palmary surface of the hand	0 0	1 1	2 2
		less than 3/4 correct or absence	**3/4 correct or considerable difference**	**correct 100%, little or no difference**
Position small alterations in the position	shoulder elbow wrist thumb (IP-joint)	0 0 0 0	1 1 1 1	2 2 2 2
			Total H (max12)	

J. PASSIVE JOINT MOTION, upper extremity, sitting position, compare with the unaffected side				**J. JOINT PAIN** during passive motion, upper extremity		
	only few degrees (less than 10° in shoulder)	decreased	normal	pronounced pain during movement or very marked pain at the end of the movement	some pain	no pain
Shoulder						
Flexion (0° - 180°)	0	1	2	0	1	2
Abduction (0°-90°)	0	1	2	0	1	2
External rotation	0	1	2	0	1	2
Internal rotation	0	1	2	0	1	2
Elbow						
Flexion	0	1	2	0	1	2
Extension	0	1	2	0	1	2
Forearm						
Pronation	0	1	2	0	1	2
Supination	0	1	2	0	1	2
Wrist						
Flexion	0	1	2	0	1	2
Extension	0	1	2	0	1	2
Fingers						
Flexion	0	1	2	0	1	2
Extension	0	1	2	0	1	2
Total (max 24)				**Total** (max 24)		

A. UPPER EXTREMITY	/36
B. WRIST	/10
C. HAND	/14
D. COORDINATION / SPEED	/ 6
TOTAL A-D (motor function)	/66

H. SENSATION	/12
J. PASSIVE JOINT MOTION	/24
J. JOINT PAIN	/24

APPENDIX II

Gene table shows gene position, symbol and description for M1 and M2 microglia biomarkers.

A01 ***Bdnf*** Brain-derived neurotrophic factor
A02 ***Arg1*** Arginase
A03 ***Camk2a*** Calcium/calmodulin-dependent protein kinase II alpha
A04 ***Camk2g*** Calcium/calmodulin-dependent protein kinase II gamma
A05 ***Cbln1*** Cerebellin 1 precursor
A06 ***Ccl11*** Chemokine (C-C motif) ligand 11
A07 ***Bdnf*** Brain-derived neurotrophic factor
A08 ***Arg1*** Arginase
A09 ***Camk2a*** Calcium/calmodulin-dependent protein kinase II alpha
A10 ***Camk2g*** Calcium/calmodulin-dependent protein kinase II gamma
A11 ***Cbln1*** Cerebellin 1 precursor
A12 ***Ccl11*** Chemokine (C-C motif) ligand 11
B01 ***Cd163*** CD163 molecule
B02 ***Cd40*** CD40 molecule, TNF receptor superfamily member 5
B03 ***Cntf*** Ciliary neurotrophic factor
B04 ***Cntfr*** Ciliary neurotrophic factor receptor
B05 ***Creb1*** CAMP responsive element binding protein 1
B06 ***Crh*** Corticotropin releasing hormone
B07 ***Cd163*** CD163 molecule
B08 ***Cd40*** CD40 molecule, TNF receptor superfamily member 5
B09 ***Cntf*** Ciliary neurotrophic factor
B10 ***Cntfr*** Ciliary neurotrophic factor receptor
B11 ***Creb1*** CAMP responsive element binding protein 1
B12 ***Crh*** Corticotropin releasing hormone
C01 ***Crhbp*** Corticotropin releasing hormone binding protein
C02 ***Crhr1*** Corticotropin releasing hormone receptor 1

C03 ***Crhr2*** Corticotropin releasing hormone receptor 2
C04 ***Cxcr4*** Chemokine (C-X-C motif) receptor 4
C05 ***Fgf9*** Fibroblast growth factor 9
C06 ***Fos*** FBJ osteosarcoma oncogene
C07 ***Crhbp*** Corticotropin releasing hormone binding protein
C08 ***Crhr1*** Corticotropin releasing hormone receptor 1
C09 ***Crhr2*** Corticotropin releasing hormone receptor 2
C10 ***Cxcr4*** Chemokine (C-X-C motif) receptor 4
C11 ***Fgf9*** Fibroblast growth factor 9
C12 ***Fos*** FBJ osteosarcoma oncogene
D01 ***Galr1*** Galanin receptor 1
D02 ***Gfra3*** GDNF family receptor alpha 3
D03 ***Gmfg*** Glia maturation factor, gamma
D04 ***Il1b*** Interleukin 1 beta
D05 ***il10ra*** Interleukin 10 receptor, alpha
D06 ***Il6*** Interleukin 6
D07 ***Galr1*** Galanin receptor 1
D08 ***Gfra3*** GDNF family receptor alpha 3
D09 ***Gmfg*** Glia maturation factor, gamma
D10 ***Il1b*** Interleukin 1 beta
D11 ***il10ra*** Interleukin 10 receptor, alpha
D12 ***Il6*** Interleukin 6
E01 ***Nos2*** Nitric oxide synthase 2, inducible
E02 ***Nell1*** NEL-like 1
E03 ***Npy1r*** Neuropeptide Y receptor Y1
E04 ***Npy2r*** Neuropeptide Y receptor Y2
E05 ***Sox2*** SRY (sex determining region Y)-box 2
E06 ***Stat1*** Signal transducer and activator of transcription 1
E07 ***Nos2*** Nitric oxide synthase 2, inducible
E08 ***Nell1*** NEL-like 1

E09 ***Npy1r*** Neuropeptide Y receptor Y1
E10 ***Npy2r*** Neuropeptide Y receptor Y2
E11 ***Sox2*** SRY (sex determining region Y)-box 2
E12 ***Stat1*** Signal transducer and activator of transcription 1
F01 ***Stat3*** Signal transducer and activator of transcription 3
F02 ***Stat4*** Signal transducer and activator of transcription 4
F03 ***Stat6*** Signal transducer and activator of transcription 6
F04 ***Tgfb1*** Transforming growth factor, beta 1
F05 ***Tnf*** Tumor necrosis factor (TNF superfamily, member 2)
F06 ***Plat*** Plasminogen activator, tissue
F07 ***Stat3*** Signal transducer and activator of transcription 3
F08 ***Stat4*** Signal transducer and activator of transcription 4
F09 ***Stat6*** Signal transducer and activator of transcription 6
F10 ***Tgfb1*** Transforming growth factor, beta 1
F11 ***Tnf*** Tumor necrosis factor (TNF superfamily, member 2)
F12 ***Plat*** Plasminogen activator, tissue
G01 ***Grip1*** Glutamate receptor interacting protein 1
G02 ***Vegfa*** Vascular endothelial growth factor A
G03 ***Ppih*** Peptidylprolyl isomerase H (cyclophilin H)
G04 ***Actb*** Actin, beta
G05 ***Hprt1*** Hypoxanthine phosphoribosyltransferase 1
G06 ***Ldha*** Lactate dehydrogenase A
G07 ***Grip1*** Glutamate receptor interacting protein 1
G08 ***Vegfa*** Vascular endothelial growth factor A
G09 ***Ppih*** Peptidylprolyl isomerase H (cyclophilin H)
G10 ***Actb*** Actin, beta
G11 ***Hprt1*** Hypoxanthine phosphoribosyltransferase 1
G12 ***Ldha*** Lactate dehydrogenase A
H01 ***Nono*** Non-POU domain containing, octamer-binding
H02 **GDC** Genomic DNA control

H03 **RTC** Reverse-transcription control
H04 **RTC** Reverse-transcription control
H05 **PPC** Positive PCR control
H06 **PPC** Positive PCR control
H07 ***Nono*** Non-POU domain containing, octamer-binding
H08 **GDC** Genomic DNA control
H09 **RTC** Reverse-transcription control
H10 **RTC** Reverse-transcription control
H11 **PPC** Positive PCR control
H12 **PPC** Positive PCR control

APPENDIX III

Gene table shows gene position, symbol and description for neurotrophins and receptors RT² Profiler PCR Array

A01 ***Adcyap1r1*** Adenylate cyclase activating polypeptide 1 receptor 1
A02 ***Artn*** Artemin
A03 ***Bax*** Bcl2-associated X protein
A04 ***Bcl2*** B-cell CLL/lymphoma 2
A05 ***Bdnf*** Brain-derived neurotrophic factor
A06 ***Cbln1*** Cerebellin 1 precursor
A07 ***Cckar*** Cholecystokinin A receptor
A08 ***Cd40*** CD40 molecule, TNF receptor superfamily member 5
A09 ***Cntf*** Ciliary neurotrophic factor
A10 ***Cntfr*** Ciliary neurotrophic factor receptor
A11 ***Crh*** Corticotropin releasing hormone
A12 ***Crhbp*** Corticotropin releasing hormone binding protein
B01 ***Crhr1*** Corticotropin releasing hormone receptor 1
B02 ***Crhr2*** Corticotropin releasing hormone receptor 2
B03 ***Cx3cr1*** Chemokine (C-X3-C motif) receptor 1
B04 ***Cxcr4*** Chemokine (C-X-C motif) receptor 4
B05 ***Fas*** Fas (TNF receptor superfamily, member 6)
B06 ***Fgf2*** Fibroblast growth factor 2
Fgf9 ***Fibroblast*** growth factor 9
B08 ***Fgfr1*** Fibroblast growth factor receptor 1
B09 ***Fos*** FBJ osteosarcoma oncogene
B10 ***Frs2*** Fibroblast growth factor receptor substrate 2
B11 ***Frs3*** Fibroblast growth factor receptor substrate 3
B12 ***Fus*** Fusion (involved in t(12;16) in malignant liposarcoma) (human)
C01 ***Galr1*** Galanin receptor 1
C02 ***Galr2*** Galanin receptor 2

C03 ***Gdnf*** Glial cell derived neurotrophic factor
C04 ***Gfra1*** GDNF family receptor alpha 1
C05 ***Gfra2*** GDNF family receptor alpha 2
C06 ***Gfra3*** GDNF family receptor alpha 3
C07 ***Gmfb*** Glia maturation factor, beta
C08 ***Gmfg*** Glia maturation factor, gamma
C09 ***Grpr*** Gastrin releasing peptide receptor
C10 ***HcRt*** Hypocretin
C11 ***Hcrtr1*** Hypocretin (orexin) receptor 1
C12 ***Hcrtr2*** Hypocretin (orexin) receptor 2
D01 ***Hspb1*** Heat shock protein 1
D02 ***Il10*** Interleukin 10
D03 ***Il10ra*** Interleukin 10 receptor, alpha
D04 ***Il1b*** Interleukin 1 beta
D05 ***Il1r1*** Interleukin 1 receptor, type I
D06 ***Il6*** Interleukin 6
D07 ***Il6r*** Interleukin 6 receptor
D08 ***Il6st*** Interleukin 6 signal transducer
D09 ***Lif*** Leukemia inhibitory factor
D10 ***Lifr*** Leukemia inhibitory factor receptor alpha
D11 ***Maged1*** Melanoma antigen, family D, 1
D12 ***Mc2r*** Melanocortin 2 receptor
E01 ***Mt3*** Metallothionein 3
E02 ***Myc*** Myelocytomatosis oncogene
E03 ***Nell1*** NEL-like 1
E04 ***Nf1*** Neurofibromin 1
E05 ***Ngf*** Nerve growth factor (beta polypeptide)
E06 ***Ngfr*** Nerve growth factor receptor (TNFR superfamily, member 16)
E07 ***Ngfrap1*** Nerve growth factor receptor (TNFRSF16) associated protein 1
E08 ***Npffr2*** Neuropeptide FF receptor 2

E09 ***Npy*** Neuropeptide Y
E10 ***Npy1r*** Neuropeptide Y receptor Y1
E11 ***Npy2r*** Neuropeptide Y receptor Y2
E12 ***Nr1i2*** Nuclear receptor subfamily 1, group I, member 2
F01 ***Nrg1*** Neuregulin 1
F02 ***Nrg2*** Neuregulin 2
F03 ***Ntf3*** Neurotrophin 3
F04 ***Ntf4*** Neurotrophin 4
F05 ***Ntrk1*** Neurotrophic tyrosine kinase, receptor, type 1
F06 ***Ntrk2*** Neurotrophic tyrosine kinase, receptor, type 2
F07 ***Ntsr1*** Neurotensin receptor 1
F08 ***Ppyr1*** Pancreatic polypeptide receptor 1
F09 ***Pspn*** Persephin
F10 ***Ptger2*** Prostaglandin E receptor 2 (subtype EP2)
F11 ***Stat1*** Signal transducer and activator of transcription 1
F12 ***Stat2*** Signal transducer and activator of transcription 2
G01 ***Stat3*** Signal transducer and activator of transcription 3
G02 ***Stat4*** Signal transducer and activator of transcription 4
G03 ***Tacr1*** Tachykinin receptor 1
G04 ***Tfg*** Trk-fused gene
G05 ***Tgfa*** Transforming growth factor alpha
G06 ***Tgfb1*** Transforming growth factor, beta 1
G07 ***Tgfb1i1*** Transforming growth factor beta 1 induced transcript 1
G08 ***Tp53*** Tumor protein p53
G09 ***Ucn*** Urocortin
G10 ***Vgf*** VGF nerve growth factor inducible
G11 ***Zfp110*** Zinc finger protein 110
G12 ***Zfp91*** Zinc finger protein 91
H01 ***Actb*** Actin, beta
H02 ***B2m*** Beta-2 microglobulin

H03 ***Hprt1*** Hypoxanthine phosphoribosyltransferase 1
H04 ***Ldha*** Lactate dehydrogenase A
H05 ***Rplp1*** Ribosomal protein, large, P1
H06 **RGDC** Rat Genomic DNA Contamination
H07 **RTC** Reverse Transcription Control
H08 **RTC** Reverse Transcription Control
H09 **RTC** Reverse Transcription Control
H10 **PPC** Positive PCR Control
H11 **PPC** Positive PCR Control
H12 **PPC** Positive PCR Control

APPENDIX IV

Gene table shows gene position, symbol and description for synaptic plasticity RT² Profiler PCR Array.

A01 ***Adam10*** ADAM metallopeptidase domain 10
A02 ***Adcy1*** Adenylate cyclase 1 (brain)
A03 ***Adcy8*** Adenylate cyclase 8 (brain)
A04 ***Akt1*** V-akt murine thymoma viral oncogene homolog 1
A05 ***Arc*** Activity-regulated cytoskeleton-associated protein
A06 ***Bdnf*** Brain-derived neurotrophic factor
A07 ***Camk2a*** Calcium/calmodulin-dependent protein kinase II alpha
A08 ***Camk2g*** Calcium/calmodulin-dependent protein kinase II gamma
A09 ***Cdh2*** Cadherin 2
A10 ***Cebpb*** CCAAT/enhancer binding protein (C/EBP), beta
A11 ***Cebpd*** CCAAT/enhancer binding protein (C/EBP), delta
A12 ***Cnr1*** Cannabinoid receptor 1 (brain)
B01 ***Creb1*** CAMP responsive element binding protein 1
B02 ***Crem*** CAMP responsive element modulator
B03 ***Dlg4*** Discs, large homolog 4 (Drosophila)
B04 ***Egr1*** Early growth response 1
B05 ***Egr2*** Early growth response 2
B06 ***Egr3*** Early growth response 3
B07 ***Egr4*** Early growth response 4
B08 ***Ephb2*** Eph receptor B2
B09 ***Fos*** FBJ osteosarcoma oncogene
B10 ***Gabra5*** Gamma-aminobutyric acid (GABA) A receptor, alpha 5
B11 ***Gnai1*** Guanine nucleotide binding protein (G protein), alpha inhibiting 1
B12 ***Gria1*** Glutamate receptor, ionotropic, AMPA 1
C01 ***Gria2*** Glutamate receptor, ionotropic, AMPA 2
C02 ***Gria3*** Glutamate receptor, ionotrophic, AMPA 3

C03 ***Gria4*** Glutamate receptor, ionotrophic, AMPA 4
C04 ***Grin1*** Glutamate receptor, ionotropic, N-methyl D-aspartate 1
C05 ***Grin2a*** Glutamate receptor, ionotropic, N-methyl D-aspartate 2A
C06 ***Grin2b*** Glutamate receptor, ionotropic, N-methyl D-aspartate 2B
C07 ***Grin2c*** Glutamate receptor, ionotropic, N-methyl D-aspartate 2C
C08 ***Grin2d*** Glutamate receptor, ionotropic, N-methyl D-aspartate 2D
C09 ***Grip1*** Glutamate receptor interacting protein 1
C10 ***Grm1*** Glutamate receptor, metabotropic 1
C11 ***Grm2*** Glutamate receptor, metabotropic 2
C12 ***Grm3*** Glutamate receptor, metabotropic 3
D01 ***Grm4*** Glutamate receptor, metabotropic 4
D02 ***Grm5*** Glutamate receptor, metabotropic 5
D03 ***Grm7*** Glutamate receptor, metabotropic 7
D04 ***Grm8*** Glutamate receptor, metabotropic 8
D05 ***Homer1*** Homer homolog 1 (Drosophila)
D06 ***Igf1*** Insulin-like growth factor 1
D07 ***Inhba*** Inhibin beta-A
D08 ***Jun*** Jun oncogene
D09 ***Junb*** Jun B proto-oncogene
D10 ***Kruppel***-like factor 10
D11 ***Mapk1*** Mitogen activated protein kinase 1
D12 ***Mmp9*** Matrix metallopeptidase 9
E01 ***Ncam1*** Neural cell adhesion molecule 1
E02 ***Nfkb1*** Nuclear factor of kappa light polypeptide gene enhancer in B-cells 1
E03 ***Nfkbib*** Nuclear factor of kappa light polypeptide gene enhancer in B-cells inhibitor, beta
E04 ***Ngf*** Nerve growth factor (beta polypeptide)
E05 ***Ngfr*** Nerve growth factor receptor (TNFR superfamily, member 16)
E06 ***Nos1*** Nitric oxide synthase 1, neuronal
E07 ***Nptx2*** Neuronal pentraxin 2

E08 ***Nr4a1*** Nuclear receptor subfamily 4, group A, member 1
E09 ***Ntf3*** Neurotrophin 3
E10 ***Ntf4*** Neurotrophin 4
E11 ***Ntrk2*** Neurotrophic tyrosine kinase, receptor, type 2
E12 ***Pcdh8*** Protocadherin 8
F01 ***Pick1*** Protein interacting with PRKCA 1
F02 ***Pim1*** Pim-1 oncogene
F03 ***Plat*** Plasminogen activator, tissue
F04 ***Plcg1*** Phospholipase C, gamma 1
F05 ***Ppp1ca*** Protein phosphatase 1, catalytic subunit, alpha isoform
F06 ***Ppp1cc*** Protein phosphatase 1, catalytic subunit, gamma isoform
F07 ***Ppp1r14a*** Protein phosphatase 1, regulatory (inhibitor) subunit 14A
F08 ***Ppp2ca*** Protein phosphatase 2, catalytic subunit, alpha isoform
F09 ***Ppp3ca*** Protein phosphatase 3, catalytic subunit, alpha isoform
F10 ***Prkca*** Protein kinase C, alpha
F11 ***Prkcg*** Protein kinase C, gamma
F12 ***Prkg1*** Protein kinase, cGMP-dependent, type 1
G01 ***Rab3a*** RAB3A, member RAS oncogene family
G02 ***Rela V***-rel reticuloendotheliosis viral oncogene homolog A (avian)
G03 ***Reln*** Reelin
G04 **RGD1562511** Similar to MmKIF17
G05 ***Rgs2*** Regulator of G-protein signaling 2
G06 ***Rheb*** Ras homolog enriched in brain
G07 ***Sirt1*** Sirtuin (silent mating type information regulation 2 homolog) 1 (S. cerevisiae)
G08 ***Srf*** Serum response factor (c-fos serum response element-binding transcription factor)
G09 ***Synpo*** Synaptopodin
G10 ***Timp1*** TIMP metallopeptidase inhibitor 1 theta polypeptide
H01 ***Actb*** Actin, beta

H02 ***B2m*** Beta-2 microglobulin
H03 ***Hprt1*** Hypoxanthine phosphoribosyltransferase 1
H04 ***Ldha*** Lactate dehydrogenase A
H05 ***Rplp1*** Ribosomal protein, large, P1
H06 **RGDC** Rat Genomic DNA Contamination
H07 **RTC** Reverse Transcription Control
H08 **RTC** Reverse Transcription Control
H09 **RTC** Reverse Transcription Control
H10 **PPC** Positive PCR Control
H11 **PPC** Positive PCR Control
H12 **PPC** Positive PCR Control

APPENDIX V

Neurotrophins & Receptors PCR Array: Functional Gene Grouping

Neuropeptides and Receptors:

Adcyap1r1, Artn, Bdnf, Cntf, Cntfr, Crh, Crhbp, Crhr1, Crhr2, Frs2, Frs3, Gdnf, Gfra1, Gfra2, Gfra3, Gmfb, Gmfg, Hcrtr1, Hcrtr2, Mt3, Ngf, Ngfr, Ngfrap1, Nr1i2, Nrg1 (Hgl), Nrg2, Ntf3, Ntf4, Ntrk1, Ntrk2, Pspn, Ptger2, Tfg, Cd40 (Tnfrsf5), Fas (Tnfrsf6), Ucn, Vgf, Zfp110, Zfp91.

Neuropeptides and Receptors:

Galanin Receptors: *Galr1, Galr2.*
Neuropeptide Y Receptors: *Npy1r, Npy2r, Npy4r.*
Other Neuropeptides and Receptors: *Cckar, Grpr, Npffr2 (Gpr74), Ntsr1, HcRt, Mc2r, Npy, Nrg1 (Hgl), Tacr1.*

Neurogenesis:
Central Nervous System Development: *Cxcr4, Fgfr1, Ngfr, Ntf3.*
Peripheral Nervous System Development: *Artn, Gdnf, Gfra3, Ngf, Nrg1 (Hgl), Ntf3.*
Axon Guidance: Artn, Gfra3, Ngfr.
Gliogenesis: *Fgf2 (bFGF), Nrg1 (Hgl), Ntf3.*
Dendrite Morphogenesis: *Bdnf, Mt3.*
Other Neurogenesis Genes: *Bax, Fos, Cbln1, Galr2, Gfra1, Gfra2, Nell1, Ntf4, Ntrk1, Ntrk2.*

Cell Growth and Differentiation:
Growth Factors and Receptors: *Artn, Bdnf, Fgf2 (bFGF), Fgf9, Fgfr1, Gdnf, Gmfb, Gmfg, Il10, Il1b, Il6, Lif, Mt3, Ngf, Nrg2, Ntf3, Ntf4, Pspn, Tgfa, Tgfb1, Tgfb1i1, Tp53, Vgf.*
Cell Cycle: *Fgf2 (bFGF), Fgf9, Il1b, Ntrk1, Tgfa, Tgfb1, Tp53.*
Cell Proliferation: *Bax, Cxcr4, Fgf2 (bFGF), Fgf9, Grpr, Il10, Il1b, Myc, Stat4, Tgfa,*

Tgfb1, Tp53.

Cell Differentiation*: Cntf, Fgf2 (bFGF), Fgf9, Nf1, Nrg1 (Hgl), Stat3, Tp53, Zfp91.*

Cytokines and Receptors:

Cx3cr1, Cxcr4, Il10, Il10ra, Il1b, Il1r1, Il6, Il6r, Il6st (Gp130), Lif, Lifr,.

Apoptosis:

Bax, Bcl2, Cd40 (Tnfrsf5), Hspb1 (Hsp27), Il10, Il6, Myc, Ngfr, Ngfrap1, Fas (Tnfrsf6), Tp53.

Inflammatory Response:

Il10, Il1b, Il6, Stat3, Tgfb1.

Immune Response:

Il10, Cd40 (Tnfrsf5), Lif, Fas (Tnfrsf6).

Transcription Factors and Regulators:

Fos, Fus, Maged1, Myc, Nr1i2, Ntf3, Stat1, Stat2, Stat3, Stat4, Tp53, Tgfb1i1, Zfp110.

APPENDIX VI

Rat Synaptic Plasticity PCR Array: Functional Gene Grouping

Immediate-Early Response Genes (IEGs):

Arc, Bdnf, Cebpb, Cebpd, Creb1, Crem, Egr1, Egr2, Egr3, Egr4, Fos, Homer1, Jun, Junb, Klf10, Mmp9 (Gelatinase B), Nfkb1, Nfkbib (Trip9), Ngf, Nptx2, Nr4a1, Ntf3, Pcdh8, Pim1, Plat (tPA), Rela, Rgs2, Rheb, Srf, Tnf.

Late Response Genes: *Inhba, Synpo.*

Long Term Potentiation (LTP): *Adcy1, Adcy8, Bdnf, Camk2a, Camk2g, Cdh2 (N-cadherin), Cnr1, Gabra5, Gnai1, Gria1, Gria2, Grin1, Grin2a, Grin2b, Grin2c, Grin2d, Mapk1, Mmp9 (Gelatinase B), Ntf4, Ntrk2, Plcg1, Ppp1ca, Ppp1cc, Ppp3ca, Prkca, Prkcg, Rab3a, Ywhaq (14-3-3).*

Long Term Depression (LTD): *Gnai1, Gria1, Gria2, Gria3, Gria4, Grip1, Grm1, Grm2, Igf1, Mapk1, Nos1, Ngfr, Pick1, Plat (tPA), Ppp1ca, Ppp1cc, Ppp1r14a (Cpi-17), Ppp2ca, Ppp3ca, Prkca, Prkg1.*

Cell Adhesion: *Adam10, Cdh2 (N-cadherin), Grin2a, Grin2b, Ncam1, Pcdh8, Ppp2ca, Reln, Tnf.*

Extracellular Matrix & Proteolytic Processing: *Adam10, Mmp9 (Gelatinase B), Plat (tPA), Reln, Timp1.*

CREB Cofactors: *Akt1, Camk2g, Grin1, Grin2a, Grin2b, Grin2c, Grin2d, Mapk1 (Erk2), Ppp1ca, Ppp1cc.*

Neuronal Receptors: *Ephb2, Gabra5, Gria1, Gria2, Gria3, Gria4, Grin1, Grin2a, Grin2b, Grin2c, Grin2d, Grm1, Grm2, Grm3, Grm4, Grm5, Grm7, Grm8, Ntrk2.*

Postsynaptic Density: *Adam10, Arc, Dlg4 (Psd95), Gria1, Gria3, Gria4, Grin1, Grin2a, Grin2b, Grin2c, Grm1, Grm3, Homer1, Pick1, Synpo.*

APPENDIX VII

Fold Chang and Fold Regulation Values

Tables below show data from RT^2 PCR including gene symbol, *p*-value, fold change and fold regulation. Data are sorted by *p*-value from lowest to highest. Fold-change and fold-regulation values greater than 2 are indicated in red; fold-change values less than 0.5 and fold-regulation values less than -2 are indicated in blue.

A. FSA-treated Male Rats Comparing to Control Male Rats

Gene Symbol	*p*-value	fold change	fold regulation
Ccl11	0.03234	3.7352	3.7352
Stat4	0.041333	2.0813	2.0813
Bdnf	0.089873	3.851	3.851
Nos2	0.094423	0.50001	-2.0004
Crhbp	0.158613	1.6378	1.6378
Nell1	0.227599	1.2708	1.2708
Cbln1	0.280965	1.8809	1.8809
Arg1	0.291588	0.7505	-1.3325
Crh	0.35071	1.4626	1.4626
Cntfr	0.423522	0.874	-1.1442
Galr1	0.436634	1.1068	1.1068
Sox2	0.534786	0.8478	-1.1795
Creb1	0.550981	0.719	-1.3908
Il1b	0.554228	0.5653	-1.7691
Npy2r	0.566378	1.0393	1.0393
Vegfa	0.589248	0.9202	-1.0867
Cd163	0.633102	0.995	-1.0051
Camk2a	0.673144	0.8677	-1.1525
Fgf9	0.719273	1.019	1.019
Crhr1	0.721574	0.956	-1.046
Grip1	0.754236	0.9615	-1.04
Npy1r	0.75501	0.9634	-1.038
Il6	0.760602	0.6318	-1.5827
Cd40	0.771506	0.7912	-1.264
Gmfg	0.771657	0.7572	-1.3206
Camk2g	0.774906	0.9605	-1.0411
Tnf	0.785379	0.617	-1.6207
Gfra3	0.828051	0.4734	-2.1123

Cntf	0.850348	0.8518	-1.1739
Stat1	0.851229	0.6064	-1.649
Stat3	0.895215	1.0923	1.0923
il10ra	0.895902	0.8025	-1.246
Crhr2	0.953413	0.897	-1.1148
Fos	0.971686	1.0238	1.0238
Plat	0.972077	0.9203	-1.0866
Tgfb1	0.97797	0.6633	-1.5077
Cxcr4	0.991455	0.6021	-1.6608
Stat6	0.992385	0.8349	-1.1977

B. FSA-treated Female Rats Comparing to Control Female Rats

Gene Symbol	*p*-value	fold change	fold regulation
Sox2	0.047631	2.5115	2.5115
Cntf	0.057901	1.6898	1.6898
Creb1	0.059055	1.4316	1.4316
Fos	0.076262	1.3918	1.3918
Cntfr	0.099695	1.7101	1.7101
Crhr2	0.101033	1.4342	1.4342
Crhr1	0.10333	2.4755	2.4755
Camk2g	0.125511	2.1039	2.1039
Crh	0.147916	2.3538	2.3538
Arg1	0.155278	0.3795	-2.6353
Galr1	0.155288	1.7544	1.7544
Plat	0.165041	1.3647	1.3647
il10ra	0.202232	1.4973	1.4973
Crhbp	0.215802	2.2195	2.2195
Fgf9	0.225599	1.8046	1.8046
Gfra3	0.253349	1.3295	1.3295
Bdnf	0.272128	1.9904	1.9904
Cbln1	0.310568	2.0208	2.0208
Vegfa	0.337747	1.2386	1.2386
Camk2a	0.351778	1.8665	1.8665
Stat4	0.356739	1.3098	1.3098
Stat1	0.362456	1.1966	1.1966
Npy2r	0.367681	1.4132	1.4132
Il6	0.3708	0.7732	-1.2933
Tgfb1	0.378224	1.487	1.487
Grip1	0.379007	1.3269	1.3269
Ccl11	0.395425	1.2771	1.2771
Nell1	0.412523	2.1142	2.1142
Cd163	0.4487	1.2084	1.2084
Nos2	0.536738	0.8217	-1.217
Npy1r	0.57088	1.425	1.425
Tnf	0.638525	1.0934	1.0934
Cd40	0.63938	1.1124	1.1124
Stat3	0.646504	1.0171	1.0171
Gmfg	0.715201	0.7491	-1.335
Stat6	0.811588	1.1616	1.1616
Il1b	0.824719	0.974	-1.0267
Cxcr4	0.962157	1.0542	1.0542

C. Simvastatin-treated Male Rats Comparing to Control Male Rats

Gene Symbol	*p*-value	fold change	fold regulation
Ccl11	0.022319	2.3405	2.3405
Crhr2	0.067797	1.4184	1.4184
Cd163	0.073125	1.7696	1.7696
Fos	0.167572	1.3642	1.3642
Nos2	0.181671	0.7392	-1.3528
Cbln1	0.185183	2.0057	2.0057
Galr1	0.19592	1.4718	1.4718
Bdnf	0.200537	3.0055	3.0055
Crhbp	0.222841	1.4558	1.4558
Stat6	0.223868	1.6405	1.6405
Plat	0.256844	1.1847	1.1847
Cntf	0.2591	1.412	1.412
Cntfr	0.264005	1.1983	1.1983
Tgfb1	0.275765	1.4401	1.4401
il10ra	0.292258	1.6629	1.6629
Camk2a	0.30005	1.2253	1.2253
Sox2	0.316827	1.2873	1.2873
Camk2g	0.327571	1.1834	1.1834
Grip1	0.346105	1.2544	1.2544
Il6	0.415327	0.865	-1.1561
Stat3	0.425231	1.4677	1.4677
Npy2r	0.426295	1.2733	1.2733
Cxcr4	0.429465	1.4594	1.4594
Npy1r	0.441851	1.2411	1.2411
Cd40	0.489159	1.485	1.485
Creb1	0.504883	1.1676	1.1676
Fgf9	0.521157	1.1251	1.1251
Arg1	0.524046	1.1999	1.1999
Nell1	0.550677	1.1268	1.1268
Tnf	0.554736	1.1165	1.1165
Gmfg	0.574405	1.3142	1.3142
Crhr1	0.5775	1.0366	1.0366
Il1b	0.723912	1.1045	1.1045
Crh	0.824846	0.8641	-1.1573
Gfra3	0.880793	0.7031	-1.4223
Stat4	0.918165	1.0875	1.0875
Vegfa	0.947222	0.9915	-1.0085
Stat1	0.982461	0.9063	-1.1034

D. FSA-treated Female Rats Comparing to FSA-treated Male Rats

Gene Symbol	*p*-value	fold change	fold regulation
Fos	0.051224	1.47	1.47
Gfra3	0.084574	5.8624	5.8624
Cd163	0.089223	3.0674	3.0674
Cntf	0.105728	2.2289	2.2289
Il1b	0.150449	3.2735	3.2735
Cntfr	0.159912	1.4477	1.4477
Nos2	0.174178	2.371	2.371
Crhr2	0.194493	1.5751	1.5751
Sox2	0.199428	1.7685	1.7685
Crhr1	0.235838	1.6742	1.6742
Arg1	0.243321	1.9596	1.9596
Creb1	0.243441	1.7837	1.7837
Camk2g	0.265644	1.5051	1.5051
Tnf	0.273191	3.012	3.012
Tgfb1	0.295521	2.6995	2.6995
Stat3	0.321568	1.6189	1.6189
Plat	0.327347	1.5035	1.5035
Cxcr4	0.346437	3.4937	3.4937
Stat1	0.352873	2.3304	2.3304
Ccl11	0.429505	0.6515	-1.5348
Grip1	0.440118	1.163	1.163
il10ra	0.464164	2.0297	2.0297
Cd40	0.487533	2.4509	2.4509
Vegfa	0.493297	1.133	1.133
Stat6	0.496305	1.7039	1.7039
Crhbp	0.51346	1.4907	1.4907
Gmfg	0.582022	2.2929	2.2929
Il6	0.639032	2.3906	2.3906
Camk2a	0.656883	1.4105	1.4105
Npy2r	0.783806	1.0019	1.0019
Nell1	0.844901	1.0061	1.0061
Stat4	0.849211	1.0134	1.0134
Fgf9	0.873117	1.1626	1.1626
Galr1	0.885226	1.3016	1.3016
Npy1r	0.887996	1.0873	1.0873
Cbln1	0.906738	0.6692	-1.4944
Crh	0.910133	1.2329	1.2329
Bdnf	0.958841	1.2839	1.2839

E. Control Female Rats Comparing to Control Male Rats

Gene Symbol	*p*-value	fold change	fold regulation
Sox2	0.046977	0.403	-2.4814
Cntfr	0.074848	0.4995	-2.0022
Creb1	0.101809	0.6047	-1.6536
Vegfa	0.129834	0.5682	-1.76
Camk2g	0.130036	0.4639	-2.1558
Fgf9	0.1307	0.4431	-2.2566
Npy2r	0.151455	0.4974	-2.0105
Crh	0.162665	0.5171	-1.9337
Crhr1	0.172162	0.4365	-2.2911
Grip1	0.213425	0.5689	-1.7579
Cd163	0.221681	1.7048	1.7048
Ccl11	0.242341	1.2864	1.2864
Galr1	0.266493	0.5543	-1.8041
Npy1r	0.268385	0.4962	-2.0152
Cntf	0.27722	0.7585	-1.3185
Crhr2	0.27996	0.665	-1.5038
Cbln1	0.286772	0.4205	-2.3784
Stat1	0.306141	0.7972	-1.2544
Plat	0.317554	0.6844	-1.4611
Arg1	0.343563	2.6161	2.6161
Camk2a	0.415672	0.4426	-2.2593
Nell1	0.443202	0.4082	-2.4496
il10ra	0.443591	0.7343	-1.3618
Fos	0.464762	0.7299	-1.3701
Gfra3	0.537377	1.4092	1.4092
Cxcr4	0.711004	1.347	1.347
Gmfg	0.728997	1.5647	1.5647
Il1b	0.737027	1.2825	1.2825
Tgfb1	0.815698	0.8128	-1.2303
Stat4	0.817578	1.087	1.087
Crhbp	0.834578	0.7425	-1.3468
Tnf	0.845661	1.1474	1.1474
Stat6	0.873237	0.8267	-1.2096
Nos2	0.877283	0.9906	-1.0095
Bdnf	0.915087	1.6769	1.6769
Il6	0.969347	1.3186	1.3186
Stat3	0.989123	1.1736	1.1736
Cd40	0.992662	1.1767	1.1767

F. Neurotrophic Factors-regulated Gene Expressions in FSA treated Male Rats Comparing to Control

Gene Symbol	*p*-value	fold change	fold regulation
Gdnf	0.027147	0.5286	-1.8919
Fas	0.03166	0.4035	-2.4784
Il1b	0.032286	0.3877	-2.5795
Nr1i2	0.039786	3.7774	3.7774
Cntf	0.051449	0.6523	-1.533
Il10	0.059186	0.4512	-2.2165
Pspn	0.11014	1.6954	1.6954
Mt3	0.116473	0.7846	-1.2746
Zfp91	0.119956	1.4965	1.4965
Galr2	0.120142	1.5424	1.5424
HcRt	0.128589	9.9214	9.9214
Npffr2	0.129714	0.5853	-1.7085
Grpr	0.132977	2.2403	2.2403
Lif	0.149851	0.2841	-3.5205
Hspb1	0.160027	0.3582	-2.7916
Ucn	0.184827	1.5905	1.5905
Stat3	0.196704	0.6712	-1.49
Fus	0.200037	0.7883	-1.2686
Il6	0.210604	0.3641	-2.7461
Zfp110	0.210782	1.2478	1.2478
Hcrtr2	0.212278	1.4767	1.4767
Nell1	0.235502	1.4848	1.4848
Cckar	0.237235	0.6939	-1.4411
Npy	0.251874	1.3044	1.3044
Crhr2	0.255905	1.4652	1.4652
Cxcr4	0.260175	0.4393	-2.2765
Bdnf	0.275876	3.9795	3.9795
Ntrk1	0.27955	0.7334	-1.3636
Ntrk2	0.291239	1.3084	1.3084
Nf1	0.317303	1.2141	1.2141
Ptger2	0.326239	0.554	-1.8049
Ngfrap1	0.335346	1.2111	1.2111
Npy1r	0.336204	1.377	1.377
Fgf2	0.348263	0.789	-1.2674
Stat4	0.357587	1.5701	1.5701
Ngf	0.363967	1.2321	1.2321
Tgfb1i1	0.369922	1.2762	1.2762
Lifr	0.375133	1.2643	1.2643

Tp53	0.381005	1.1799	1.1799
Bax	0.407826	0.6913	-1.4465
Gfra2	0.414646	1.2027	1.2027
Frs3	0.439885	1.1153	1.1153
Cx3cr1	0.452364	0.562	-1.7793
Cbln1	0.454712	1.6227	1.6227
Hcrtr1	0.457167	1.1227	1.1227
Npy4r	0.45726	1.3753	1.3753
Fgf9	0.481014	0.9783	-1.0222
Myc	0.490162	0.4904	-2.0393
Ntf3	0.506506	1.4581	1.4581
Vgf	0.523186	0.9217	-1.0849
Fgfr1	0.545401	0.7876	-1.2696
Frs2	0.566019	1.1046	1.1046
Crh	0.571825	0.9597	-1.042
Maged1	0.58919	1.0137	1.0137
Ntf4	0.591481	0.6727	-1.4865
Il1r1	0.643553	0.6298	-1.5877
Il10ra	0.659463	0.5726	-1.7464
Stat1	0.663928	0.754	-1.3263
Tgfb1	0.682868	0.7713	-1.2965
Cntfr	0.690641	0.7825	-1.2779
Il6r	0.691259	0.6581	-1.5195
Crhbp	0.696538	0.8017	-1.2473
Nrg2	0.698461	1.0591	1.0591
Artn	0.72308	0.8388	-1.1921
Tacr1	0.730063	1.0187	1.0187
Il6st	0.736219	0.9564	-1.0456
Npy2r	0.739882	1.4755	1.4755
Fos	0.741683	0.8284	-1.2071
Nrg1	0.743462	0.9605	-1.0412
Adcyap1r1	0.764325	0.7279	-1.3739
Galr1	0.779722	0.619	-1.6154
Cd40	0.785942	0.5142	-1.9447
Gfra1	0.786957	0.8671	-1.1532
Ngfr	0.817439	0.7037	-1.4211
Tfg	0.817747	1.0206	1.0206
Gmfg	0.828249	0.5432	-1.841
Mc2r	0.831922	0.8033	-1.2449
Gmfb	0.883504	0.9415	-1.0621
Tgfa	0.908245	0.9966	-1.0034

Crhr1	0.923336	0.7899	-1.266
Stat2	0.932098	0.9141	-1.094
Gfra3	0.937607	0.5988	-1.6699
Ntsr1	0.985155	0.8096	-1.2353
Bcl2	0.995706	0.9074	-1.102

F. Synaptic Plasticity-regulated Gene Expression in FSA treated Male Rats Comparing to Control

gene	***p*** value	**fod change**	**fold regulation**
Pim1	0.12664	0.6422	-1.5572
Klf10	0.151032	0.5412	-1.8478
Nr4a1	0.167991	1.8715	1.8715
Mmp9	0.177072	0.4552	-2.1968
Cebpd	0.186163	0.3841	-2.6035
Jun	0.192471	0.6844	-1.461
Pcdh8	0.218854	2.851	2.851
Timp1	0.219116	0.5087	-1.9657
Cdh2	0.235217	0.6657	-1.5023
Ntf3	0.25607	1.555	1.555
Akt1	0.269585	0.7898	-1.2661
Sirt1	0.291652	1.1592	1.1592
Tnf	0.295738	0.5748	-1.7399
Cebpb	0.308731	0.5608	-1.7832
Cnr1	0.330611	0.5847	-1.7102
Rab3a	0.342813	1.0856	1.0856
Pick1	0.371536	1.1874	1.1874
Nfkbib	0.374321	0.7592	-1.3172
Nos1	0.374801	1.2927	1.2927
Rela	0.380306	0.8689	-1.1509
Gria1	0.386969	0.5336	-1.8742
Egr2	0.394857	1.1844	1.1844
Grin2c	0.397816	0.5966	-1.6761
Igf1	0.401632	0.4222	-2.3683
Synpo	0.402157	1.2184	1.2184
Ntf4	0.439379	0.811	-1.233
Prkcg	0.443998	1.0263	1.0263
Gnai1	0.446055	0.6494	-1.5398
Egr1	0.455676	1.0975	1.0975
Reln	0.468039	1.0898	1.0898

Nfkb1	0.474956	1	1
Egr4	0.491043	1.0349	1.0349
Gabra5	0.505539	0.5208	-1.9201
Prkg1	0.506751	1.1523	1.1523
Plat	0.521329	0.928	-1.0775
Ngfr	0.521657	0.9013	-1.1095
Ncam1	0.530234	1.1187	1.1187
Junb	0.540034	1.1783	1.1783
Ppp2ca	0.541094	1.2053	1.2053
Creb1	0.546866	0.7586	-1.3183
Ppp1cc	0.553437	0.9584	-1.0434
Bdnf	0.56377	0.8524	-1.1731
Ywhaq	0.567824	1.0896	1.0896
Rheb	0.590702	1.1023	1.1023
Grm3	0.598756	0.7269	-1.3756
Grin2d	0.610027	0.913	-1.0953
Gria3	0.620373	0.8035	-1.2446
Gria2	0.629791	0.775	-1.2904
Ppp3ca	0.637036	1.0658	1.0658
Ngf	0.640312	1.2567	1.2567
Grm7	0.649373	0.9665	-1.0347
Fos	0.657628	0.7617	-1.3129
Grin1	0.66239	0.6966	-1.4355
Ppp1ca	0.677821	0.9423	-1.0612
Homer1	0.699038	1.0384	1.0384
Ephb2	0.715093	0.8469	-1.1807
Ppp1r14a	0.7184	1.0842	1.0842
Camk2g	0.731992	0.8209	-1.2182
Srf	0.75282	1.0424	1.0424
Gria4	0.759192	0.8568	-1.1671
Camk2a	0.760477	0.7767	-1.2874
Mapk1	0.768616	0.8512	-1.1748
Grip1	0.77556	0.8592	-1.1638
Grin2a	0.777394	0.8951	-1.1172
Prkca	0.794296	0.8962	-1.1159
Plcg1	0.799546	1.0633	1.0633
Egr3	0.799952	0.934	-1.0706
Dlg4	0.806109	0.6941	-1.4407
Grm8	0.82198	0.719	-1.3907
Inhba	0.834537	0.7964	-1.2557
Adcy8	0.840848	0.9416	-1.062

Crem	0.847683	0.8908	-1.1226
Nptx2	0.851677	1.0505	1.0505
Grin2b	0.856433	0.8759	-1.1417
Ntrk2	0.858551	1.1388	1.1388
Kif17	0.920053	0.9983	-1.0017
Grm5	0.921761	0.7531	-1.3279
Arc	0.93635	0.7814	-1.2798
Grm4	0.947561	0.7526	-1.3287
Grm2	0.968087	0.9456	-1.0576
Adam10	0.972659	0.9301	-1.0751
Rgs2	0.97654	1.0286	1.0286
Grm1	0.987763	0.7249	-1.3795
Adcy1	0.995551	0.8225	-1.2158